Vol. 67 • No. 12

December 2024

Microwave Journal

horizon house®

Founded in 1958

mwjournal.com

MILLER MMIC

Advancing RF MMIC Design Through Human-AI collaboration and competition

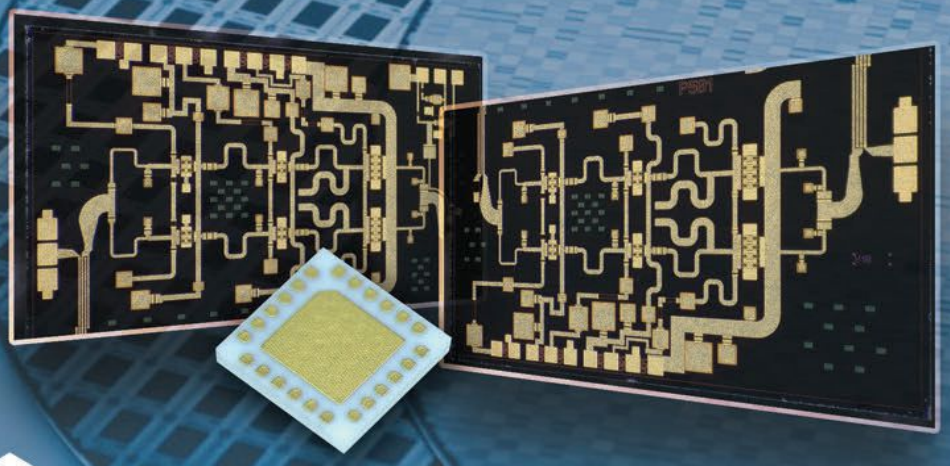

Miller MMIC is a global provider of RF semiconductor solutions with expertise in GaAs and GaN processes. We offer a diverse range of products tailored to various wireless applications. Our product lineup encompasses a wide array of offerings, including Low Noise Amplifiers, Distributed Amplifiers, Power Amplifiers, Driver Amplifiers, RF Switches, RF PIN Diode Switches, and numerous other voltage- and digitally-controllable RF components.

RapidRF MILLER MMIC RapidRF AI Platform for RF MMIC Design

RF Distributed Low Noise Amplifiers

PN	Freq Low (GHz)	Freq High (GHz)	Gain (dB)	NF(dB)	P1dB (dBm)	Voltage (VDC)	Current (mA)	Package
MMW001T	DC	20.0	17~19	1~3.5	23 @ 10GHz	8.0	145	die
MMW4FP	DC	50.00	16.00	4.00	24.00	10	200	die
MMW507	0.20	22.0	14.0	4 - 6	28.0	10.0	350	die
MMW508	DC	30.0	14.0	2.5dB @ 15GHz	24.5	10.0	200	die
MMW509	30KHz	45.0	15.0		20.0	6.0	190	die
MMW510	DC	45.0	11.0	4.5	15.5	6.0	100	die
MMW510F	DC	30.00	20.00	2.50	22.00			die
MMW511	0.04	65.0	10.0	9.0	18.0	8.0	250	die
MMW512	DC	65.0	10.0	5.0	14.5	4.5	85	die
MMW5FN	DC	67.00	14.00	2.00	19.00	4.5	81	die
MMW5FP	DC	67.00	14.00	4.00	21.00	8	140	die
MMW011	DC	12.0	14.0		30.5	12.0	350	die

Low Noise Amplifiers

PN	Freq Low (GHz)	Freq High (GHz)	Gain (dB)	NF(dB)	P1dB (dBm)	Voltage (VDC)	Current (mA)	Package
MML040	6.0	18.0	24.0	1.5	14.0	5.0	35	die
MML058	1.0	18.0	15.0	1.7	17.0	5.0	35	die
MML063	18.0	40.0	11.0	2.9	15.0	5.0	52	die
MML080	0.8	18.0	16.5/15.5	1.9/1.7	18/17.5	5.0	65/40	die
MML081	2.0	18.0	25/23	1.0/1.0	16/9.5	5.0	37/24	die
MML083	0.1	20.0	23.0	1.6	11.0	5.0	58	die

RF Driver Amplifier

PN	Freq Low (GHz)	Freq High (GHz)	Gain (dB)	NF(dB)	P1dB (dBm)	Voltage (VDC)	Current (mA)	Package
MM3006	2.0	20.0	19.5	2.5	22.0	7.0	130	die
MM3014	6.0	20.0	15.0	-	19.5	5.0	107	die
MM3017T	17.0	43.0	25.0		22.0	5.0	140	die
MM3031T	20.0	43.0	20.0		24.0	5.0	480	die
MM3051	17.0	24.0	25.0	-	25.0	5.0	220	die
MM3058	18.0	40.0	20/19.5	2.5/2.3	16/14	5/4	69/52	die
MM3059	18.0	40.0	16/16	2.5/2.3	16/15	5/4	67/50	die

GaAs Medium Power Amplifier

PN	Freq Low (GHz)	Freq High (GHz)	Gain (dB)	P1dB (dBm)	Psat (dBm)	Voltage (VDC)	Current (mA)	Package
MMP107	17.0	21.0	19.0	30.0	30.0	6.0	400	die
MMP108	18.0	28.0	14.0	31.5	31.0	6.0	650	die
MMP111	26.0	34.0	25.5	33.5	33.5	6.0	1300	die
MMP112	2.0	6.0	20.0	31.5	32.0	8.0	365	die
MMP501	20.0	44.0	15.0	27 -- 32	29 - 34	5.0	1200	die
MMP502	18.0	47.0	14.0	28.0	30.0	5.0	1500	die

PN: MMW5FP

RF GaAs MMIC DC-67GHz

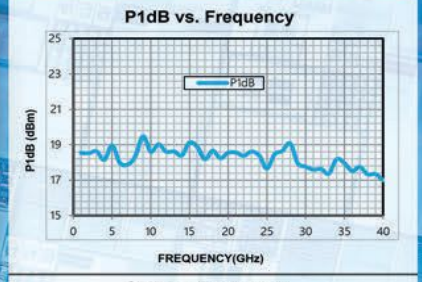

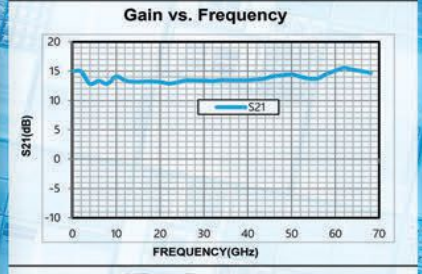

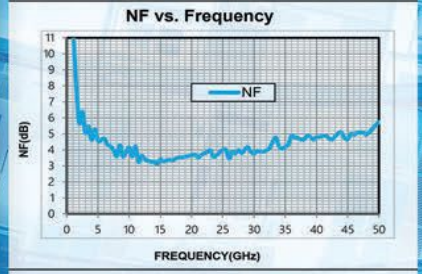

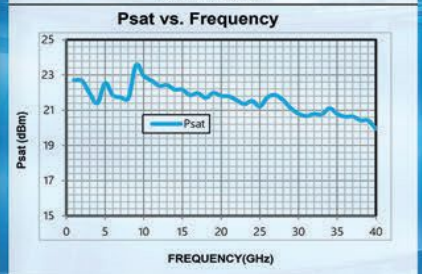

CALL US 1-833-2MILLER(264-5537)

WWW.MILLERMMIC.COM

RapidRF sales@millermmic.com support@millermmic.com

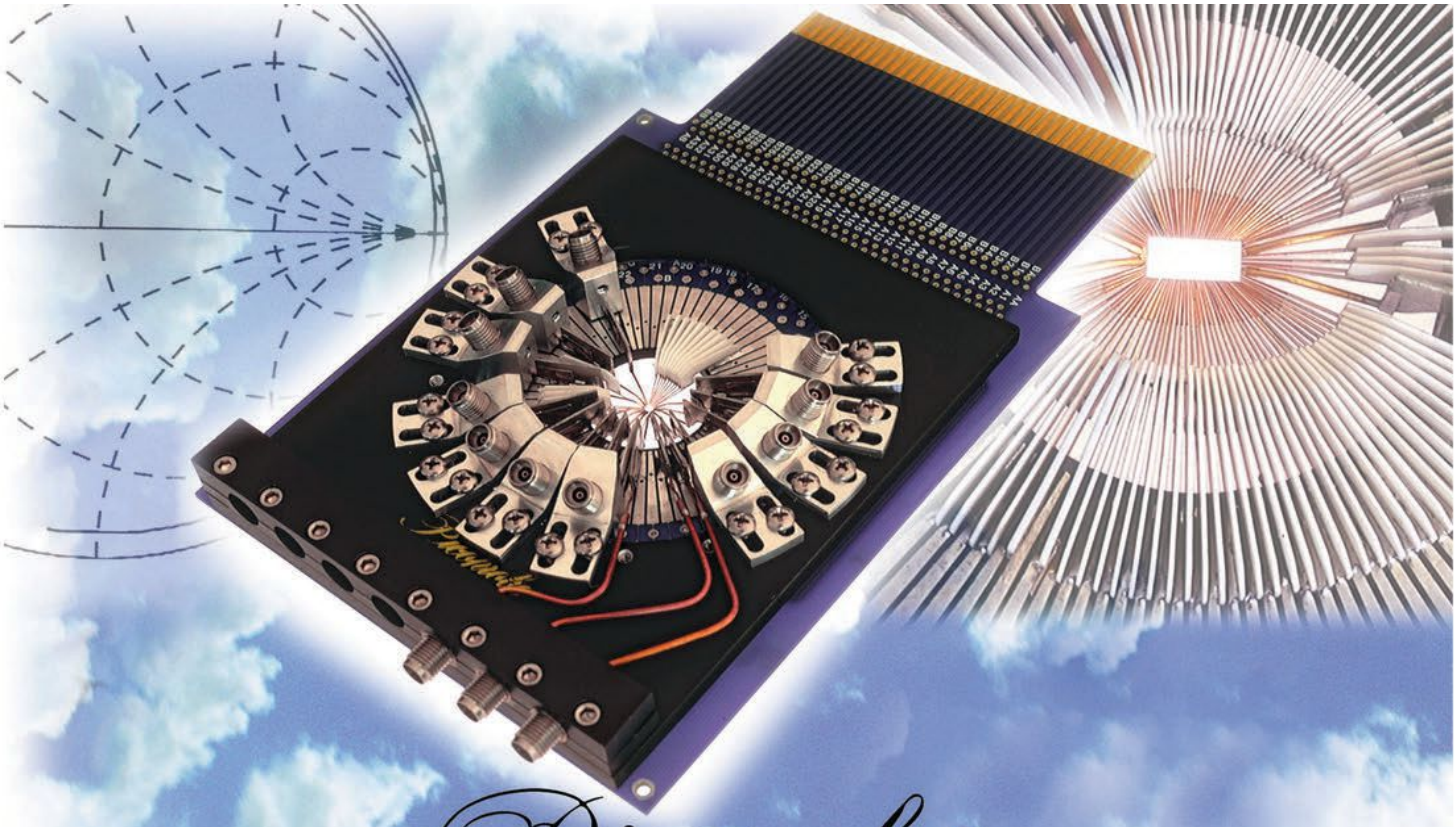

Picoprobe®

Picoprobe elevates probe cards to a higher level…

(…110 GHz to be exact.)

Since 1981, GGB Industries, Inc., has blazed the on-chip measurement trail with innovative designs, quality craftsmanship, and highly reliable products. Our line of custom microwave probe cards continues our tradition of manufacturing exceptional testing instruments.

Through unique modular design techniques, hundreds of low frequency probe needles and a variety of microwave probes with operating frequencies from DC to 40, 67, or even 110 GHz can be custom configured to your layout.

Our patented probe structures provide the precision and ruggedness you require for both production and characterization testing. And only Picoprobe® offers the lowest loss, best match, low inductance power supplies, and current sources on a single probe card.

Our proven probe card design technology allows full visibility with inking capability and ensures reliable contacts, even when probing non-planar structures.

Not only do you get all the attractive features mentioned, but you get personal, professional service, rapid response, and continuous product support--all at an affordable price so your project can be completed on time and within budget.

Typical Specs	10GHz	20GHz	40GHz
Insertion Loss	0.6 dB	0.8 dB	1.3 dB
Return Loss	22 dB	18 dB	15 dB

For technical assistance, custom product designs, or off-the-shelf delivery,call GGB Industries, Inc., at (239) 643-4400.

GGB INDUSTRIES, INC. • 4196 CORPORATE SQUARE • NAPLES, FL 34104

Telephone (239) 643-4400 • E-mail email@ggb.com • www.picoprobe.com

DC TO 110 GHz

RF & Microwave Test Accessories

One-Stop Shopping from R&D to Production

LEARN MORE

ADAPTERS
Coax & Waveguide

AMPLIFIERS
DC to 110 GHz

ATTENUATORS
DC to 65 GHz

GAUGES, CAL KITS & WRENCHES

BIAS TEES
0.1 MHz to 54 GHz

CABLES
Test Leads
& System Cables

COUPLERS
0.005 MHz to 65 GHz

DC BLOCKS
0.1 MHz to 65 GHz

EQUALIZERS
DC to 40 GHz

FILTERS
DC to 86 GHz

HYBRIDS,
90° & 180°
0.01 to 4200 MHz

IMPEDANCE
MATCHING PADS
DC to 3000 MHz

LIMITERS
0.2 to 8200 MHz

MIXERS
0.0005 MHz to 65 GHz

MODULATORS
& DEMODULATORS
1 to 200 MHz

MULTIPLIERS
0.05 MHz to 20 MHz

PHASE DETECTORS
1 MHz to 100 MHz

PHASE SHIFTERS
250 MHz to 430 MHz

POWER
DETECTORS
10 MHz to 43.5 GHz

POWER SPLITTERS
& COMBINERS
DC to 67 GHz

SWITCHES
DC to 67 GHz

TERMINATIONS
DC to 65 GHz

TRANSFORMERS
& BALUNS
DC to 2500 MHz

Mini-Circuits®

RF EXCELLENCE.
MISSION-CRITICAL SUCCESS.

NIC

Innovative Solutions - DC-40GHz | Quick Prototype Delivery (3-4 wks)

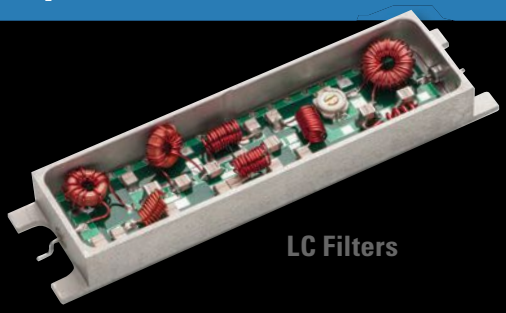

LC Filters

Cavity Filters

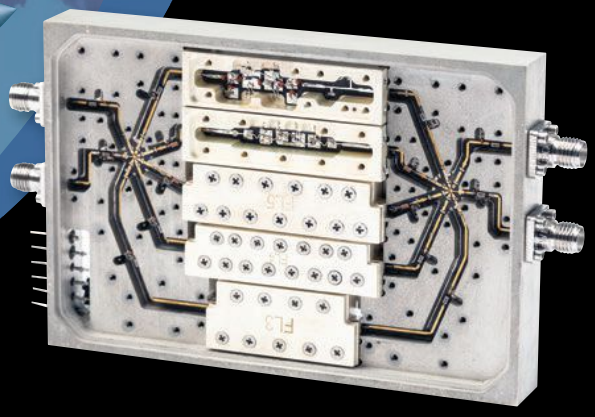

Switched Filter Banks

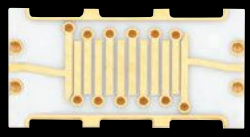

Printed Filters

Ceramic & Crystal Filters • Space-Qualified Filters • Multiplexers • Integrated Assemblies

Radar | EW | Guidance & Navigation | Communications | GPS & Satellite

ISO 9001:2015
AS9100
CERTIFIED

NIC NETWORKS INTERNATIONAL CORPORATION
www.nickc.com

913.685.3400
15237 Broadmoor
Overland Park, KS
e-mail: sales@nickc.com

Take Control.

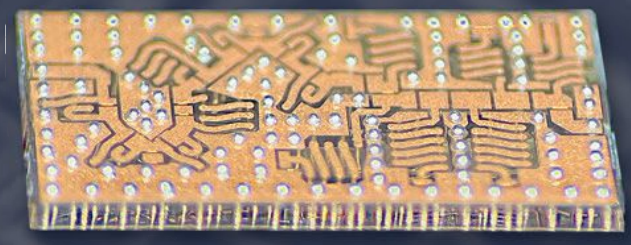

2.6 mm x 5.4 mm

Meet the new ultra-miniature, high Q filters from Spectrum Control

Until now, high performance RF filters, like traditional lumped elements, were not small enough to fit on your board. Now you can take back control of your miniature RF circuits with a new family of standard and custom filters from Spectrum Control; operating in bands from 0.5 to 10 GHz, with extremely low insertion loss and excellent out-of-band rejection.

These new filters are manufactured using a highly repeatable, wafer-scale process in glass. And the results are revolutionary – incredible filtering performance delivered in a 2.6 x 5.4 mm BGA package. The MMG family is ideal for lowpass, high-pass, bandpass, notch, and multiplexer filtering in a wide range of defense, space, and commercial applications.

Learn more at spectrumcontrol.com/High-Q

SPECTRUM CONTROL™

spectrumcontrol.com © 2024 Spectrum Control, Inc. All rights reserved

All Test and Measurement Components are In-Stock

Pasternack RF test and measurement equipment, calibration kits, cable assembly and other precision interconnects cover a broad range of uses and applications across the radio frequency spectrum to provide phase stability with many cycles of repeatability over a wide temperature range.

In-Stock & Shipped Same-Day

pasternack.com
+1 (800) 715-4396

PASTERNACK®
an INFINITE brand

RF-LAMBDA

THE LEADER OF RF BROADBAND SOLUTIONS

BROADBAND SSPA / EMC BENCHTOP

SOLID STATE POWER AMPLIFIER

0.1-22GHZ ULTRA BROADBAND SSPA

RFLUPA01M22GA
4W 0.1-22GHZ

RFLUPA0218GB
20W 1-19GHZ

300W 6-18GHZ SOLID STATE BROADBAND

400W 8-11GHZ
SOLID STATE BROADBAND

0. 1-6GHZ VHZ, UHF, L, S, C BAND

RFLUPA02G06GC
100W 2-6GHZ

RFLUPA0706GD
30W 0.7-6GHZ

MADE IN USA

6-18GHZ C, X, KU BAND

RFLUPA0618GD
60W 6-18GHZ

RFLUPA08G11GA
50W 8-11GHZ

RFLUPA06G12GB
25W 6-12GHZ

18-50GHZ K, KA, V BAND

RFLUPA18G47GC
2W 18-47GHZ

RFLUPA27G34GB
15W 27-34GHZ

RFLUPA47G53GA2
10W 47-53GHZ

RFLUPA27G34GB
30W 18-40GHZ

BENCHTOP RF MICROWAVE SYSTEM POWER AMPLIFIER

RAMP00G06GA- 30W 0.01-6GHZ

RAMP39G48GA- 4W 39-48GHZ

RAMP01G22GA- 8W 1-22GHZ

RAMP27G34GA- 8W 27-34GHZ

www.rflambda.com 1-888-976-8880 San Diego, CA, US Ottawa, ONT, Canada
sales@rflambda.com 1-972-767-5998 Carrollton, TX, US Frankfurt, Germany

Microwave Journal
CONTENTS

December 2024
Vol. 67 • No. 12
Government & Military Electronics
mwjournal.com

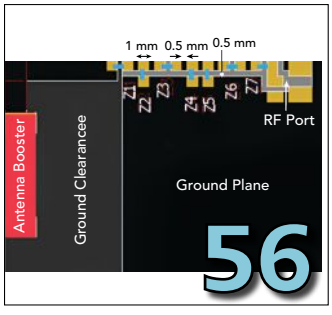

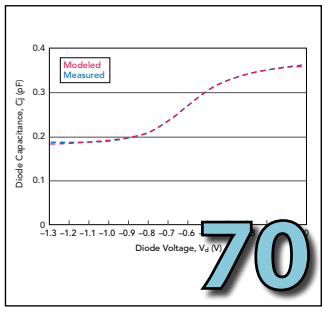

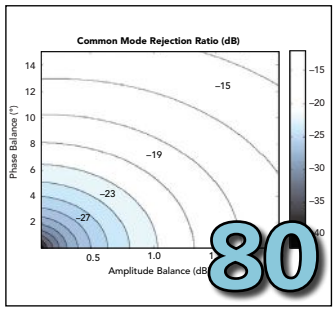

Cover Feature

18 **Countering the Evolving UAS Threat**
Graeme Forsyth, SPX Communication Technologies, formed by TCI and Enterprise Control Systems

Special Report

44 **The Future of Wireless: Technologies Overcoming 5G Struggles**
Ali Sadri, Airgain and Kyei Anim and Kapil Dandekar, Drexel University

2024 Editorial Index

A complete listing of 2024 Microwave Journal articles, organized by subject and indexed alphabetically by author, can be found at mwjournal.com/edindex2024.

Technical Feature

56 **Designing IoT Devices Embedding Antenna Boosters Using Freeware and Low-Cost Equipment**
J. Valle, A. Andújar** and J. Anguera*,**, Smart Society Research Group, Universitat Ramon Llull* and Ignion***

Tutorials

70 **Extracting Diode Parameters Using Optimization in Excel Part 2: AC Parameters from Capacitance Measurements**
Charles Trantanella, Retired from Custom MMIC

80 **Advantages and Applications of GaN Push-Pull Amplifiers**
Paramita Maity, Ashish Shinde, Sritama Dutta and Manish Shah, TagoreTech

ACCESS NOW!
digital.microwavejournal.com

eXclusive Digital Content ›››

109 **Nonlinear Algorithm for Small-Signal GaN HEMT Modeling**
Ziyue Ding, Haiyi Cai, Jincan Zhang, Yuhao Ren and Jinchan Wang Henan University of Science and Technology

114 **CPW-Fed Microstrip Antenna Design Uses Machine Learning Approach**
Sonmati Verma, Rajiv Kumar Singh and Neelam Srivstava, Institute of Engineering & Technology and Pinku Ranjan, ABV-Indian Institute of Information Technology and Management

67 YEARS OF PUBLISHING EXCELLENCE

Has Amplifier Performance or Delivery Stalled Your Program?

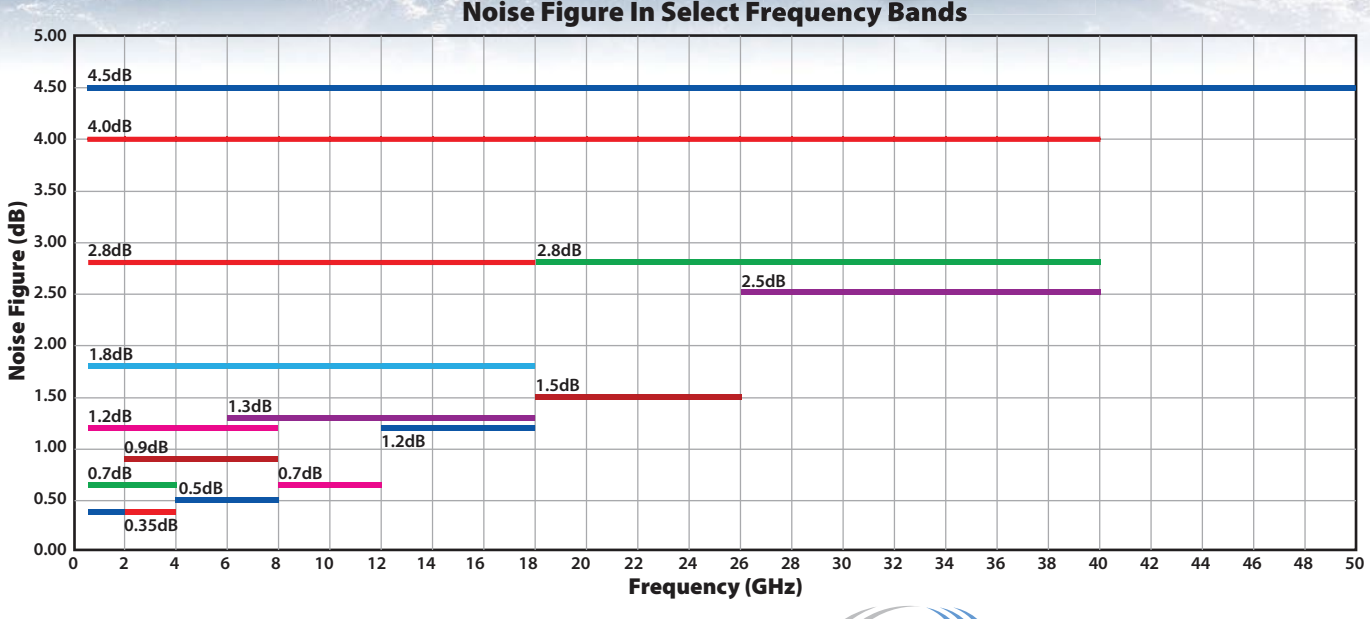

B&Z TECHNOLOGIES
Innovating to Excel

www.bnztech.com

Microwave Journal
CONTENTS
mwjournal.com

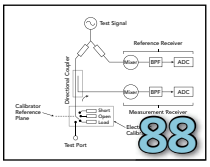

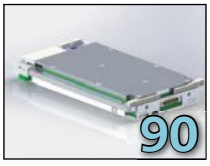

Product Features

88 **Vector Network Analyzer for Embedded OEM Applications**
LA Techniques Ltd and AAI Robotics Ltd

90 **20 GHz 3U VPX Module Speeds EW and Radar Design Times**
Analog Devices, Inc.

92 **Millimeter Wave Filters Shrink EW and Radar Systems**
Benchmark Lark Technology

Tech Briefs

96 **Chamber Enables 110 GHz 4K Testing**
Eravant (formerly Sage Millimeter Inc.)

96 **High-Power SSPA Produces 600 W**
Exodus Advanced Communications

Departments

17 Mark Your Calendar
29 Defense News
33 Commercial Market
36 Around the Circuit
98 Making Waves
99 New Products
102 Book End
104 Ad Index
104 Sales Reps
106 Fabs & Labs

Microwave Journal (USPS 396-250) (ISSN 0192-6225) is published monthly by Horizon House Publications Inc., 685 Canton St., Norwood, MA 02062. Periodicals postage paid at Norwood, MA 02062 and additional mailing offices.

Photocopy Rights: Permission to photocopy for internal or personal use, or the internal or personal use of specific clients, is granted by Microwave Journal for users through Copyright Clearance Center provided that the base fee of $5.00 per copy of the article, plus $1.00 per page, is paid directly to the Copyright Clearance Center, 222 Rosewood Drive, Danvers, MA 01923 USA (978) 750-8400. For government and/or educational classroom use, the Copyright Clearance Center should be contacted. The rate for this use is 0.03 cents per page. Please specify ISSN 0192-6225 Microwave Journal International. Microwave Journal can also be purchased on 35 mm film from University Microfilms, Periodic Entry Department, 300 N. Zeeb Rd., Ann Arbor, MI 48106 (313) 761-4700. Reprints: For PDF reprints, contact Barbara Walsh at (781) 769-9750.

POSTMASTER: Send address corrections to Microwave Journal, PO Box 1028, Lowell, MA 01853 or e-mail mwj@e-circ.net. com. Subscription information: (978) 671-0446. This journal is issued without charge upon written request to qualified persons working in the RF & microwave industry. Other subscriptions are: domestic, $130.00 per year, two-year subscriptions, $200.00; foreign, $225.00 per year, two-year subscriptions, $400.00; back issues (if available) and single copies, $20.00 domestic and $30.00 foreign. Claims for missing issues must be filed within 90 days of date of issue for complimentary replacement.

©2024 by Horizon House Publications Inc.
Posted under Canadian international publications mail agreement #PM40612608

STAFF

Group Director: Carl Sheffres
Associate Publisher: Michael Hallman
Media Director: Patrick Hindle
Brand & Content Director: Jennifer DiMarco
Technical Editor: Eric Higham
Associate Technical Editor: Cliff Drubin
Editorial & Media Specialist: Kelley Roche
Associate Editor: Kaitlyn Joyner
Multimedia Staff Editor: Barbara Walsh
Electronic Marketing Manager: Chris Stanfa
Senior Digital Content Specialist: Lauren Tully
Digital Content Specialist: Vincent Carrabino
Director of Production & Distribution: Edward Kiessling
Art Director: Janice Levenson
Graphic Designer: Ann Pierce

EUROPE
Office Manager: Nina Plesu

CORPORATE STAFF
CEO: William M. Bazzy
President: Ivar Bazzy
Vice President: Jared Bazzy

EDITORIAL REVIEW BOARD
A. Chenakin
R. Dahle
B. Derat
K. Galitskaya
R. Hershtig
D. Jorgesen
W. Lohmeyer
M. Ozalas
A. Poddar
C. Puente
B. Rautio
M. Roberg
U. Rohde
F. Schindler
R. Smith
D. Vye

EXECUTIVE EDITORIAL OFFICE
685 Canton Street, Norwood, MA 02062
Tel: (781) 769-9750
FAX: (781) 769-5037
e-mail: mwj@mwjournal.com

EUROPEAN EDITORIAL OFFICE
16 Sussex Street, London SW1V 4RW, England
Tel: Editorial: +44 207 596 8730 Sales: +44 207 596 8740
FAX: +44 207 596 8749

SUBSCRIPTION SERVICES
Send subscription inquiries and address changes to:
Tel: (978) 671-0446
e-mail: mwj@e-circ.net

www.mwjournal.com

Printed in the USA

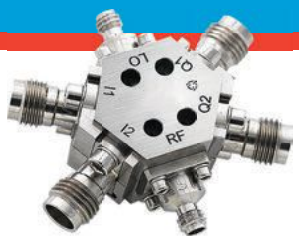

RFMW®

From Introduction to Production

Strategically Aligned Distribution

With World-leading Manufacturers in
RF, Microwave, and Power

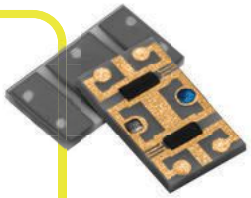

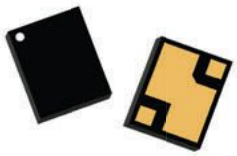

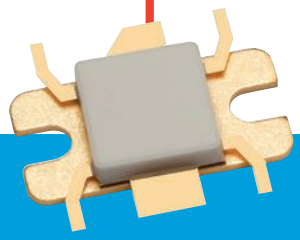

Amplifiers | Antennas | Attenuators | Beamformers | Cable Assemblies | Couplers
Combiners & Splitters | Diodes | Filters | Interconnect | Mixers | MMICs & RFICs
Resistors & Terminations | Switches | Test & Measurement | Transistors | Oscillators & Timing

Ask the Experts
www.RFMW.com

Sales@RFMW.com | Toll Free: +1-877-367-7369
188 Martinvale Lane, San Jose, CA 95119 U.S.A.

Microwave Journal ONLINE .COM

E LEARNING CENTER

Recent Advances in Broadband RF Amplifiers: Beyond Distributed Amps
Sponsored by: Marki Microwave 12/10

Catch *Frequency Matters*, the industry update from *Microwave Journal*,
microwavejournal.com/FrequencyMatters

Sponsored By RFMW

WHITE PAPERS

ERZIA

Characterizing Wide-Band Converters for EW

soitec

Engineered Substrates for Intelligent IoT Connectivity

Look for additional content from:

Signal Hound

Executive Interviews

Scott Sentz, Vice President of Sales and Marketing at **Q-Tech**, discusses his background and role at the company, Q-Tech's acquisition of Axtal, the combined company's product offerings and strengths and the vision for the future of Q-Tech.

Steve McGeary, President of **San-tron**, discusses some of the challenges and benefits of working for a family-owned business that has been around for 65 years. Steve will also talk about his background and role at the company, San-tron's product portfolio and what has them excited about the future.

Join Us Online

Follow us
@Pathindle
@MWJEric
@MWJEditor

Join us at the RF and Microwave Community

Become a fan at facebook.com/microwavejournal

Visit us @ mwjournal.com

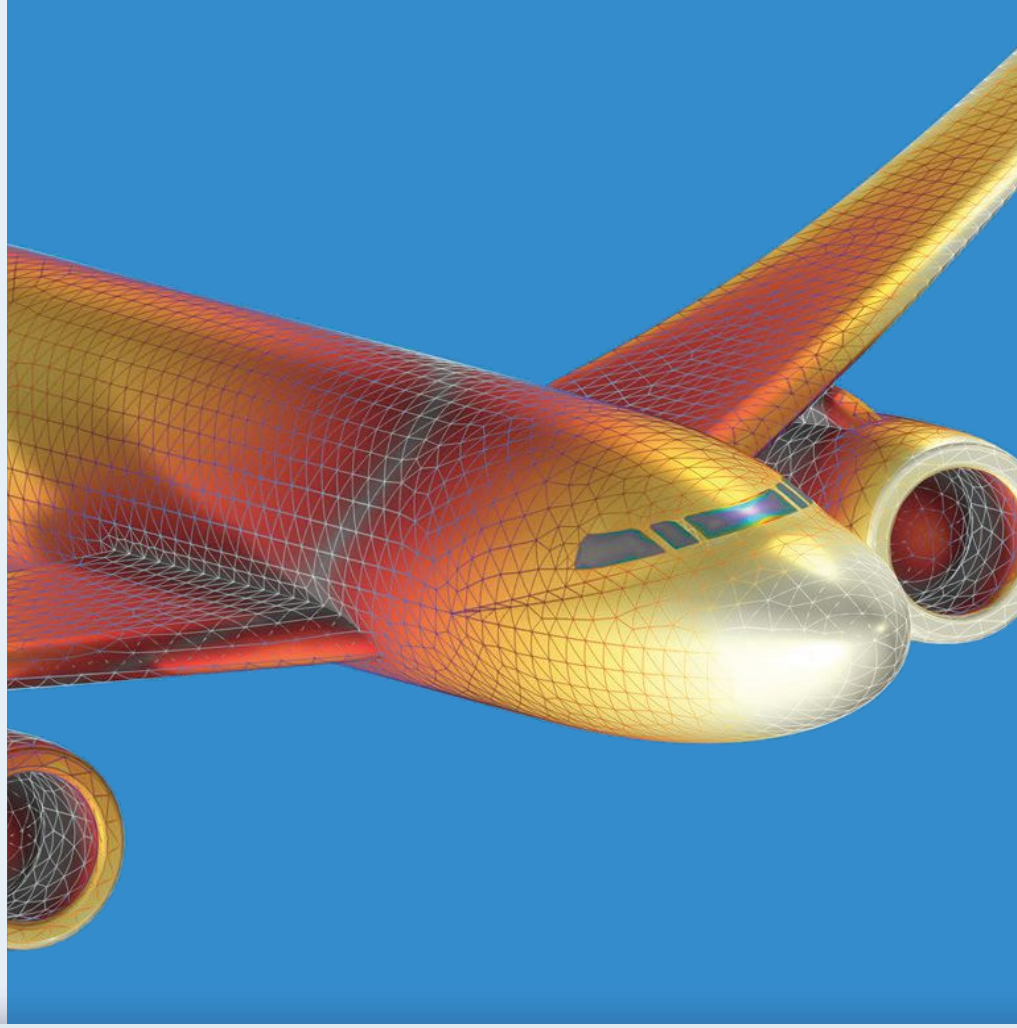

Take the Lead in Aerospace & Defense Design

with COMSOL Multiphysics®

Multiphysics simulation software feeds the innovation of A&D products that deliver on safety and performance. By building models that accurately represent the real world, engineers are able to develop, test, and verify their designs faster.

» *comsol.com/feature/aerospace-defense*

COMSOL

DC TO 50 GHz

MMIC Amplifiers

300+ Models Designed in House

Options for Every Requirement

CATV (75Ω)

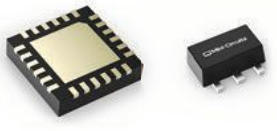

Supporting DOCSIS® 3.1 and 4.0 requirements

Dual Matched

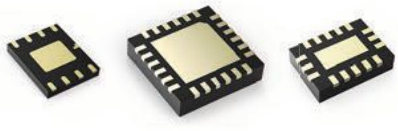

Save space in balanced and push-pull configurations

Hi-Rel

Rugged ceramic package meets MIL requirements for harsh operating conditions

High Linearity

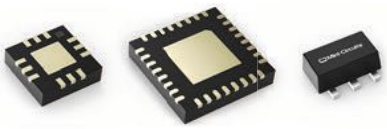

High dynamic range over wide bandwidths up to 45 GHz

Low Noise

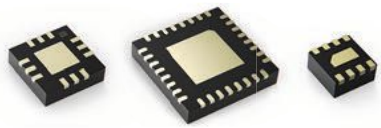

NF as low as 0.38 dB for sensitive receiver applications

Low Additive Phase Noise

As low as -173 dBc/Hz @ 10 kHz offset

RF Transistors

<1 dB NF with footprints as small as 1.18 x 1.42mm

Variable Gain

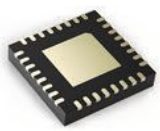

Up to 31.5 dB digital gain control

Wideband Gain Blocks

Flat gain for broadband and multi-band use

Mini-Circuits®

MARK YOUR CALENDAR

STAY CONNECTED TO COMING EVENTS

DECEMBER

16-18
IEEE WiSEE
Daytona Beach, Fla.
https://attend.ieee.org/wisee-2024/

JANUARY 2025

7-10
CES 2025
Las Vegas, Nev.
www.ces.tech

19-22
104th ARFTG
San Juan, Puerto Rico
https://arftg.org/104-conference/

28-30
DesignCon 2025
Santa Clara, Calif.
www.designcon.com

MARCH

1-8
IEEE Aerospace Conference
Big Sky, Mont.
www.aeroconf.org

3-6
MWC
Barcelona, Spain
www.mwcbarcelona.com

10-13
Satellite 2025
Washington, DC
www.satshow.com

15-20
IPC APEX EXPO 2025
Anaheim, Calif.
www.ipcapexexpo.org

25-27
EMV
Stuttgart, Germany
https://emv.mesago.com/events/en.html

30-4/5
EuCAP 2025
Stockholm, Sweden
www.eucap2025.org

APRIL

8-9
IEEE Texas Symposium
Waco, Texas
https://texassymposium.org

Register online at signalintegrityjournal.com

ONLINE PANEL SERIES

3/14
Using AI in the Design of Electronic Systems

Call for Papers Deadlines

1/13 IEEE EMC+ SIPI 2025

2/7 WAMICON

FOR DETAILS VISIT MWJOURNAL.COM/EVENTS

Countering the Evolving UAS Threat

Graeme Forsyth
SPX Communication Technologies, formed by TCI (Fremont, USA) and Enterprise Control Systems (Wappenham, UK)

In recent years, global conflict and geopolitical and social unrest have fueled an unprecedented deployment of uncrewed aerial systems (UAS). These events include the war in Ukraine along with the war in the Middle East and tensions in other global hotspots. In parallel, electronic warfare (EW) has continued to evolve, leading to more frequent and increasingly sophisticated threats. More than ever, nations have heightened their security and are investing in the right solutions to counter these new threats. Governments and defense teams worldwide require flexible, adaptable counter-UAS (C-UAS) systems that can be easily deployed and match their unique requirements.

However, the complexity and speed at which modern conflict develops means it is practically impossible for a single provider to own all the necessary technologies and provide a best-in-class solution suitable for all forms of threats today and in the future. This, paired with a crowded UAS space, means decisions may be hard for end-users to make and costly when not adequately matched to the threat they face. The ability to counter threats and provide communication security is considered among the highest global priorities and is where RF plays a vital role. But what can governments and defense teams do to future-proof their nations from UAS threats? What should be front of mind when choosing and upgrading C-UAS capabilities?

COMINT FOR C-UAS

It is critical to understand how tactical communications intelligence (COMINT) enables teams to survey and map the electromagnetic spectrum and provide key data and information supporting missions and C-UAS operations. Today, COMINT RF receivers are not only capable of delivering superior threat analysis at a time of heightened EW activity but are also being deployed by teams as the first line of C-UAS. From a defense perspective, COMINT has never been used on the massive scale that is now being deployed on worldwide battlefields.

This presents unique challenges as teams seek to adapt to an increasingly congested RF environment. Some of the threats facing COMINT and C-UAS are the fragility of library-based systems and the speed of evolution and operating frequency values. For instance, library systems can be susceptible to frequent pattern alterations by malicious actors, resulting in compromised systems.

The passive nature of COMINT also allows successful forward positioning and the ability to perform two important roles remotely with one piece of equipment. For example, the SPX Communication Technologies BLACKTALON C-UAS system can effectively jam a combination of GNSS, command, control and telemetry signals used by both commercial and military UAS. This ensures a decisive advantage in countering threats while safeguarding friendly RF signals from unintended inhibition. BLACKTALON is an open architecture solution that can be configured for a user interface, passive RF detectors, active radars, electro-optical sensors and a multi-band RF inhibitor that relies on SDR. The solution enables an ecosystem, allowing users to integrate legacy or preferred sensors and incorporate their command-and-control system of choice. The system operates over a frequency range of 20 MHz to 8 GHz with a detection range of more than 20 kilometers. High gain, directional antennas transmit the inhibition waveforms, ensuring that the antennas affect the target. These antennas have a nominal 20-degree beamwidth, ultimately providing

Find the Right Part Faster

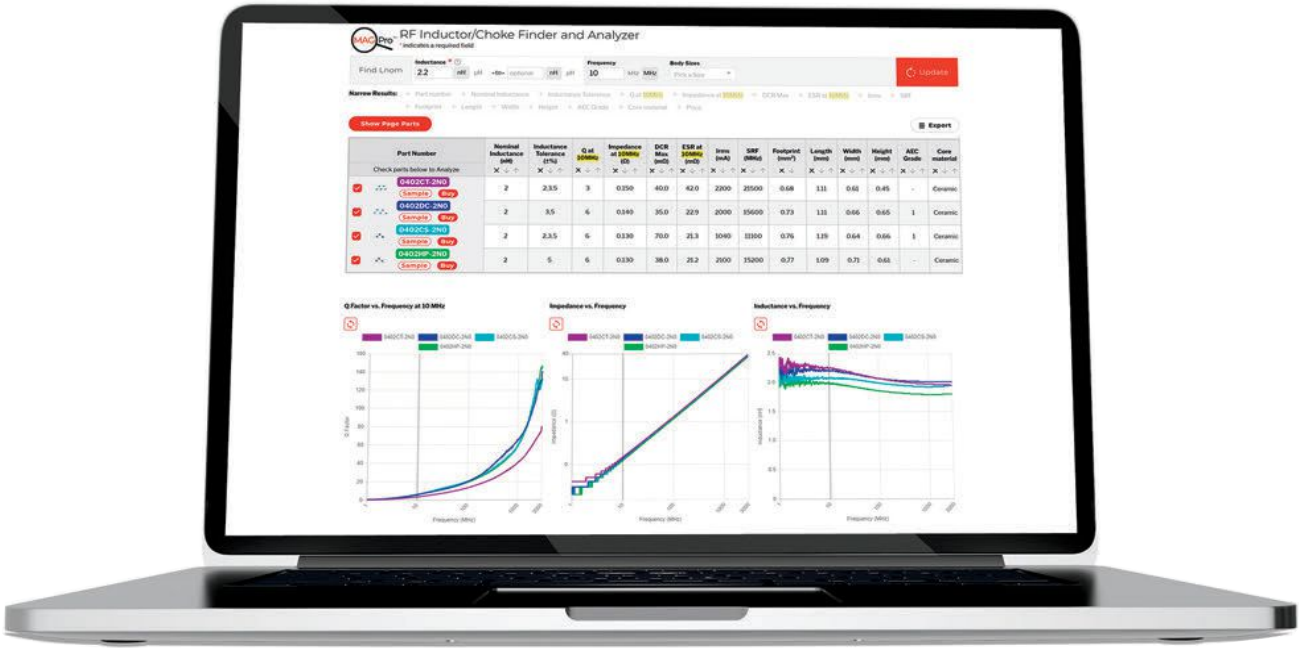

Designed by Engineers for Engineers, our MAGPro™ RF Inductor and Choke Finder helps you find the optimal parts for your desired L@frequency or Z@frequency quickly, reducing your design cycle time.

Coilcraft's MAGPro suite of online inductor analysis tools are designed to enable inductor selection and circuit optimization based on sound engineering principles and measured data.

The RF Inductor/Choke Finder and Analyzer offers two search options. The L @ Frequency option identifies inductors suitable for your L, Q, and current requirements and displays a full range of performance graphs including L, Q and ESR at frequency.

For RF choke applications, the Z @ Frequency tool searches thousands of part numbers for your desired impedance and lets you select the desired choke based on size, performance, or a combination of the two.

Reduce your design cycle time with confidence at **www.coilcraft.com/tools.**

Coilcraft®

WWW.COILCRAFT.COM

Fig. 1 **Example of the BLACKTALON Ecosystem with integrated sensors.**

the power density required at the target UAS while mitigating collateral impact upon other systems. An example of the BLACKTALON Ecosystem containing the BLACKTALON system along with a Weibel radar, OpenWorks camera and Claw jammer is shown in ***Figure 1***.

DEVELOPMENTS IN C-UAS TECHNOLOGY

A steady evolution of UAS has led to deploying directional and omnidirectional RF inhibitor systems. While every scenario requires a tailored approach, both jamming configurations have proven effective for governments and defense teams in Europe, the Middle East and Africa.

Designed for defense, security and critical national infrastructure operational environments, directional RF inhibitors, like the Claw system by Enterprise Control Systems (ECS), which is part of SPX Communication Technologies, are tailored to focus specifically on the UAS threat and the command-and-control video links these systems use. By utilizing software-defined radios, which leverage software instead of hardware components to generate signals, teams can improve

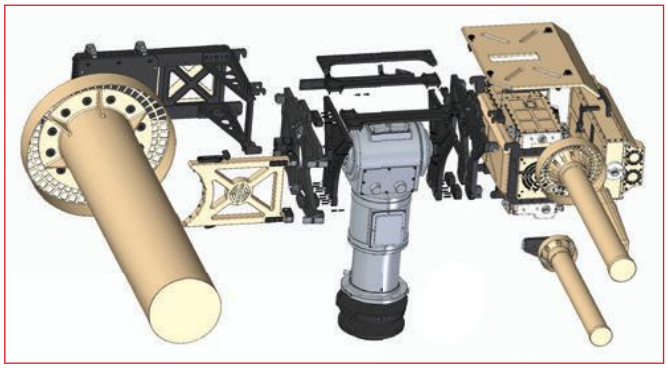

Fig. 2 **Claw RF jammer exploded view on a positioner.**

control of their source images and tailor the output across a particular band, creating additional flexibility in the process.

The Claw system combines RF power electronics with a high gain quintuple-band antenna system designed to be mounted on suitable pan-and-tilt platforms. The inhibitor comprises two RF units covering the GNSS, 433 MHz, 915 MHz, 2.4 GHz and 5.8 GHz ISM and Wi-Fi frequency bands with RF output powers to the antennas of up to 40 W. The antennas have a nominal gain of 15 to 17 dBiC, producing an EIRP of over 300 W each for the 433 MHz and 915 MHz bands, over 1250 W for the 2.4 GHz band and 500 W for the 5.8 GHz band. ***Figure 2*** shows an exploded view rendering of the ECS Claw RF jammer mounted on a positioner in a side-mount configuration.

On the other hand, omnidirectional RF inhibitors have become widely deployed for close self-protection applications. These application cases range from individual team members to vehicles. While unable to reach the ranges of a directional jammer, omnidirectional systems have been successfully deployed as the last line of defense with ranges of up to 400 m. It should also be noted that this last line of defense will continue to play a key role in protecting teams world-

MILLER MMIC

AI Powered RFIC Design Platform

RapidRF

Revolutionizing RFIC Design with AI-Driven Innovation.
Our AI driven design platform is redefining the future of the RFIC design industry. We automate the design of RFICs for the next generation of wireless communication, accelerating innovation for a smarter future.

AI-Driven Design Automation – Multiplying Engineers Productivity

- Technology Independent: GaAs, GaN, and Silicon proven
- Fast and reliable: more than 100x faster than an experienced design engineer
- AI-Driven Layout Optimization: cutting down costs, maximizing performance

Reference Design Done by Experienced Engineer

≈10 Days/Design

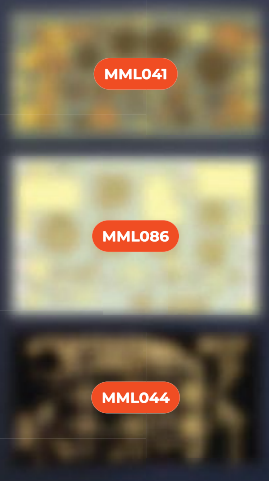

AI MMIC Design Process

1. Set Design Target
2. Schematic & Layout Generation & Optimization
3. GDS Generation
4. Learning

Design Done by RapidRF AI Platform

≈5 Hours/Design

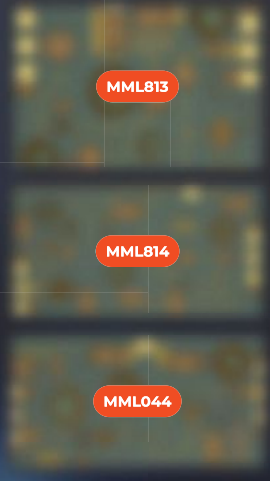

Performance Comparisons: RapidRF AI vs Human Engineer Designs

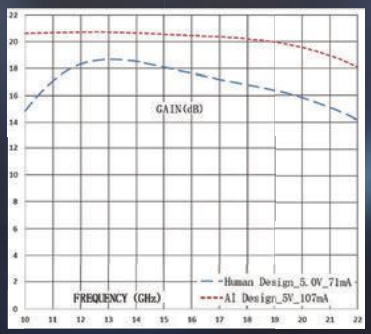

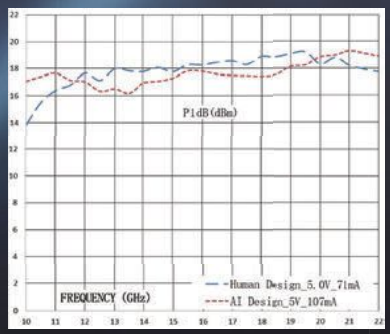

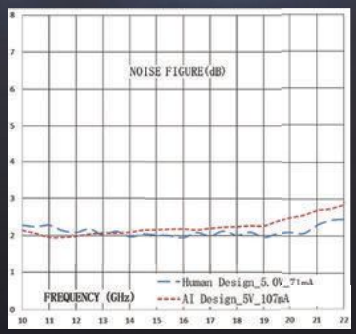

wide as warfighters face increasing threat levels.

Furthermore, reactive inhibiting is an additional and more bespoke approach, allowing end-users to act only when a signal is detected. Ultimately, reactive jamming will enable teams to assess the core frequencies used to control a threat and deploy a proportionately targeted response in near real-time. While this may seem ideal, it can also create significant compromises around filter constraints, power amplifiers and other signal conditioning elements. Solutions like the Claw RF inhibitor help keep pace with change and enable added flexibility.

It is also important to note a global resurgence in high frequency (HF) band (3 to 30 MHz) communications as a replacement for modern-day satellite communications (satcom). The challenge with satcom is that it can fall short in today's uneasy environment since hostile forces can easily disrupt or interfere with the signals. First deployed in the 1930s, HF was a popular choice for safe, omnidirectional communication like shore-to-shore and ship-to-shore over distances of around 500 to 5000 km. In turn, this has created an urgent need to be able to intercept HF communication to counter any nefarious activity being enabled by its use. In addition to directional and omnidirectional inhibitors, HF direction finding (HF/DF) is increasingly used as a critical tool to provide the intercept and source transmission location when HF frequencies are used as an alternative to beyond-line-of-sight satcom.

THE ROLE OF DATA

Software is proving to be a key element in C-UAS efforts, working in conjunction with these RF-inhibiting systems and antennas. To help coordinate and standardize missions, teams must work closely with the broader EW and defense intelligence communities to ensure that COMINT teams have real-time and remote data access. For instance, the SPX Communication Technologies Blackbird software detects, identifies, direction-finds and tracks signals of interest to enable support, find, fix and strike operations and mitigate EW threats. Integrated into an SPX Communication Technologies COMINT RF receiver, it also helps track the RF emission of UAS and their controllers or data links to support counter-responses. Blackbird can record the signal environment for look-back analysis without interrupting the mission. It simplifies the collection task, triggers automated actions and supports unattended operations. An example of the screen display and environment for the Blackbird software tracking four emitters in an industrial setting in Fremont, Calif., is shown in ***Figure 3***.

Understanding and managing the electromagnetic spectrum is critical to all operations. SPX Communication Technologies has enhanced Blackbird to enable greater coordination and command-and-control functions. While many are discussing the creation of NATO's Recognized Electromagnetic Picture (REMP) concept as a desirable option, it is largely already available and utilized to good ef-

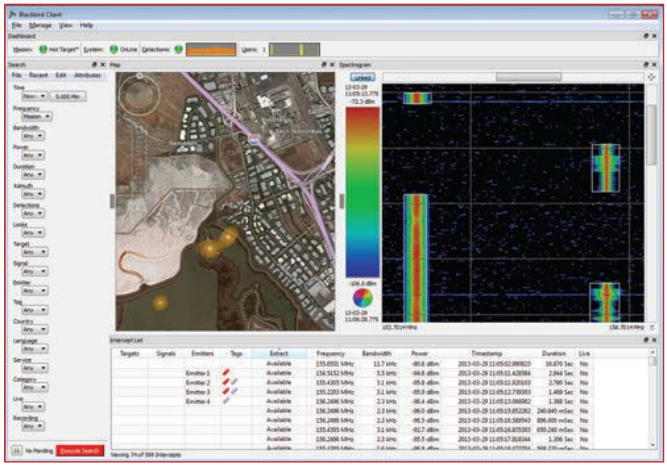

Fig. 3 **Blackbird COMINT software display.**

ERAVANT
FORMERLY SAGE MILLIMETER

MAKING MMW ACCESSIBLE

INTRODUCING OUR **FOUR BUSINESS UNITS**

1

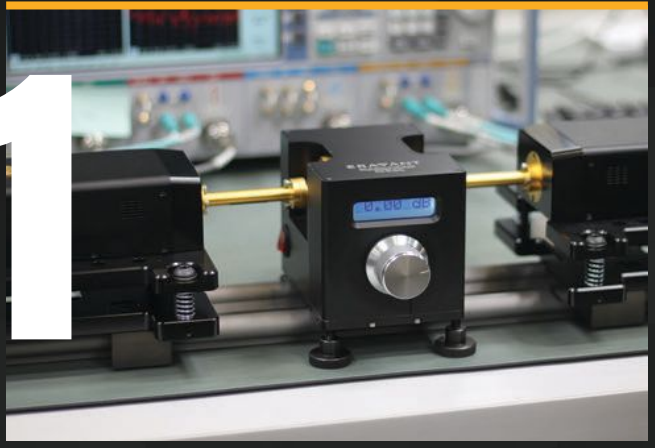

Test & Measurement Equipment

2

Calibration & Measurement Services

3

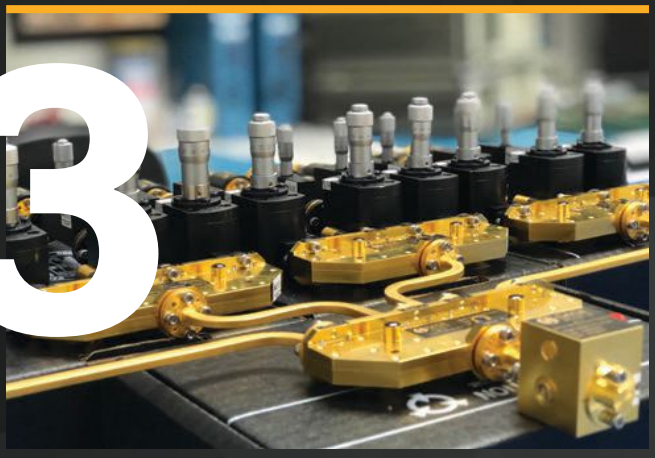

Custom System Applications

4

Millimeter Wave & Sub-THz COTS

Scan the code to explore our
60,000 sq. ft. facility in Torrance, CA

RoHS COMPLIANT · MADE IN USA · ITAR INTERNATIONAL TRAFFIC IN ARMS REGULATIONS · Management System AS9100 D · DEKRA Certification · DEKRA certified · Accredited by ANAB

WWW.ERAVANT.COM
www.eravant.com 501 Amapola Avenue Torrance, CA 90501
T: 424-757-0168 F: 424-757-0188 support@eravant.com

Adapters • Amplifiers • Antenna Feeds • Antennas • Attenuators • Bias Tees • Cable Assemblies • Corner Reflectors • Couplers • DC Blocks • Detectors • Ferrite Devices • Filters • Frequency Converters • Frequency Multipliers • Limiters • Magic Tees • Mixers • Noise Sources • Oscillators • Phase Shifters • Power Dividers • Radar Sensors • Subassemblies • Switches • Termination Loads • Test Equipment • Test Hardware & Accessories • TX/RX Modules • Uni-Guide™ • Waveguide Sections

fect. By building better and more robust systems, we can help retrieve devices and their data that may otherwise be destroyed on the battlefield or in conflict. This allows teams to keep ahead of the curve and anticipate new threats.

COLLABORATING FOR A BETTER FUTURE

SPX Communication Technologies supports governments and defense teams in the most challenging of missions by providing them with directional and omnidirectional inhibiting, along with HF/DF capabilities. The ultimate goal of these activities is to deliver enhanced range, flexibility and accuracy for existing and new systems. These capabilities will enable agencies and companies to maintain a clear tactical advantage and a more targeted approach to ensure a brighter, more secure future for all. As tensions have grown, the interest in the HF frequency range has grown significantly and this will only increase going forward due to its secure transmission capabilities.

The last few years have seen changes resulting in many new challenges facing the industry and the ecosystem. An important part of the role of the supply chain ecosystem is to educate global defense and security teams on what solutions and capabilities best fit their needs, expertise and even geography. Collaboration among providers and end-users is necessary to ensure the best possible outcome. A key example of this approach is the BLACKTALON C-UAS Ecosystem. Systems like these are already helping break down barriers of threat response and will continue evolving to support future C-UAS needs.

The BLACKTALON Ecosystem integrates SPX Communication Technologies' BLACKTALON C-UAS technology and decades of expertise in the space with a vendor-agnostic framework. This approach ensures that solutions can meet every customer's unique set of requirements. In addition to the system flexibility, defense and security teams can create solutions tailored to their specific concepts of operations, threats, user groups, existing capabilities and budgets.

The core BLACKTALON solution includes carefully selected active radars, EOIR, passive RFDF, RF jammers and mast configurations. In addition to this standard configuration, a new, open architecture approach to the BLACKTALON Ecosystem allows any of these elements to be customized or replaced. This flexibility provides customers access to the latest systems and hardware capabilities without unnecessary barriers and in a suitable time frame.

For instance, customers can choose autonomous optical tracking from OpenWorks Engineering, cutting-edge 3D radar from U.S. provider Echodyne, RF subsystems from SPX and mount them on a range of dispersed or centrally located mobile or transportable masts to provide a single scalable BLACKTALON C-UAS capability. An example of a BLACKTALON system configured with these suppliers is

KRATOS®
MICROWAVE USA

High-Performance SSPAs with demonstrated reliability

Kratos Microwave USA, formerly CTT, has over 40 years of experience in the design and manufacture of microwave amplifiers, frequency converters and integrated assemblies delivering high-performance solutions for advanced defense platforms.

Since our inception, we have delivered thousands of microwave products for various military applications. Our San Jose, California manufacturing facility supports a mix of both low-volume and high-volume builds based on program specific needs. Design and construction utilize both SMT and hybrid chip and wire manufacturing techniques as necessary for specific products and applications.

Additionally, we offer rapid prototype development, highest packaging density, and a flexible engagement model including build-to-print capabilities.

Kratos has an extensive portfolio of power amplifiers covering 1 to 50 GHz with power levels ranging from 50W CW to 2kW pulsed for aerospace, defense, and instrumentation customers. Our capabilities extend into Integrated Microwave Assemblies supporting various Radar, EW, and Communications applications meeting unique mission specific electrical and environmental requirements.

Kratos amplifier products utilize GaAs and GaN technologies selected to meet SWAP-C challenges. Kratos engineering is constantly evaluating new semiconductor devices to develop market-leading high-density and high-efficiency SSPAs. Amplifiers can be supplied as individual modules, as part of integrated assemblies, or in rack-mount configurations. Options include integrated power supply, heat sink and microcontroller for control and display.

Kratos GaN SSPAs are designed for

- ❑ Small Form Factor
- ❑ Decoys & Expendables
- ❑ SAR, TCDL, UAVs
- ❑ AESA Radar Systems
- ❑ EW: ECM, ECCM & ESM

Contact Kratos Microwave USA today for more information.

Narrowband Capability		Broadband Capability	
Band	Output Power	Freq. (GHz)	Output Power
L & S	2000W (Pulse)	1-2, 2-4, 2-6	200W (CW
C & X	1000W (Pulse)	4-8, 6-12	150W (CW)
Ku	100W (CW)	6-18	80W (CW)
Ka	50W (CW)	2-18	40W (CW)

AS9100D
ISO 9001:2015

New product development in 2024 includes frequency coverage of V- and W-Bands

❖ High Power Amplifiers ❖ Integrated Microwave Assemblies ❖ Frequency Converters ❖

www.kratosdefense.com
Kratos Microwave USA • 5870 Hellyer Avenue • San Jose • California 95138
Phone: 408-541-0596 • E-mail: microwavesales@kratosdefense.com

Nxbeam™

Ka / V / E - Band GaN MMIC Power

Ka

- NPA2001-DE | 26.5-29.5 GHz | 35 W
- NPA2002-DE | 27.0-30.0 GHz | 35 W
- NPA2003-DE | 27.5-31.0 GHz | 35 W
- NPA2004-DE | 25.0-28.5 GHz | 35 W
- NPA2020-DE | 24.0-25.0 GHz | 8 W
- NPA2030-DE | 27.5-31.0 GHz | 20 W
- NPA2040-DE | 27.5-31.0 GHz | 10 W
- NPA2050-SM | 27.5-31.0 GHz | 8 W

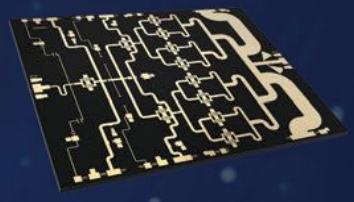

V

- NPA4000-DE | 47.0-52.0 GHz | 1.5 W
- NPA4010-DE | 47.0-52.0 GHz | 3.5 W

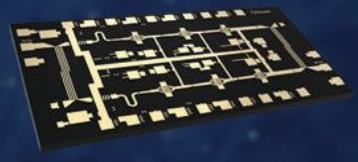

E

- NPA7000-DE | 65.0-76.0 GHz | 1 W

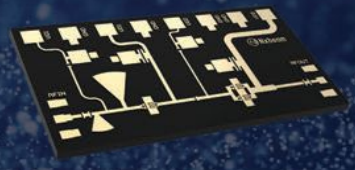

4388 Cerritos Avenue
Los Alamitos, CA 90720

www.nxbeam.com
info@nxbeam.com

Phone: 949-656-2883
info@nxbeam.com

© Copyright 2024 Nxbeam

shown in ***Figure 4***. ***Figure 5*** shows another implementation of the ecosystem that uses the BLACKTALON C-UAS solution alongside existing providers Chess Dynamics, a supplier of surveillance, fire control and large positioning systems and Blighter, the U.K.'s leading supplier of ground-based electronic scanning radar systems. This version of the system is mounted on a vehicle from Iveco Defence Vehicles.

LOOKING AHEAD

Since threats continue to evolve rapidly, the tools that provide teams with critical protection must keep pace before the potential threats materialize into reality. In the future, as UAS and other uncrewed attacks continue to evolve, the effectiveness of C-UAS solutions will depend mainly upon the ability to understand and foresee next-generation technology that is likely to be deployed and adapt solutions rapidly to counter these threats. C-UAS must ultimately form part of every country's overall strategic defense capability. To ensure defense and security organizations remain ahead of threats, the industry continues to review them and innovate to solve the challenges governments and defense teams often do not yet know they face.

The rate of change within this segment in the last 24 months has been unprecedented. Some concepts currently being dreamed up online suggest this pace will continue accelerating and permeating every aspect of our lives. Building relationships and collaborating with trusted partners will be essential to deliver the best and most appropriate technologies. Solutions manufacturers must focus on innovation and progress as their primary goals. Providers like SPX Communication Technologies will continue to do so by delivering the right capabilities, supported by proven technology, in collaboration with customers and the industry. ■

Fig. 4 **C-UAS system with BLACKTALON and integrated sensors.**

Fig. 5 **C-UAS system with BLACKTALON and different integrated sensors.**

saetta labs
saettalabs.com
Boulder, Colorado USA

- Thermally Stabilized
- Ext Ref Input (PLL)
- Status Display
- Lock Detect

Sapphire Loaded Cavity Oscillators
X-Band

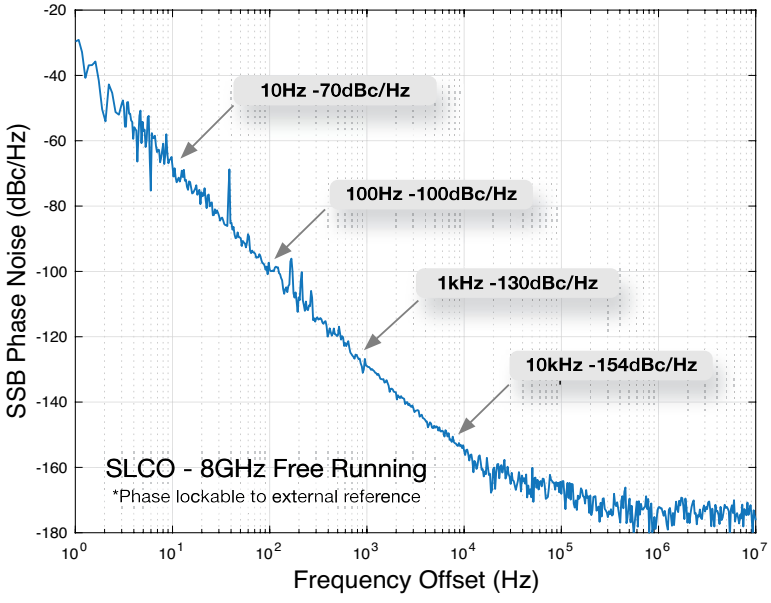

RF-LAMBDA

MADE IN USA

THE LEADER OF RF BROADBAND SOLUTIONS

EMC Broadband RF Power Amplifier

High Power Solid State

HUNDREDS IN STOCK

FAST SHIPPING

FREQUENCY UP TO 90GHZ

POWER UP TO 2KW CW

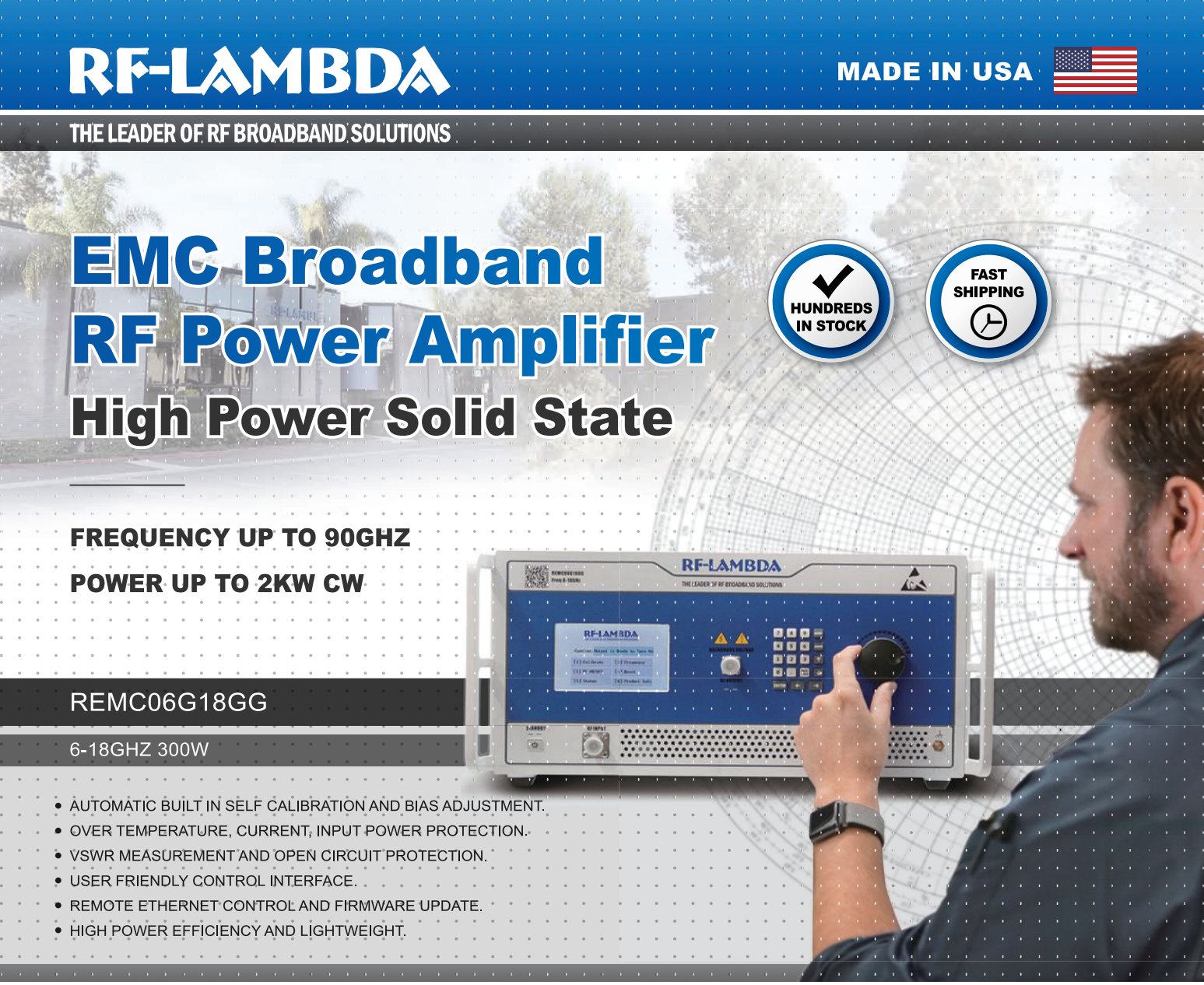

REMC06G18GG

6-18GHZ 300W

- AUTOMATIC BUILT IN SELF CALIBRATION AND BIAS ADJUSTMENT.
- OVER TEMPERATURE, CURRENT, INPUT POWER PROTECTION.
- VSWR MEASUREMENT AND OPEN CIRCUIT PROTECTION.
- USER FRIENDLY CONTROL INTERFACE.
- REMOTE ETHERNET CONTROL AND FIRMWARE UPDATE.
- HIGH POWER EFFICIENCY AND LIGHTWEIGHT.

RAMP42G47GA 42-47GHZ 8W

RAMP18G40GB-U 18-40G 20W

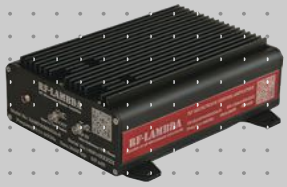

RAMP05M80GC 0.5-80GHZ

REMC02G06GE 2-6GHZ 500W

REMC08G11GE 8-11GHZ 400W

RF Amplifiers and Sub-Assemblies for Every Application

Delivery from Stock to 2 Weeks ARO from the catalog or built to your specifications!

- Competitive Pricing & Fast Delivery
- Military Reliability & Qualification
- Various Options: Temperature Compensation, Input Limiter Protection, Detectors/TTL & More
- Unconditionally Stable (100% tested)

ISO 9001:2000 and AS9100B CERTIFIED

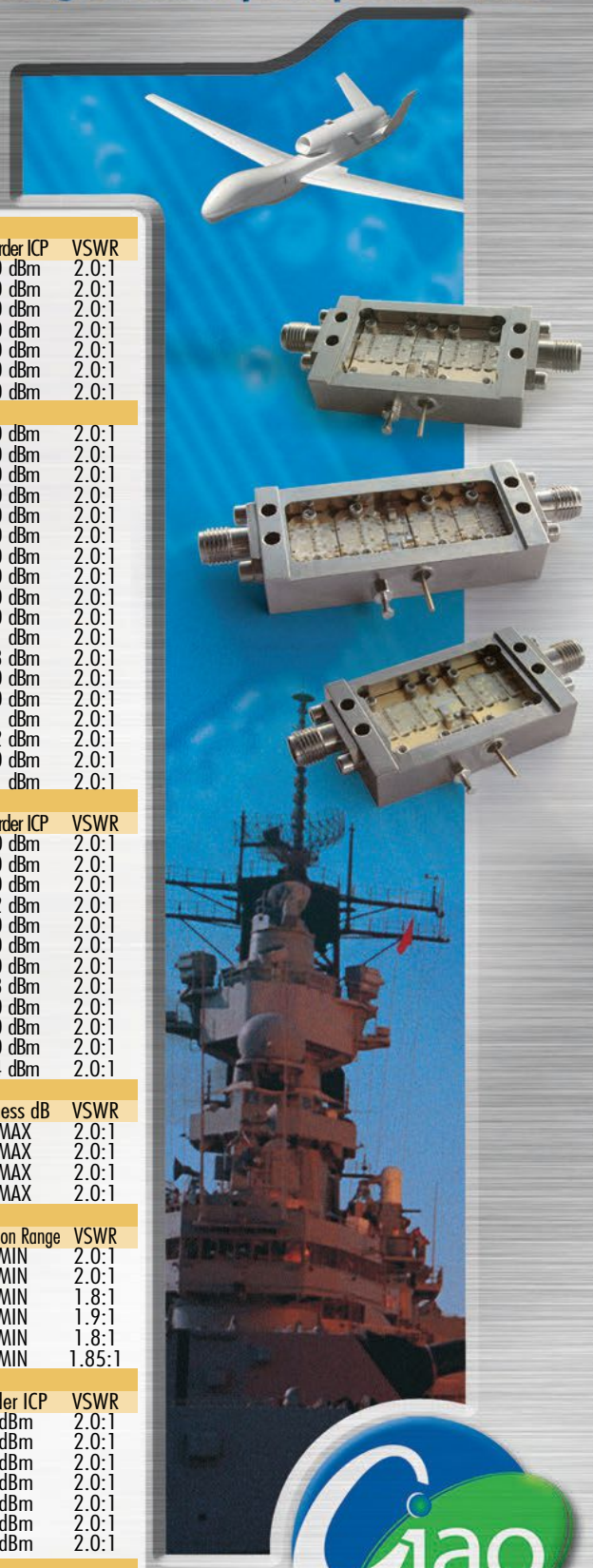

OCTAVE BAND LOW NOISE AMPLIFIERS

Model No.	Freq (GHz)	Gain (dB) MIN	Noise Figure (dB)	Power-out @ P1-dB	3rd Order ICP	VSWR
CA01-2110	0.5-1.0	28	1.0 MAX, 0.7 TYP	+10 MIN	+20 dBm	2.0:1
CA12-2110	1.0-2.0	30	1.0 MAX, 0.7 TYP	+10 MIN	+20 dBm	2.0:1
CA24-2111	2.0-4.0	29	1.1 MAX, 0.95 TYP	+10 MIN	+20 dBm	2.0:1
CA48-2111	4.0-8.0	29	1.3 MAX, 1.0 TYP	+10 MIN	+20 dBm	2.0:1
CA812-3111	8.0-12.0	27	1.6 MAX, 1.4 TYP	+10 MIN	+20 dBm	2.0:1
CA1218-4111	12.0-18.0	25	1.9 MAX, 1.7 TYP	+10 MIN	+20 dBm	2.0:1
CA1826-2110	18.0-26.5	32	3.0 MAX, 2.5 TYP	+10 MIN	+20 dBm	2.0:1

NARROW BAND LOW NOISE AND MEDIUM POWER AMPLIFIERS

Model No.	Freq (GHz)	Gain (dB) MIN	Noise Figure (dB)	Power-out @ P1-dB	3rd Order ICP	VSWR
CA01-2111	0.4 - 0.5	28	0.6 MAX, 0.4 TYP	+10 MIN	+20 dBm	2.0:1
CA01-2113	0.8 - 1.0	28	0.6 MAX, 0.4 TYP	+10 MIN	+20 dBm	2.0:1
CA12-3117	1.2 - 1.6	25	0.6 MAX, 0.4 TYP	+10 MIN	+20 dBm	2.0:1
CA23-3111	2.2 - 2.4	30	0.6 MAX, 0.45 TYP	+10 MIN	+20 dBm	2.0:1
CA23-3116	2.7 - 2.9	29	0.7 MAX, 0.5 TYP	+10 MIN	+20 dBm	2.0:1
CA34-2110	3.7 - 4.2	28	1.0 MAX, 0.5 TYP	+10 MIN	+20 dBm	2.0:1
CA56-3110	5.4 - 5.9	40	1.0 MAX, 0.5 TYP	+10 MIN	+20 dBm	2.0:1
CA78-4110	7.25 - 7.75	32	1.2 MAX, 1.0 TYP	+10 MIN	+20 dBm	2.0:1
CA910-3110	9.0 - 10.6	25	1.4 MAX, 1.2 TYP	+10 MIN	+20 dBm	2.0:1
CA1315-3110	13.75 - 15.4	25	1.6 MAX, 1.4 TYP	+10 MIN	+20 dBm	2.0:1
CA12-3114	1.35 - 1.85	30	4.0 MAX, 3.0 TYP	+33 MIN	+41 dBm	2.0:1
CA34-6116	3.1 - 3.5	40	4.5 MAX, 3.5 TYP	+35 MIN	+43 dBm	2.0:1
CA56-5114	5.9 - 6.4	30	5.0 MAX, 4.0 TYP	+30 MIN	+40 dBm	2.0:1
CA812-6115	8.0 - 12.0	30	4.5 MAX, 3.5 TYP	+30 MIN	+40 dBm	2.0:1
CA812-6116	8.0 - 12.0	30	5.0 MAX, 4.0 TYP	+33 MIN	+41 dBm	2.0:1
CA1213-7110	12.2 - 13.25	28	6.0 MAX, 5.5 TYP	+33 MIN	+42 dBm	2.0:1
CA1415-7110	14.0 - 15.0	30	5.0 MAX, 4.0 TYP	+30 MIN	+40 dBm	2.0:1
CA1722-4110	17.0 - 22.0	25	3.5 MAX, 2.8 TYP	+21 MIN	+31 dBm	2.0:1

ULTRA-BROADBAND & MULTI-OCTAVE BAND AMPLIFIERS

Model No.	Freq (GHz)	Gain (dB) MIN	Noise Figure (dB)	Power-out @ P1-dB	3rd Order ICP	VSWR
CA0102-3111	0.1-2.0	28	1.6 Max, 1.2 TYP	+10 MIN	+20 dBm	2.0:1
CA0106-3111	0.1-6.0	28	1.9 Max, 1.5 TYP	+10 MIN	+20 dBm	2.0:1
CA0108-3110	0.1-8.0	26	2.2 Max, 1.8 TYP	+10 MIN	+20 dBm	2.0:1
CA0108-4112	0.1-8.0	32	3.0 MAX, 1.8 TYP	+22 MIN	+32 dBm	2.0:1
CA02-3112	0.5-2.0	36	4.5 MAX, 2.5 TYP	+30 MIN	+40 dBm	2.0:1
CA26-3110	2.0-6.0	26	2.0 MAX, 1.5 TYP	+10 MIN	+20 dBm	2.0:1
CA26-4114	2.0-6.0	22	5.0 MAX, 3.5 TYP	+30 MIN	+40 dBm	2.0:1
CA618-4112	6.0-18.0	25	5.0 MAX, 3.5 TYP	+23 MIN	+33 dBm	2.0:1
CA618-6114	6.0-18.0	35	5.0 MAX, 3.5 TYP	+30 MIN	+40 dBm	2.0:1
CA218-4116	2.0-18.0	30	3.5 MAX, 2.8 TYP	+10 MIN	+20 dBm	2.0:1
CA218-4110	2.0-18.0	30	5.0 MAX, 3.5 TYP	+20 MIN	+30 dBm	2.0:1
CA218-4112	2.0-18.0	29	5.0 MAX, 3.5 TYP	+24 MIN	+34 dBm	2.0:1

LIMITING AMPLIFIERS

Model No.	Freq (GHz)	Input Dynamic Range	Output Power Range Psat	Power Flatness dB	VSWR
CLA24-4001	2.0 - 4.0	-28 to +10 dBm	+7 to +11 dBm	+/- 1.5 MAX	2.0:1
CLA26-8001	2.0 - 6.0	-50 to +20 dBm	+14 to +18 dBm	+/- 1.5 MAX	2.0:1
CLA712-5001	7.0 - 12.4	-21 to +10 dBm	+14 to +19 dBm	+/- 1.5 MAX	2.0:1
CLA618-1201	6.0 - 18.0	-50 to +20 dBm	+14 to +19 dBm	+/- 1.5 MAX	2.0:1

AMPLIFIERS WITH INTEGRATED GAIN ATTENUATION

Model No.	Freq (GHz)	Gain (dB) MIN	Noise Figure (dB)	Power-out @ P1-dB	Gain Attenuation Range	VSWR
CA001-2511A	0.025-0.150	21	5.0 MAX, 3.5 TYP	+12 MIN	30 dB MIN	2.0:1
CA05-3110A	0.5-5.5	23	2.5 MAX, 1.5 TYP	+18 MIN	20 dB MIN	2.0:1
CA56-3110A	5.85-6.425	28	2.5 MAX, 1.5 TYP	+16 MIN	22 dB MIN	1.8:1
CA612-4110A	6.0-12.0	24	2.5 MAX, 1.5 TYP	+12 MIN	15 dB MIN	1.9:1
CA1315-4110A	13.75-15.4	25	2.2 MAX, 1.6 TYP	+16 MIN	20 dB MIN	1.8:1
CA1518-4110A	15.0-18.0	30	3.0 MAX, 2.0 TYP	+18 MIN	20 dB MIN	1.85:1

LOW FREQUENCY AMPLIFIERS

Model No.	Freq (GHz)	Gain (dB) MIN	Noise Figure dB	Power-out @ P1-dB	3rd Order ICP	VSWR
CA001-2110	0.01-0.10	18	4.0 MAX, 2.2 TYP	+10 MIN	+20 dBm	2.0:1
CA001-2211	0.04-0.15	24	3.5 MAX, 2.2 TYP	+13 MIN	+23 dBm	2.0:1
CA001-2215	0.04-0.15	23	4.0 MAX, 2.2 TYP	+23 MIN	+33 dBm	2.0:1
CA001-3113	0.01-1.0	28	4.0 MAX, 2.8 TYP	+17 MIN	+27 dBm	2.0:1
CA002-3114	0.01-2.0	27	4.0 MAX, 2.8 TYP	+20 MIN	+30 dBm	2.0:1
CA003-3116	0.01-3.0	18	4.0 MAX, 2.8 TYP	+25 MIN	+35 dBm	2.0:1
CA004-3112	0.01-4.0	32	4.0 MAX, 2.8 TYP	+15 MIN	+25 dBm	2.0:1

CIAO Wireless can easily modify any of its standard models to meet your "exact" requirements at the Catalog Pricing.

Visit our web site at www.ciaowireless.com for our complete product offering.

Ciao Wireless, Inc. 4000 Via Pescador, Camarillo, CA 93012

Tel (805) 389-3224 Fax (805) 389-3629 sales@ciaowireless.com

Cliff Drubin, Associate Technical Editor

Thales Demonstrates its Capacity to Deploy Drone Swarms with Unparalleled Levels of Autonomy Using AI

The operational value of drones on the battlefield is now firmly established, but their effectiveness is still limited by two factors: they usually require one operator per drone and a secure, resilient datalink must be available throughout the mission. Recent flight tests showcased the latest breakthroughs by Thales and its partners in their efforts to overcome these limitations and support drone swarm operations tailored to military requirements. In the tests, Thales's COHESION demonstrator showed how AI and intelligent agents can be used to achieve an unparalleled level of autonomous operation in drone swarm deployments.

The system architecture of the COHESION demonstrator enables operators to adapt the level of autonomy of their drone swarms to the operational requirements of each phase of the mission. This new possibility offers an unprecedented level of flexibility in contested environments, where electronic warfare measures can saturate communication systems and jam datalinks that rely on GNSS signals. Autonomous operation by single drones and/or entire swarms overcomes the need for a permanent datalink with the control station. The drones are capable of perceiving and analyzing their local environment, sharing target information, analyzing enemy intent and prioritizing missions. They can also use collaborative tactics and optimize their trajectories to increase resilience and boost force effectiveness, helping to accelerate the Observe, Orient, Decide and Act (OODA) loop and enhance battlefield transparency.

This innovative approach acts as a force multiplier without increasing the cognitive load on operators, who remain in charge of the most critical decisions. The use of trusted, cybersecure, human-in-the-loop AI guarantees safe human supervision at all times, in line with Thales's principles of TrUE AI.

Positioned as a systems provider and integrator, Thales has developed its Drone Warfare offering to accelerate interoperability between a wide range of land, airland, air and naval platforms. The group is also a key player in an ecosystem of French industries and tech companies working to expand the capabilities of frontline drones in the theater of operations.

Drone Swarm (Source: Thales)

Indra Showcases its Crow System's Ability to Thwart Complex Drone Swarm Attacks

During the Anti-Drone Interoperability Exercises (TIE24) organized by the NATO Communications and Information Agency (NCIA), Indra demonstrated the ability of its Crow anti-drone system to interoperate with all kinds of systems and adapt to each mission and type of attack, including those in which swarms of drones modified to resist countermeasures are used.

Given the wide range of settings and different types of drones in existence, the most advanced armies are searching for anti-drone systems that can adapt to each specific mission and scenario in a flexible manner. With this premise in mind, Crow's command-and-control system demonstrated its ability to integrate with 27 sensors and effectors made by different manufacturers in Europe during these exercises, the most important ones organized by NATO held in September in the Netherlands.

The system used the new NATO interoperability standard (C-UAS AEDP-4869), previously known as SAPIENT, which can integrate all kinds of technologies almost as simply as a plug-and-play device.

Indra took part in it during "blind" exercises, known as the Performance Challenge, with which NATO sought to validate the new interoperability standard that should ensure that the technologies of the allied countries can be combined to constantly guarantee the most advanced anti-drone solution.

Juan López Campos, Indra's head of the solution, explained, "Crow's command and control system provides each army with complete freedom to configure the system to best meet its needs. The solution is capable of operating in combination with the command and control systems of other allied countries, while it can also be integrated into the future combat cloud."

Another important benefit of Indra's system is its high degree of usability. In fact, Crow was used by military operators who had no previous training in operating it without any problems arising.

During the exercises, Indra also tried out its new RF sensor as part of the specific tests carried out by the study group of the Unmanned Aerial Systems Detection and Classification by Radio Frequency (NATO SET-204) project. This system also used the new NATO interoperability standard to integrate with other command-and-control systems.

Crow (Source: Indra)

For More Information Visit mwjournal.com for more defense news.

This is the latest sensor to be added to Indra's existing range of systems, which include state-of-the-art radars, electro-optical systems, RF systems and jammers.

The Spanish Air Force has used Indra's Crow system during real missions, including one carried out in Mali. Other state security forces and corps have employed it to protect the airspace at major international conventions and events.

The USMC Completes a Successful First Live-Fire Exercise with Iron Dome Interceptor

The U.S. Marine Corps (USMC) has successfully completed its first live-fire training exercise using an air defense system that integrates the Iron Dome interceptor.

The system is based on an American radar and command-and-control center, combined with the Iron Dome (Tamir) interceptor and a mobile launcher developed by Rafael, with Raytheon as the prime contractor.

During the exercise, the USMC operated the system fully, leading to successful target interceptions. Additionally, the continuous launch capability of Iron Dome interceptors from a mobile launcher developed for the USMC was evaluated.

Iron Dome Interceptor (Source: Rafael Advanced Defense Systems)

The exercise followed the completion of a full training program and a series of tests, part of a development and procurement plan led by the USMC to assess a new prototype system for medium range intercept capability.

The training exercise demonstrated both the proficiency of the forces in fully operating the system and the performance of the mobile launcher, as well as the capabilities of the Iron Dome interceptor in relevant and challenging interception scenarios.

The Tamir interceptor is capable of intercepting cruise missiles, unmanned aerial vehicles and various rockets, shells and mortars. Developed by Rafael, the interceptor was adapted for the USMC configuration in collaboration with Raytheon as the primary contractor. They also provided training support.

The Israel Missile Defense Organization leads the development of Israel's multi-layered defense array, which includes four operational defense layers: the Iron Dome, David's Sling and Arrow-2 and Arrow-3 systems.

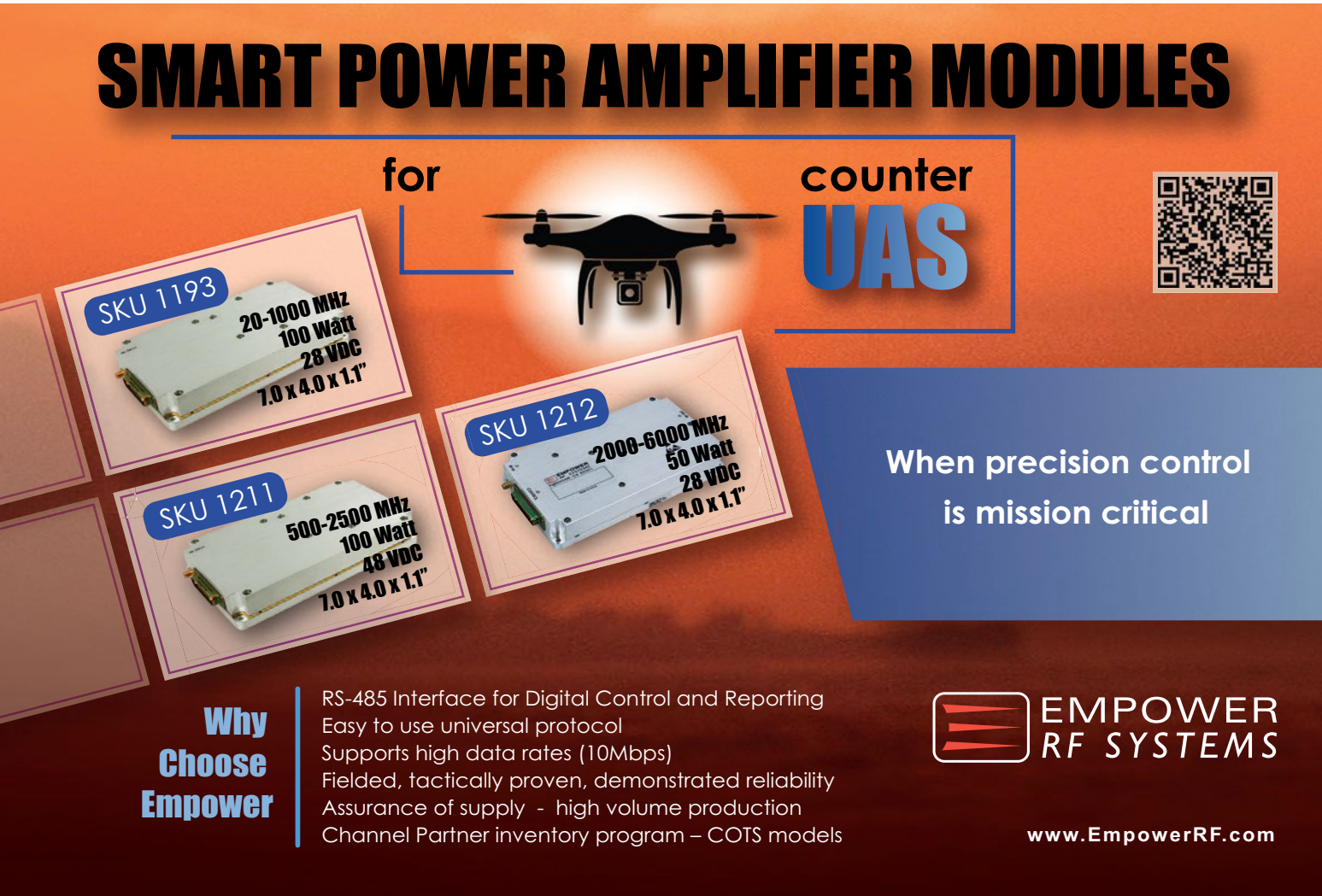

Reactel, Inc.

Reacting First to All Your Filter Needs.

Filter Solutions For Mission Critical Applications

High Performance, Rugged Packaging, Small Size and Weight

Great things *can* come in small packages. Reactel filters are ideally suited for the demanding environments that unmanned vehicles encounter.

Many manufacturers rely on Reactel to provide units which are:
High performance - Lightweight - Low profile

Contact a Reactel engineer with your filter or multiplexer requirements. We can create a unit which will be the perfect fit for your applications.

RF & Microwave Filters - Multiplexers - Multifunction Assemblies

8031 Cessna Avenue • Gaithersburg, Maryland 20879 • (301) 519-3660 • reactel@reactel.com • reactel.com

Intertek

RoHS Compliant 2002/95/EC

MADE IN MD
Since 1979

PROPRIETARY TECHNOLOGIES

LTCC Filter Innovations

The Industry's Widest Selection

Ultra-High Rejection

- Rejection floor down to 100+ dB
- Excellent selectivity
- Built-in shielding
- 1812 package style
- Patent pending

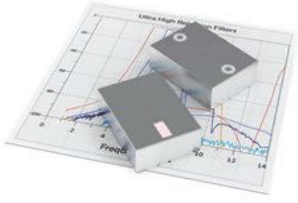

LEARN MORE

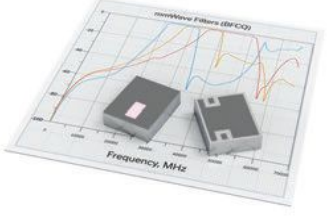

mmWave Passbands

- Passbands to 50+ GHz
- The industry's widest selection of LTCC filters optimized for 5G FR2 bands
- Growing selection of models for Ku- and Ka-band Satcom downlink
- 1812 & 1008 package styles

Substrate Integrated Waveguide

- First commercially available SIW LTCC filter in the industry
- Narrow bandwidth (~5%) and good selectivity
- Internally shielded to prevent detuning
- 1210 package style

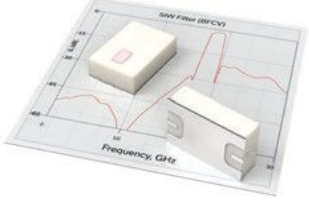

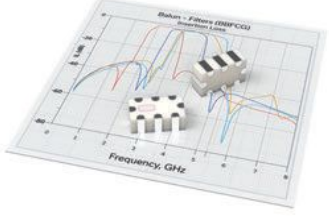

Integrated Balun-Bandpass Filters

- Combine balun transformer and bandpass filter in a single device
- Saves space and simplifies board layouts in ADCs, DACs and other circuits
- 1210, 1008 & 0805 package styles

Mini-Circuits

UCL Engineers Set New Record on How Fast Data Can Be Sent Wirelessly

A new world record in wireless transmission, promising faster and more reliable wireless communications, has been set by researchers from University College London (UCL). The team successfully sent data over the air at a speed of 938 Gbps over a record frequency range of 5 to 150 GHz. This speed is up to 9380x faster than the best average 5G download speed in the U.K., which is currently 100 Mb/s or over. The total bandwidth of 145 GHz is more than 5x higher than the previous wireless transmission world record.

Typically, wireless networks transmit information using radio waves over a narrow range of frequencies. Current wireless transmission methods, such as Wi-Fi and 5G mobile, predominantly operate at low frequencies below 6 GHz. But congestion in this frequency range has limited the speed of wireless communications. Researchers from UCL Electronic & Electrical Engineering overcame this bottleneck by transmitting information through a much wider range of radio frequencies by combining both radio and optical technologies for the first time. The results are described in a new study published in *The Journal of Lightwave Technology*. This more efficient use of the wireless spectrum is expected to help meet the growing demand for wireless data capacity and speed over the next three to five years.

> Demonstrated up to 9380x faster than the best average 5G download speed in the U.K.

Dr. Zhixin Liu, senior author of the study from UCL Electronic & Electrical Engineering, said, "Current wireless communication systems are struggling to keep up with the increasing demand for high speed data access, with capacity in the last few meters between the user and the fiber-optic network holding us back.

"Our solution is to use more of the available frequencies to increase bandwidth, while maintaining high signal quality and providing flexibility in accessing different frequency resources. This results in super-fast and reliable wireless networks, overcoming the speed bottleneck between user terminals and the internet.

"Our new approach combines two existing wireless technologies for the first time, high speed electronics and mmWave photonics, to overcoming these barriers. This new system allows for the transmission of large amounts of data at unprecedented speeds, which will be crucial for the future of wireless communications."

To address the current limitations of wireless technology, researchers from UCL developed a novel approach that combines advanced electronics, which performs well in the 5 to 50 GHz range and a technology called photonics that uses light to generate radio information, which performs well in the 50 to 150 GHz range.

The team generated high-quality signals by combining electronic digital-to-analog signal generators with light-based radio signal generators, allowing data to be transmitted across a wide range of frequencies from 5 to 150 GHz.

State-of-the-art communications networks rely on several technologies to function. Optical fiber communications systems transmit data over long distances, between continents and from data centers to people's homes. Wireless technology often comes in at the final stage, when data is transmitted a short distance, for example from a household internet router to the devices connected to it over Wi-Fi.

While optical fiber, which forms the backbone of modern communications networks, has made big advances in bandwidth and speed in recent years, these gains are limited without similar advances in the wireless technology that transmits information the final few meters in homes, workplaces and public spaces.

The new UCL-developed technology has the potential to revolutionize various sectors, not least the Wi-Fi connectivity that people rely on at home and in other public places.

Spectrum in the 7 to 8 GHz Range Could Enable Future 6G Networks

The next generation of wireless technology is already being planned as the spectrum in the 7.125 to 8.400 GHz range has been identified as a key enabler of future connectivity. 5G Americas announced the publication of its latest white paper, 'The 6G Upgrade in the 7-8 GHz Spectrum Range: Coverage, Capacity, and Technology,' highlighting the potential of this emerging spectrum for delivering unparalleled capacity, faster data rates and better coverage, all while reusing existing infrastructure.

"The 7 to 8 GHz spectrum will potentially be a cornerstone of 6G technology, enabling faster, more reliable networks that are essential for the next wave of innovation in AI, smart cities and immersive experiences," said Viet Nguyen, vice president of PR and technology at 5G Americas.

The white paper outlines how the spectrum in the 7 to 8 GHz range would enable 6G to potentially provide up to 10 to 20x increase in capacity compared to current 5G networks. This will enable higher data speeds and more efficient network management, making the deployment of advanced technologies like AI and extended reality (XR) more feasible.

As the industry prepares for the next era of 6G in the 2030 timeframe, the study emphasizes that the

For More Information Visit mwjournal.com for more commercial market news.

> Crucial for achieving economies of scale and driving down costs.

availability of 1.5 to 2 GHz of mid-band spectrum per market is essential for successful 6G deployment. The 7.125 to 8.400 GHz spectrum is emerging as a globally harmonized band, dubbed the "Golden Band of 6G," crucial for achieving economies of scale and driving down costs for operators and consumers. The white paper covers the following key highlights:

- Spectrum Efficiency: The 7 to 8 GHz range combined with advanced antennas allows for four to five times higher spectral efficiency compared to current 5G bands leading to enhanced performance.
- Infrastructure Reuse: The new band enables the reuse of existing 5G base station sites, significantly reducing the cost of deployment.
- Technology Boost: Advanced beamforming, massive MIMO and AI-driven algorithms will further enhance network capacity and coverage.
- Spectrum Sharing: While exclusive licensing is ideal, the report highlights that spectrum sharing may be necessary in certain regions, ensuring flexible and rapid access to the new band.

With mobile data traffic expected to grow from three to five-fold in the next five years, driven by new applications that demand high-capacity, low latency networks, the 7 to 8 GHz spectrum is critical. The band is currently home to several incumbent users in the U.S., including federal and satellite services. As part of the transition to 6G, greater transparency, coordination and repacking will be important in ensuring efficient use of the new spectrum.

"The 7 to 8 GHz band is pivotal for the future of 6G. It offers the capacity and efficiency we need to support the exponential data growth expected with emerging applications such as AR, VR and advanced AI," said Harri Holma, senior advisor of technology leadership at Nokia and leader of the 5G Americas work group for this paper.

Amit Mukhopadhyay, principal standardization leader at Nokia and leader of the working group added, "This spectrum range is a critical component in ensuring a seamless transition from 5G to 6G, allowing operators to reuse existing infrastructure while still delivering next-generation performance and capabilities."

The paper also identifies that the success of 6G deployment relies on global collaboration to harmonize spectrum use to reduce manufacturing costs, streamline supply chains and support international roaming, benefiting both operators and consumers.

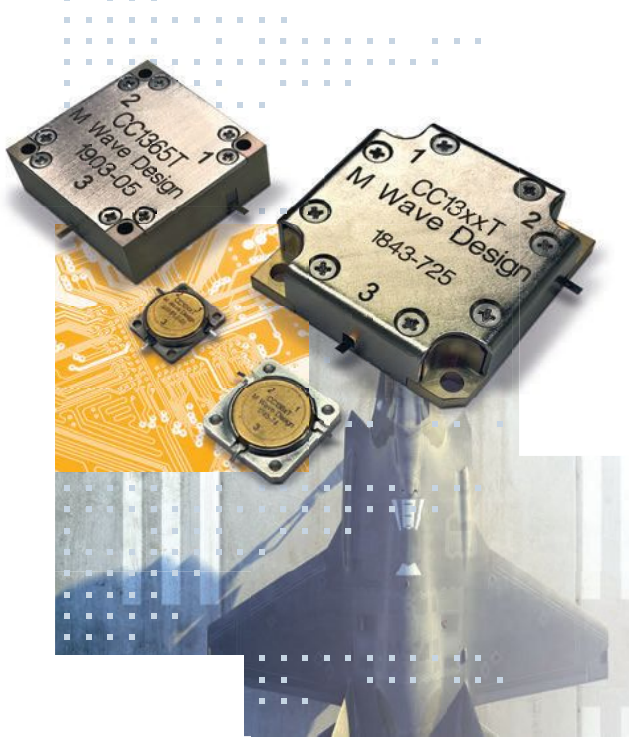

Quantic™ M-Wave

Circulators for AESA Radar

100 MHz to 40 GHz

- Specializing in the design and manufacture of ferrite-based RF/MW components
- Small form factor, high power, and low-loss performance solutions for improved efficiency and dynamic range

Contact Us

M Wave Design Corporation / info@quanticmwave.com / www.quanticmwave.com

3H Communication Systems

AS9100 & ISO9001:2015 certified

3H offers innovative, high quality and cost effective RF / Microwave Filter solutions ranging from DC to 50 GHz backed by our 5 year warranty and manufactured in our ISO 9001 facilities.

MICROWAVE AND RF FILTER PRODUCTS

LC • CERAMIC • CAVITY • PRINTED • MULTIPLEXERS • SWITCHED FILTER BANKS • MULTI-FUNCTION ASSEMBLIES

FOR YOUR DEFENSE, COMMERCIAL AND SPACE APPLICATION

CONTACT US TO DISCUSS YOUR APPLICATION

3hcommunicationsystems.com

sales@3hcomm.com | 949.529.1583

Around the **Circuit**

Barbara Walsh, Multimedia Staff Editor

COLLABORATIONS

Kratos Defense & Security Solutions, Inc. announced that it is partnering with **Radisys® Corporation** to develop cloud native 5G non-terrestrial network (NTN) solutions for satellite connectivity. These solutions will be available through Kratos OpenSpace® Platform, the only commercially available, fully software-defined satellite ground system. Radisys is a leading Radio Access Network (RAN) partner for telecom and mobile network operators around the world. Radisys and Kratos share a common vision for the future of connectivity to provide open standards-based solutions that interoperate seamlessly across terrestrial and space networks. Together, Kratos and Radisys are developing a 5G-NTN satellite base station equivalent to a cellular base station but delivered completely as cloud-native software.

Modelithics and **Signal Edge Solutions (SES)** have joined forces in a strategic partnership aimed at advancing signal integrity and power integrity modeling. By combining their advanced simulation and software model development and validation techniques, Modelithics and SES will collaborate to address critical challenges faced by high speed electronic and power electronic systems designers. Known for delivering top-tier models for RF and microwave applications, supporting a multitude of popular circuit and electromagnetic simulation tools, Modelithics brings industry-leading expertise to the table. Their comprehensive, measurement-validated, model libraries are trusted by engineers worldwide and have been widely adopted by leading semiconductor companies, defense contractors, instrumentation companies and research institutions.

Quadsat has worked with **ALL.SPACE** to conduct a comprehensive evaluation of its electronically steerable antenna (ESA) for use on LEO constellations. Conducted in the U.K. using Quadsat's unmanned aerial vehicle (UAV)-based solution, the test is the first such comprehensive evaluation of an ESA and has proven the ability of the Quadsat system to conduct complex measurements of this type. Quadsat is developing its own view of a comprehensive test procedure for ESAs. This includes both the assessment of the antenna radiation performance combined with the evaluation of the dynamic testing of the desired operational cases, including satellite passes, handover switching and multibeam tracking.

NEW STARTS

VIAVI Solutions Inc. has opened its VIAVI Automated Lab-as-a-Service (VALOR™) Open RAN testing facility in Chandler, Ariz., with a ribbon-cutting ceremony attended by senior VIAVI management, customers, partners, government officials and dignitaries. Funded by a grant from the U.S. National Telecommunications and Information Administration Public Wireless Supply Chain Innovation Fund, VALOR offers a fully automated, open and impartial lab-as-a-service/test-as-a-service suite for Open RAN interoperability, performance and security. VALOR addresses the challenges to accelerate Open RAN adoption and encourage competition by providing access to test capabilities that, typically, have only been within the reach of large, established players.

Morse Micro announced the launch of multiple open-source GitHub repositories, along with a community forum. This initiative offers a robust collection of assets, tools and resources designed to support and empower the global developer community. Both the repositories and forum are available for free, catering to engineers, developers and technology enthusiasts interested in advancing Wi-Fi HaLow. Morse Micro's GitHub repositories contain the software and tools necessary to bring up Wi-Fi HaLow on Linux based projects. Additionally, the Morse Micro community, powered by Discourse, is a dedicated platform where users can engage in discussions, share knowledge, seek advice, troubleshoot and contribute to Wi-Fi HaLow-related projects.

ACHIEVEMENTS

Telenor Pakistan and **ZTE Corporation** have set a new benchmark in telecommunications by achieving a record data transmission rate of 1.9 Gbps over 11.6 km using MIMO technology. This accomplishment marks the highest transmission rate recorded in Pakistan, representing a significant leap forward in microwave backhaul technology. Conducted within Telenor Pakistan's live network environment, the successful trial tested next-generation microwave transmission technology, aimed at enhancing network performance and capacity. Utilizing the industry's first-ever 18 GHz and 23 GHz dual-band integrated antenna alongside advanced carrier aggregation technology, the trial achieved stable transmission over 7.8 km with a capacity of 3.9 Gbps.

CesiumAstro announced its selection by the **Space Development Agency (SDA**) for the Hybrid Acquisition for Proliferated LEO (HALO) program. This award positions CesiumAstro to compete for future prototype orders in SDA's mission-critical space development initiatives. The HALO program, utilizing Other Transaction Authority (OTA), is designed to foster rapid, affordable mission feasibility demonstrations. As a selected vendor, CesiumAstro joins an elite pool of non-traditional defense contractors eligible to bid on specific flight demonstration opportunities, including the Tranche 2 Demonstration and Experimentation System (T2DES) and other SDA demonstration projects. The HALO program is structured as a multiple-step competition, aimed at increasing the pool of performers capable of bidding on future SDA programs and participating in layers of future tranches.

Radisys® Corporation announced its inclusion in the AccelerComm® 5G Ecosystem Partner Program, for-

For More Information

For up-to-date news briefs, visit mwjournal.com

GOLD STANDARD

GSDRO series

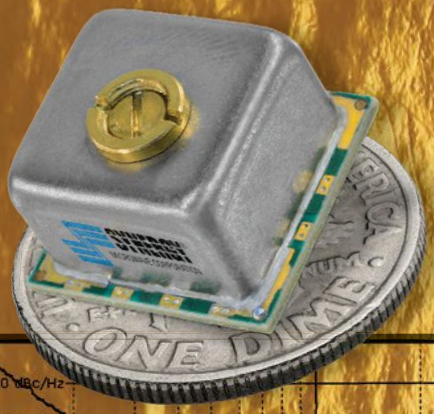

0.75" x 0.75" x 0.53"

* *Typical For 10 GHz RF Output*

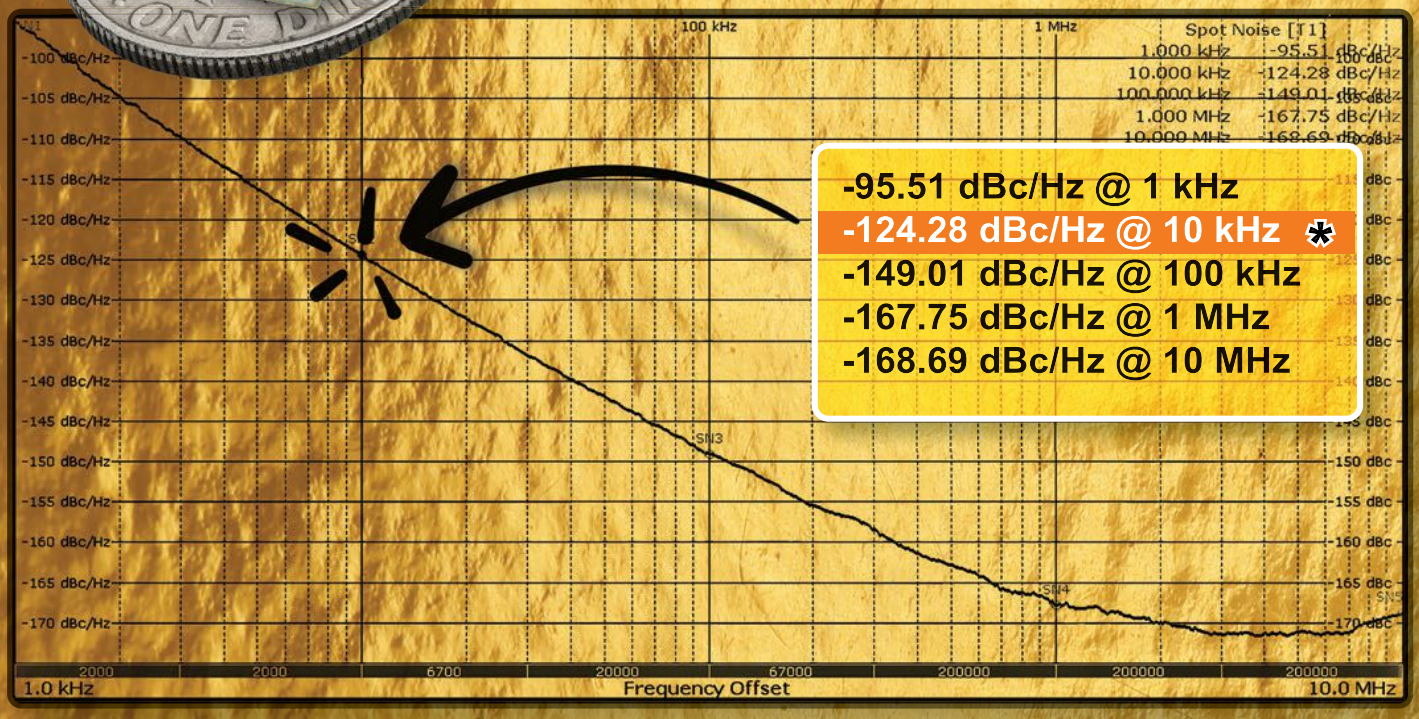

-95.51 dBc/Hz @ 1 kHz
-124.28 dBc/Hz @ 10 kHz *
-149.01 dBc/Hz @ 100 kHz
-167.75 dBc/Hz @ 1 MHz
-168.69 dBc/Hz @ 10 MHz

FEATURES:

- *Exceptional Phase Noise*
- *Lead Free RoHS Compliant*
- *Patented Technology*

Applications:
Radar, Test Equipment,
5G, Frequency Synthesizer

Now Up To 22 GHz!

Check out our website for available frequencies.

Talk To Us About Your Custom Requirements.

SYNERGY® MICROWAVE CORPORATION

Phone: (973) 881-8800 | Fax: (973) 881-8361
E-mail: sales@synergymwave.com | Web: www.synergymwave.com
Mail: 201 McLean Boulevard, Paterson, NJ 07504

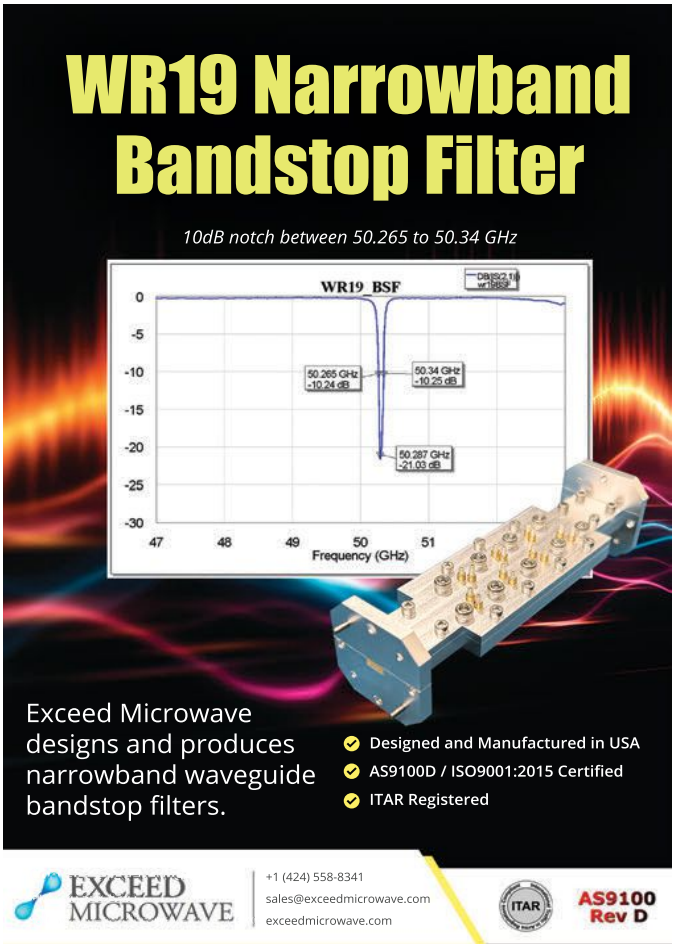

Around the **Circuit**

malizing a long-standing partnership. This collaboration will enable original equipment manufacturers to unlock new business opportunities for non-terrestrial network (NTN) 5G communication, extending coverage to areas that were previously inaccessible due to high cost and allowing companies to explore innovative applications that were previously deemed too expensive. The collaboration aims to enable satcom technology with 3GPP standards-compliant solutions, reducing costs and improving network flexibility. Additionally, it will promote cross-compatibility with Radisys' NR-NTN gNodeB software, NTN 5G Core (5GC) and multi non-3GPP interworking gateway (AGF/TWIF) software for interworking with legacy NTN technologies, and RIC for monitoring and control of multi-layer/ad-hoc reconfigurable satellite networks.

Indra has completed the implementation and testing of the new Lanza 3D long-range radar (LRR) to be used by the Air Surveillance Squadron 2 (EVA-2) of the **Spanish Air and Space Force**, located in the province of Toledo and responsible for the surveillance of the central area of the peninsula. The project being implemented by Indra is part of the ongoing process to modernize the Spanish Air and Space Force's air surveillance and control system and strives to replace systems that have reached the end of their service life with next-generation equipment. All in all, Indra will deploy five radars: four fixed Lanza 3D LRR and one deployable Lanza 3D LTR-25, a long-range tactical radar.

CONTRACTS

Raytheon, an RTX business, has been awarded a $192 million contract from the **U.S. Navy** to develop the Next Generation Jammer Mid-Band Expansion (NGJ-MBX), an upgrade to the current Next Generation Jammer Mid-Band (NGJ-MB) system. This modification will extend the frequency range of the NGJ-MB system to counter additional threats. MBX provides additional capabilities to improve operational effectiveness. NGJ-MB, to include MBX, is a cooperative development and production program with the Royal Australian Air Force. It is an airborne electronic attack system consisting of two pods containing active electronically scanned arrays that radiate in the mid-band frequency range. The U.S. Navy employs NGJ-MB on the EA-18G GROWLER® to target advanced electronic warfare threats.

Mercury Systems Inc. announced it was awarded a five-year contract worth as much as $131.3 million from the **U.S. Naval Air Systems Command** to continue providing secure data transfer systems for naval aircraft. Mercury has been delivering advanced data transfer systems (ADTS) and components to the Navy since 2017 to support numerous rotary-wing and fixed-wing aircraft. These rugged, flexible and proven systems simplify the secure transfer of data between planners on the ground and aircraft, significantly improving operational readiness of these airborne assets. The new indefinite delivery/indefinite quantity contract will allow Mercury to deliver up-

MiCable

1~18GHz 30/40dB

HIGH POWER Dual-Directional Coupler

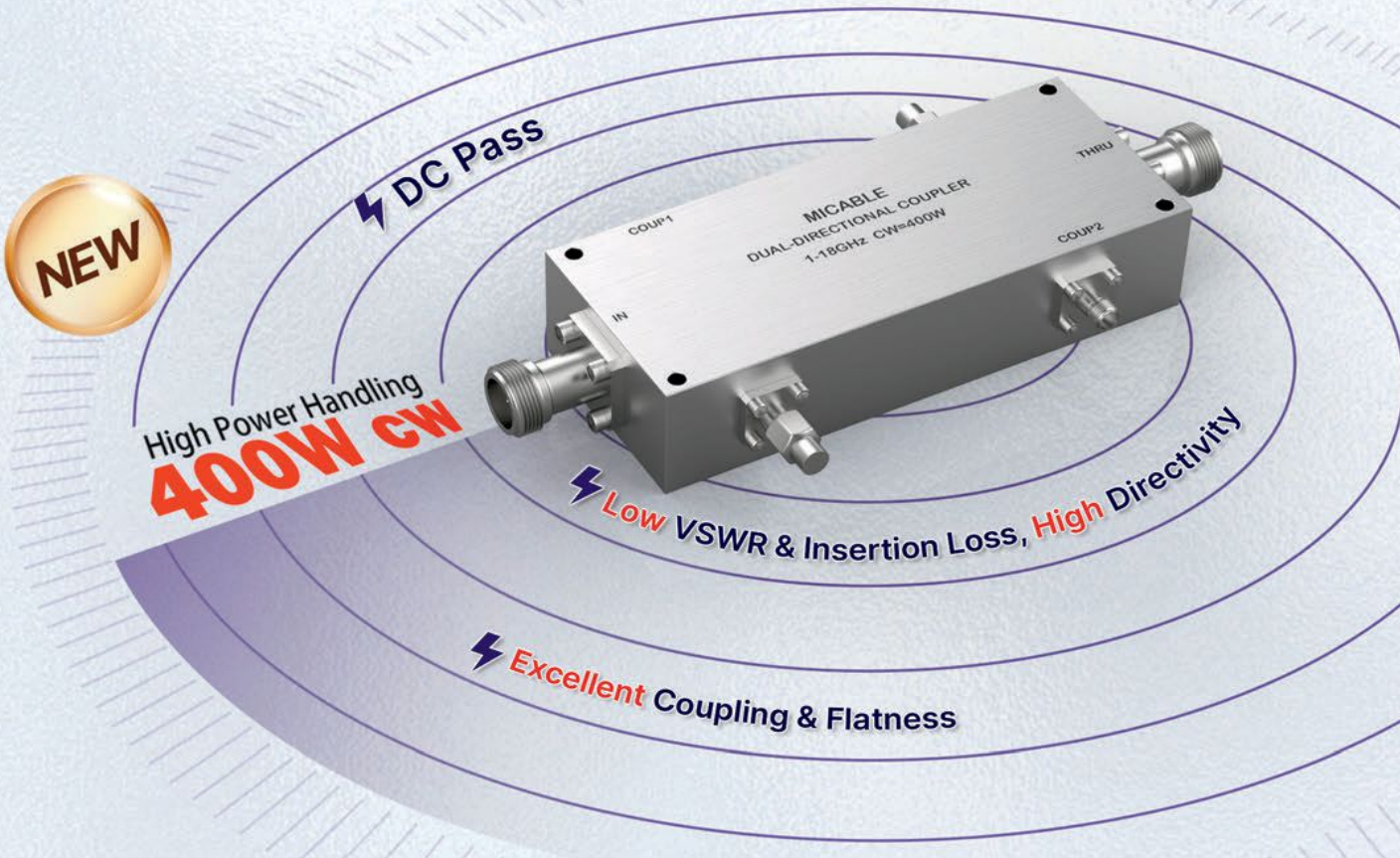

P/N	Freq. Range (GHz)	Coupling (dB) Max.	Main Line VSWR (:1) Max.	Coupling VSWR (:1) Max.	Insertion Loss* (dB) Max.	Flatness (dB) Max.	Directivity (dB) Min.	Power (W) Max.
D3008HB010180	1~18	30±1.2	1.5	1.6	0.6	±1.2	10	400
D4008HB010180		40±1.2						

*Theoretical I.L. Included

Test Curve

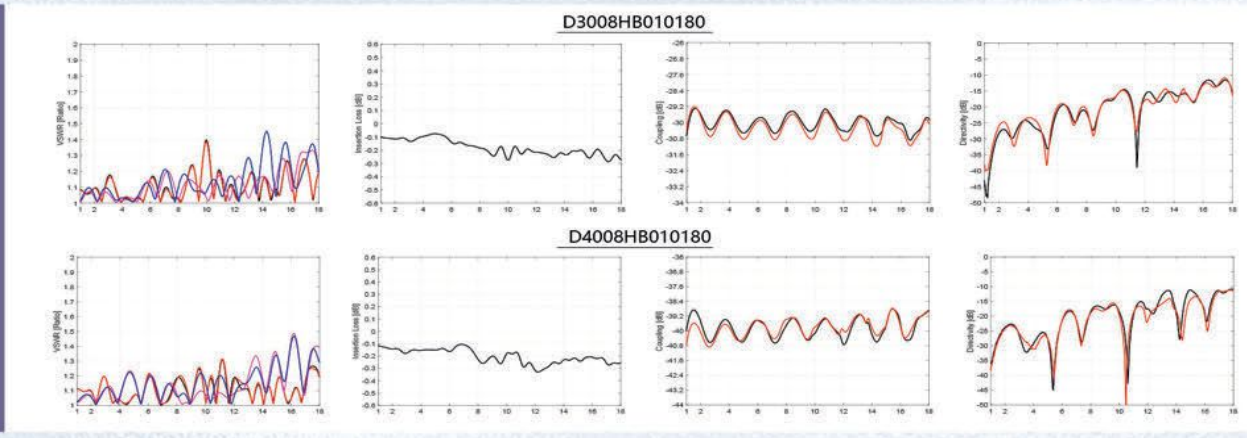

More Information-
Scan the QR Code

MIcable Inc.

www.micable.cn sales@micable.cn +86-591-87382856

QML INC.
Leading the Way in Precious Metal Reclamation

Refiners of gold, silver, platinum, palladium, rhodium, iridium, and ruthenium
(401) 490-4555 | www.qml.us

FEATURED WHITE PAPERS
The information you need, from industry experts
ERZIA
Characterizing Wide-Band Converters for EW
soitec
Engineered Substrates for Intelligent IoT Connectivity
Look for additional content from:
Signal Hound
Check out these new online Technical Papers featured at MWJournal.com
Microwave Journal

Around the **Circuit**

graded ADTS units that incorporate the company's JDAR encryption module.

Epirus announced a nearly $17 million contract modification from the **U.S. Army Rapid Capabilities and Critical Technologies Office** for the development and integration of an upgraded sensor suite in support of the Integrated Fires Protection Capability High Power Microwave (IFPC-HPM) program. Under the scope of work, Epirus will integrate a closed-loop fire control system and perform software development to increase the operational suitability and effectiveness of the IFPC-HPM systems. The upgrades will, in part, reduce engagement latency, enhance the soldier user experience and improve the accuracy of the IFPC-HPM systems.

Altum RF announced a two-year contract with the **European Space Agency (ESA)** under the Advanced Research in Telecommunications Systems Core Competitiveness (ARTES CC) Programme for the design and development of high efficiency MMIC power amplifiers. These amplifiers will be tailored for phased array Ka-Band satcom systems in space applications. Commenced in October 2024, this project aims to advance the development of high efficiency MMIC power amplifiers to enhance the performance of Ka-Band phased array satcom systems. With the rapid deployment of low Earth orbit, medium Earth orbit and geostationary orbit satellite constellations, Ka-Band phased array systems will play a critical role in future satcoms.

Gapwaves and **Valeo** have entered into an agreement regarding the development and large-scale serial production of waveguide radar antennas for advanced driver assistance systems (ADAS) applications. The contract has an expected sales value of mid-range double-digit MEUR over approximately 10 years, starting in 2025. Valeo offers a complete portfolio of ADAS on the market and keeps developing new technologies to offer more safety and comfort to drivers. Valeo has been developing and mass-producing radar technologies since 2006. In the joint development, Gapwaves supports Valeo with its antenna technology, engineering and production capabilities.

PEOPLE

▲ *Steve Shpock*

▲ *Mansoor Mosallaie*

Stellant Systems Inc. recently announced the appointment of **Mansoor Mosallaie** as its new chief operating officer (COO) and **Steve Shpock** as chief technology officer. Mosallaie brings nearly 40 years of experience in the microelectronic component and assembly manufacturing industry, holding several roles of increasing responsibility. Most recently, he was the COO of Hermetic Solutions Group, Inc. (HSG), where he oversaw the operational needs of

ANALOG DEVICES

AHEAD OF WHAT'S POSSIBLE™

Power for your world.

Simplify your designs by leveraging ADI's highly integrated power solutions.

Integrated **Solutions**

Local Design **Support**

Easy to Use **Tools**

Find your competitive advantage at analog.com/power

IEEE Wireless and Microwave Technology Conference
WAMICON 2025 - Cocoa Beach, Florida
Hilton Cocoa Beach
April 14-15, 2025

WAMICON

JOIN US
WAMICON 2025 will be held in Cocoa Beach, Florida on April 14-15, 2025. The conference addresses multidisciplinary research and technology trends in RF, Microwave and Wireless Communications.

CALL FOR PAPERS
The WAMICON 2025 focus is *"Integrated Innovations: Merging Software, Circuits, and Antennas for Next-Generation Interconnected Systems."* Submissions welcomed on all aspects of RF, Microwave and mmWave devices and systems along with hardware and software technologies enabling intelligent communications and sensing.

Prospective authors are invited to submit original work for presentation and publication in IEEE Xplore. Topics of interest include:

- Power Amplifiers, Active Components & Systems
- Passive Components & Antennas
- mmWave to THz Technologies
- Space & Emerging Applications
- Internet of Everything (IoE) & Machine Learning

Visit **www.wamicon.org** for submission details.

Important Dates

Papers Due:	***February 7, 2025***
Author Notification:	***March 10, 2025***
Final Papers Due:	***March 24, 2025***

www.wamicon.org

Exhibit/Sponsor Opportunities Available!
Email: arogers@modelithics.com
james@ace-pcb.com

Around the **Circuit**

12 business units spanning three countries. Shpock has 40 years of RF/microwave industry experience in various executive roles, including most recently as Stellant's COO. His experience will prove invaluable as Stellant continues to expand its market share while also growing its product and technology portfolio.

▲ *Isaac Pimentelli*

dB Control has hired **Isaac Pimentelli** as senior program manager. With a strong, 20+ year background in engineering, manufacturing and program management for the defense, aerospace and instrumentation industries, Pimentelli will support an exclusive dB Control program for airborne power supply development. dB Control also recently hired five additional engineers as the company continues to expand its technical capabilities and provide high-power products built to customer specifications.

Testco announced the addition of **Kimberly Hermoso-Hurst** as the new director of business development. Hermoso-Hurst brings a wealth of experience from the electronics industry, having started her career at Aromat and later with Panasonic relays. She has held various leadership roles with distributors, including marketing, value-added services and launching sales divisions for both Bell Industries and All American. Hermoso-Hurst's appointment aligns with Testco's continued commitment to providing innovative supply chain solutions to its global customer base.

▲ *Kimberly Hermoso-Hurst*

REP APPOINTMENTS

Menlo Microsystems Inc. announced a new global distribution agreement with **DigiKey**. Under the terms of the agreement, DigiKey becomes a franchised distributor for worldwide marketing and sales of Menlo Micro's innovative Ideal Switch® products. Menlo Micro's Ideal Switch technology leverages a unique combination of semiconductor technology and cutting-edge design, resulting in higher efficiency, reduced size and a longer lifespan — benefiting a wide range of products in smart energy, home automation, industrial IoT, test and measurement, aerospace and defense, telecommunications, consumer electronics and medical.

Modelithics® introduces **Exocis**, based in Limoges, France, and closely linked with AMCAD SAS, as a Modelithics Reseller. Exocis provides a comprehensive range of high performance solutions in electronics, RF and microwave technologies. In addition to distributing qualified components and systems, Exocis offers turnkey measurement solutions dedicated to the characterization, modeling and design of components, circuits and subsystems.

MI-WAVE

Millimeter Wave Products Inc.

NEW!

FREQUENCY SYNTHESIZERS

MI-WAVE SYNTHESIZER CONTROL INTERFACE

958 SERIES

GUI CONTROLLED WIDEBAND SYNTHESIZERS

0.1-8 GHz
0.1-16 GHz
0.1-32 GHz
0.1-67 GHz
V-Band (WR-15)
E-Band (WR-12)

APPLICATIONS

- Automated Test Equipment (ATE)
- Frequency Agile Radar Signal Generation
- Local Oscillators & System Clock Source
- Telecommunications/Satellite Communications
- Embedded Systems
- Secure Communications & Electronic Warfare
- Beamforming & MIMO R&D
- Spectroscopy

FEATURES

- ***Output Power +20 dBm Typical, Higher Output Power Available***
- ***Remote RF Control:*** Seamlessly operate RF signals via an intuitive GUI over Wi-Fi or Ethernet.
- ***Four Operating Modes:*** CW, Frequency Sweep, Frequency Hop, and External Trigger.
- ***Modulation:*** Supports external configuration for FSK modulation.
- ***CW Mode Filter:*** Customizable internal filter for precise and clean signal output.
- ***High Resolution:*** Achieve fine frequency adjustments with 0.01 Hz resolution.
- ***Ultra-Fast Switching:*** Less than 10 µs for rapid frequency transitions.
- ***Integrated Attenuators:*** Up to 70 dB attenuation for enhanced signal management.
- ***Low Phase Noise:*** Ensures outstanding signal clarity and quality.
- ***Reference Switching:*** Easily switch between internal and external references with a 10 MHz or 100 MHz option.
- ***Reference Compatibility:*** Supports a wide range of reference frequencies, from 10 MHz to 250 MHz.
- ***Temperature Monitoring:*** Built-in sensor for stable and consistent performance.
- ***Single Supply Operation:*** Efficiently runs on 8VDC to 15VDC power.

2007 Gandy Blvd N Suite 1310
St. Petersburg, FL 33702

Tel: (727) 563-0034
Email: sales@miwv.com

MADE IN THE USA WITH PRIDE
CERTIFIED ISO 9001-2015 COMPANY
35 ANNIVERSARY YEARS IN BUSINESS

INVITED PAPER

The Future of Wireless: Technologies Overcoming 5G Struggles

Ali Sadri
Airgain, San Diego, Calif.

Kyei Anim and Kapil Dandekar
Drexel University, Philadelphia, Pa.

In wireless communication, strong signals and reliable coverage are necessary to meet the stringent expectations and demands of users. As discussions around 5G reliability and its challenges continue, many argue that the air interface is still not yet meeting expectations. The question becomes: What is needed to unlock 5G's potential and future 6G wireless connections? This article discusses how emerging technologies can help overcome some of the current issues.

Despite substantial investment from governments and the private sector, mobile users in some countries still experience slow and sluggish internet. Analysis from cable.co.uk[1] recently found that Northern Africa has the lowest average broadband globally at 12.52 Mbps. At the same time, at the other end of the scale, residents in Iceland could experience speeds of 279.55 Mbps and the vast difference between the two is apparent. Slow download speeds frustrate consumers and have broader economic consequences. Vodafone estimates that small and medium-sized businesses are missing out on as much as £8.6 billion a year in productivity savings because the rollout of standalone 5G has been so slow.[2] Without reliable wireless 5G connectivity or 5G over Wi-Fi, the prospect of smart homes, factories and cities seems unattainable.

In the U.S., there have been challenges connecting remote communities. However, adoption rates are generally high, thanks to large coverage footprints and high speeds. The situation is even more positive in the Middle East, where countries such as Bahrain, Kuwait, Oman, Qatar, Saudi Arabia and the United Arab Emirates have been leading the way in deploying 5G networks with some of the fastest mobile internet speeds in the world.

There is no single solution for improving the 5G rollout timeline and its performance. However, innovations in antennas, repeaters and modems are now set to bridge the gap between vision and reality. In recent years, discussions about reconfigurable intelligent surfaces (RIS) and smart repeaters have become hot topics.

THE COMPLEXITIES OF WIRELESS

A whole network approach is needed to solve the problems surrounding 5G connectivity. Engineers and technology developers must focus their research, design and technical capabilities on enhancing every aspect of the user journey, from the service provider to the end-user. Engineers will appreciate the

REMCOM®

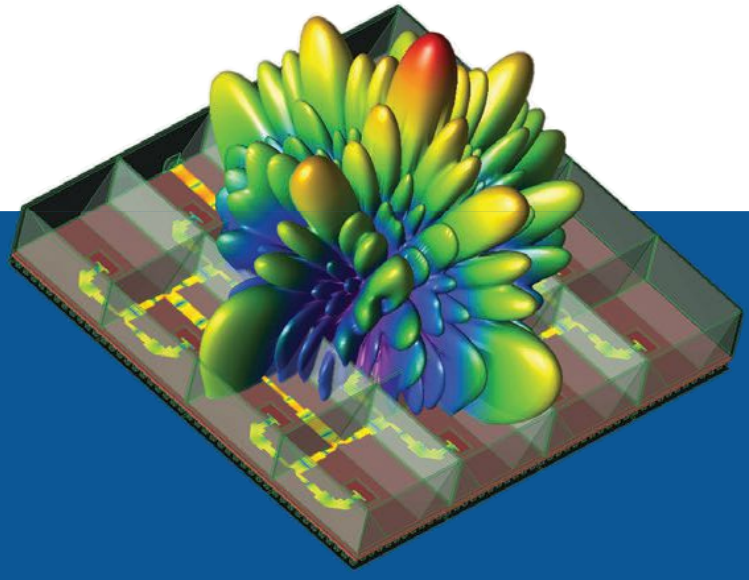

Optimize Your Device Designs

with Antenna Simulation Software from Remcom

XFdtd® 3D Electromagnetic Simulation Software provides engineers with powerful tools to shorten development time and release products to market sooner.

- In-depth analysis of 5G-capable devices and arrays
- Matching network design innovations including a schematic editor and Circuit Element Optimizer
- Huygens surface captures antenna radiation characteristics for use outside of XFdtd

Explore all of XFdtd's powerful features at | **www.remcom.com/xfdtd** ▸▸▸

30 1994 2024 REMCOM

For 30 years Remcom's software has enabled the world's most advanced engineering teams to deliver their devices to market.

+1.888.7.REMCOM (US/CAN) | +1.814.861.1299 | **www.remcom.com**

complexities inherent in wireless, starting with the propagation of 5G signals. Even though 5G can deliver lower latency, increased capacity and faster throughput, the higher frequencies result in a shorter propagation distance from the base station. The 700 MHz part of the spectrum can transmit signals over long distances and penetrate obstacles more effectively. Still, its throughput is lower due to limited available bandwidth, on the order of 10 to 20 MHz per operator.

Higher throughput is possible with the C-Band spectrum around 3.5 GHz, with hundreds of megahertz of RF signal bandwidths available. The problem is that signals in this band only travel 20 percent as far as 700 MHz signals and this propagation distance reduces further at higher frequencies. There is also an issue with limited penetration through walls and obstacles inside buildings. This leads to coverage gaps impacting user experience, network reliability and service consistency.

Demand for 5G is highest in densely populated cities, yet atmospheric pollution, buildings and people can all interrupt or block high frequency signals. To counter this, thousands of base stations or small cells would be needed to reach the highest coverage levels. At a cost of billions, networks this size would be prohibitively expensive for providers and likely incur backlash from nearby people.

RECONFIGURABLE INTELLIGENT SURFACES

An innovative solution with enormous potential to enhance 5G performance is emerging with RIS. Designed to operate in the sub-6 GHz band, primarily at the center frequency of 3.5 GHz, RIS comprises thousands of unit cells equipped with controllable elements (e.g., varactor diodes). These controllable elements enable the surface to reconfigure its response by manipulating incoming electromagnetic (EM) waves to improve signal reception in coverage blind spots. The response can be improved, potentially, by more than 15 dB when configured for a specific direction. ***Figure 1*** shows a prototype RIS board operating in the sub-6 GHz frequency band.

RIS technology promises to be a game-changer for ensuring seamless connectivity in 5G and future 6G networks. Its ability to reconfigure and direct EM waves toward areas with poor coverage can significantly boost 5G performance, efficiency and reliability. It has the potential to boost public confidence in wireless communication technologies. However, the technology is still several years away from large-scale commercialization. For all its advantages, RIS still comes with its challenges for implementation in terms of design complexities, deployment costs and energy efficiency.

5G SMART REPEATERS

In addition to RIS, 5G smart repeaters are another potentially transformative technology. These repeaters can receive, clean up, amplify and forward the signal down the line. The repeater automatically detects the optimal signal direction while mobile devices maintain fidelity and upload/download speeds even if the base stations are further away. Smart repeaters are a more traditional approach and have evolved over several years with the advancements in wireless technology. But they have proven their worth in enhancing wireless communication.

Dependable and practical, smart repeaters can reduce the cost of wireless infrastructure for operators. These repeaters do not rely

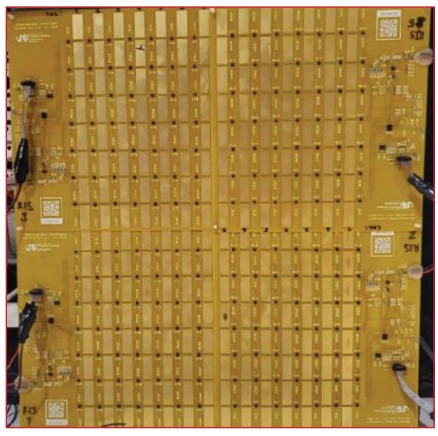

Fig. 1 **Prototype RIS.** ***Source:*** **Drexel Wireless Systems Laboratory.**

Ultra performance, high-reliability power RF switches

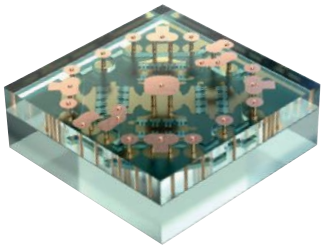

Switch array

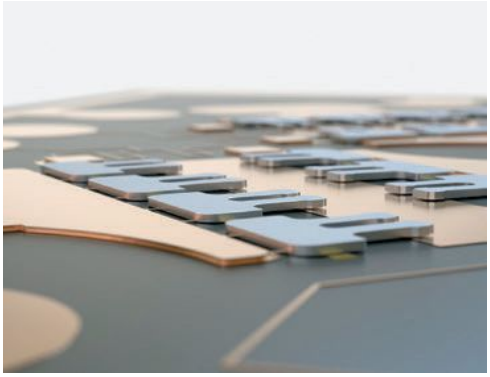

Fabrication

MM5130

DC — 60 GHz
150 W Pulsed Power
500 W Standoff Power
95 dBm IP3
1 dB Loss 40 GHz
10 B Cycles Typical

Ultra high-performance power control with scalable voltage and current

Energy Consumption Demo

Industry leading power efficiency and size – no heat sinks

	Power Consumption	Energy Consumption 1 switch	Home 40 switches	Warehouse 150 switches	LA Metro Area 35M switches	California 75M switches	Ideal Switch Savings vs relays	Energy usage vs Ideal Switch
	0.45 watt	**655 Wh/yr $0/yr**	**26 kWh/yr $8/yr**	**98 kWh/yr $29/yr**	**23 GWh/yr $7M/yr**	**49 GWh/yr $15M/yr**	–	–
Electro-mechanical relay	3.20 watt	5 kWh/yr $1/yr	187 kWh/yr $56/yr	700 kWh/yr $210/yr	163 GWh/yr $49M/yr	350 GWh/yr $105M/yr	**86% Energy Savings**	**7.1X Energy Usage**
Solid-state relay	12.89 watt	19 kWh/yr $6/yr	753 kWh/yr $226/yr	3 MWh/yr $847/yr	659 GWh/yr $198M/yr	1 TWh/yr $424M/yr	**96.5% Energy Savings**	**28.7X Energy Usage**

MM9200

AC or DC
Low R_{ON}: 8 mΩ
1,000s V & 10,000 A
10s of millions cycles
Switching: 10µs
QFN: 6.5mm x 6.0mm

Thermal image

Showing the Ideal Switch is 62 °C cooler.

130 °C — 20°C

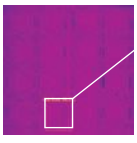

Ideal Switch

Hot spot: 56 °C

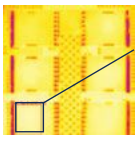

SiC

Hot spot: 118 °C

menlomicro ideal switch®

Learn more about our product portfolio at menlomicro.com

on broadband cable backhaul and only require access to power, which could include solar, making them ideal for areas that have always struggled with reliable connectivity. Repeaters receive the desired signal, amplify it from low levels and retransmit it to ensure it reaches the destination with minimal distortion. The adaptability of this solution allows smart repeaters to fit into any communication environment, making them a reliable choice. For this reason, and because the devices are easy to install without compromising performance, solution providers are rapidly moving smart repeaters into the home and enterprise market and continuing to cater to mobile network operators.

Network-controlled repeaters (NCRs) can also play an important role in boosting signal strength and improving coverage in weak zones. These devices are typically an RF repeater that can receive and process side control information (SCI) from the network. This allows NCRs to amplify the signal more efficiently than traditional repeaters.

NCRs are an advanced evolution of traditional repeaters designed to enhance wireless coverage wherever signal strength is weak, such as in dense urban environments, rural zones and indoor spaces. Unlike traditional repeaters, which amplify and retransmit signals, NCRs operate with a higher level of intelligence, utilizing real-time network data and control mechanisms to optimize signal propagation dynamically. This is enabled by accessing the network "knowledge" via the SCI. This dynamic control allows NCRs to adapt to changing conditions, such as varying user demand or physical environmental factors like vehicles, people or other objects on the move. This ensures better signal quality and coverage continuity.

NCRs incorporate intelligent features like beamforming, multi-beam antenna systems and interference cancellation. This allows them to direct signals to specific users and reduce signal losses more efficiently. For example, suppose the network detects higher congestion in one area. In that case, the NCR will optimize its transmission power or

Fig. 2 **Airgain Lighthouse™ smart NCR indoor/outdoor solution.**

beamforming direction to alleviate the issue, ensuring cleaner and more efficient signal propagation. ***Figure 2*** shows an Airgain NCR solution mounted on the side of a building for smart indoor/outdoor coverage.

RIS and NCRs have a great synergy and can work together to provide better coverage and signal quality in challenging environments. Active RIS dynamically interacts with NCR to direct signal beams, reducing interference and boosting throughput. Recent simulations using this collaborative approach have shown enormous potential for improvements in coverage and how both could be integrated into a unified system for future indoor use. Airvine, in conjunction with Drexel University researchers, used the Wireless InSite® model to display outdoor-to-indoor coverage with complete 3D path loss for several network configurations. ***Figure 3a*** shows the baseline coverage results for a 3.5 GHz base station. ***Figure 3b*** shows how the path loss changes by adding a smart repeater and ***Figure 3c*** shows the path loss profile with an RIS/smart repeater combination.

Researchers in the Drexel Wireless Systems Laboratory partially validated the concept of coexistence and cooperation of RIS technology and NCR for smart repeaters within the same network for indoor coverage. They simulated 5G network coverage in the n77 band in C-Band. Their results come from using different scenario features in Wireless InSite,[3] a commercial computational EM ray tracing system that employs 3D shooting and bouncing

EXODUS ADVANCED COMMUNICATIONS

Where Defense & EMC Solutions Begin!

Amplifiers
CW & Pulse

RF & Microwave Amplifiers
10 kHz-75 GHz

EMC
APPLICATIONS

MILITARY
APPLICATIONS

COMMERCIAL
APPLICATIONS

AMP2083P-2KW
4.0-8.0 GHz

AMP4022DBP-LC-2KW
8.0-12.0 GHz

AMP2080-LC-10KW
10 kHz -250 MHz, 10,000W

EXODUS
ADVANCED COMMUNICATIONS

MPA1081
1-18 GHz, 1W

AMP2074P-2KW
1.0–2.5 GHz, 2KW

MPA1003
2.0-8.0 GHz, 2W

3674 E. Sunset Road, Suite 100, Las Vegas, Nevada 89120 USA
Tel : 1-702-534-6564 Email : sales@exoduscomm.com

www.exoduscomm.com

SigaTek
Wide-Band Microwave Communication Components
Same Day Shipping
Power Dividers DC-70 Ghz
Directional Couplers DC-70 Ghz
90° & 180° Hybrids 0.5-40 Ghz
Bias Tees DC-40 Ghz High Current up to 2 A
Voltage Controlled Phase Shifters 180° & 360°
High Power Couplers Up to 2500 Watts
423 Black Oak Ridge Road
Wayne, NJ 07470
973-706-8475
www.sigatek.com

ray methods.

The first scenario, shown in Figure 3a, illustrates the indoor-to-outdoor coverage of a 3.5 GHz 5G New Radio (NR) macro cell used as a baseline. At 3.5 GHz, 5G signals suffer from high path loss when penetrating walls and other obstacles of a target office building about 1.5 km away. This leads to weak signals and poor reception, particularly in deeper indoor areas away from windows, where dead zones are common.

Figure 3b demonstrates using an NCR equipped with beamforming capabilities strategically placed between the macro cell base station and the target building at approximately 40 meters. The smart repeater receives the weak signal from the base station via its donor antenna, amplifies it and retransmits it through its service antenna toward the target office building. As shown in Figure 3b, the smart repeater is modeled as a service antenna with a 15 dB gain, enhancing the base station signal by about 30 dB and relaying it through the building window. However, there is a significant dead zone or shadow area within the coverage area of the building due to the limited field-of-view of the smart repeater. The efforts at Drexel University were more than just an academic exercise. ***Figure 4*** shows an example of an Airgain 5G NR smart repeater solution that operates in the n77 band of the simulation.

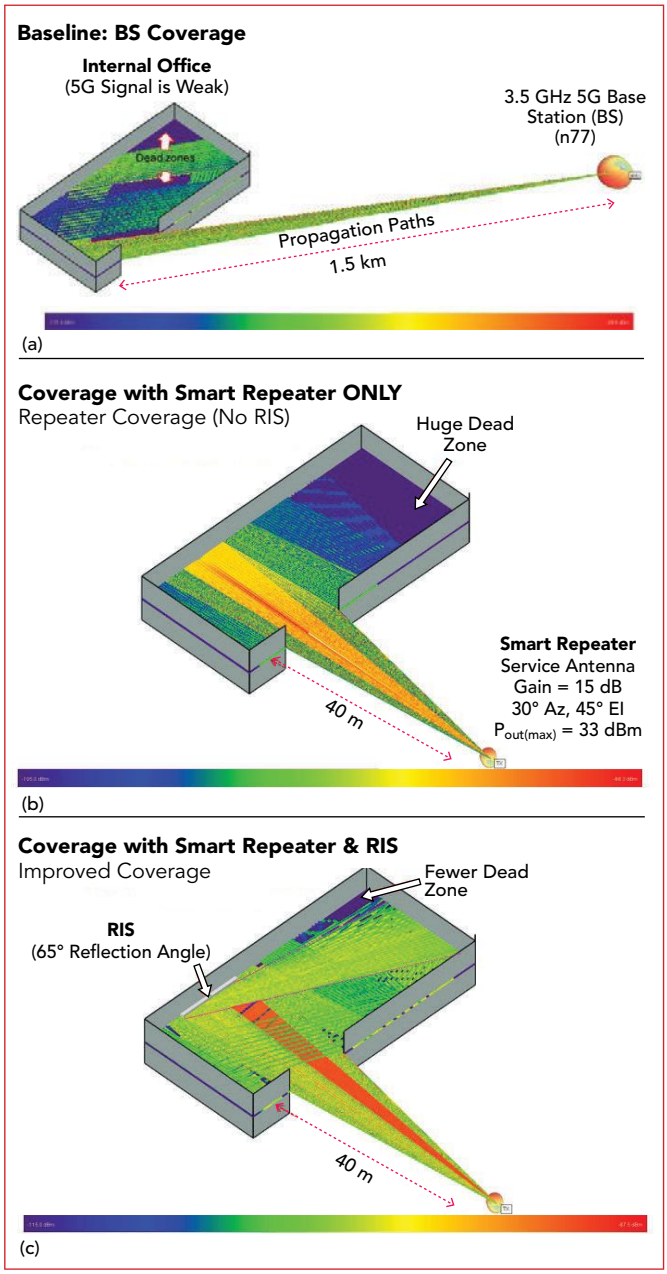

Fig. 3 (a) Baseline base station path loss characteristic. (b) Base station path loss characteristic with a smart repeater. (c) Base station path loss characteristic with smart repeater and RIS. *Source:* Drexel University.

Fig. 4 Airgain Lighthouse 5G NR smart repeater.

Dressed and Ready for Action

Custom Packaged Military Components

Micro Lambda Wireless, Inc offers a complete line of oscillators filters and harmonic generators for the military market. Whether you are designing for an Aircraft, Ship Board, Missile or Ground Based military system, check out the product capabilities available from Micro Lambda Wireless.

Oscillators covering 700 MHz to 40 GHz and filters covering 350 MHz to 50 GHz can be provided based on customer specific requirements. Individual components can also be provided utilizing industrial parts and the top levelcomponents can be screened and tested to specially designed test plans.

Micro Lambda is a ISO 9001:2015 Registered Company

- **MLFI and MLFP Series Bandpass filters**
- **MLFR and MLUN Series Bandreject (notch) filters**
- **MLOS, MLXS, MLOB, MLXB Series Oscillators**

www.microlambdawireless.com

MICRO LAMBDA WIRELESS, INC.

"Look to the leader in YIG-Technology"

46515 Landing Parkway, Fremont CA 94538 • (510) 770-9221 • sales@microlambdawireless.com

To further improve signal coverage and ensure that users in these shadowed areas receive stronger and more consistent 5G signals, an RIS is also integrated and strategically deployed on walls within the building to enhance signal quality. The Wireless InSite 3D software models the RIS using the Communication Research Centre (CRC) Canada's ray optic model.[4] This model consists of a locally periodic, passive metasurface made up of patterns of sub-wavelength scatterers printed on a substrate of glass, plastic or other materials.[5] The scattering behavior of the RIS is dynamically adjusted to steer the signal by 65 degrees, enhancing the 5G signal from the smart repeater and directing it optimally toward shadowed areas in the corner offices far from the window. This leads to fewer dead zones, as shown in Figure 3c. Future indoor RIS can potentially be made more efficient in adapting their state using power sensors integrated with the surface[6] and can be more unobtrusively deployed in indoor environments using novel materials and manufacturing techniques like fabrics.[7] The RIS/smart repeater-enabled 5G network helps overcome the indoor coverage challenges of the 3.5 GHz 5G network, ensuring reliable connectivity in complex environments like office buildings.

IN-BUILDING WIRELESS SOLUTIONS

In the early days of cellular communications, in-building wireless (IBW) coverage was not a primary concern. By the mid-2000s, the need for reliable in-building coverage had grown significantly with the advent of 3G and 4G technologies. This demand has only intensified with the introduction of 5G and now 6G. IBW solutions address these challenges by enhancing network coverage and capacity in areas where the macro network cannot adequately service the demand. This can be due to high penetration losses from building materials, low emissivity glass or the building's structure blocking the signal. Many ongoing simulations on in-building solutions could help resolve complexities around indoor 5G challenges.

Distributed antenna systems (DAS) are popular solutions for improving IBW coverage. This approach involves deploying a network of antennas throughout a building to distribute the signal from a central location. There are several types of DAS, including passive, active, hybrid and digital DAS. Each of these DAS types has advantages and limitations depending on the size and type of venue.

AMPLIFYING THE BENEFITS

Enhanced 5G connectivity has the potential to revolutionize industries while consumers seek better streaming experiences and more connected smart home devices. For telecom operators, the challenge lies in maximizing network performance using existing infrastructure without the need for an excessive number of additional base stations. Extending 5G coverage beyond urban areas to underserved regions is also cru-

iNRCORE
Family of Brands

Reliable, Intelligent Solutions Generating
A Powerful Connection Everywhere

A Family of Brands That Support Your Complete

HIGH-PERFORMANCE

Precision Electronic Component Needs

Our Products

- Broadband Conicals •
- Chip Inductors •
- Military QPL Inductors •

- Bias Tee Filters •
- Lowpass/Highpass Filters •
- EMI/RFI Filters •

- RF Beads •
- Ethernet Transformers •
- Custom Magnetics •

support@inrcore.com
www.inrcore.com/brands/
(215) 781-6400

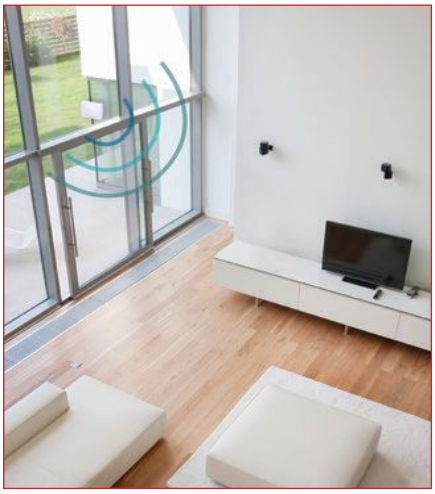

Fig. 5 **Airgain Lighthouse Micro Smart Repeater.**

cial in ensuring broader accessibility. Unobtrusive solutions, like the Airgain Lighthouse Micro Smart Repeater shown in ***Figure 5***, will help with small-office and home-office adoption of the technology.

To achieve this, network providers must adopt the latest technologies that address these challenges and unlock the numerous benefits 5G offers, such as faster download and upload speeds, improved reliability and reduced latency. Solutions like RIS, smart repeaters and NCR are helping network operators optimize their investments. These innovations reduce deployment costs by leveraging existing infrastructure while enhancing signal quality and coverage, making them valuable assets in the industry's toolkit.

The demand for reliable, high speed 5G connectivity is growing. These and other technologies are the key to overcoming challenges such as signal interference and rising operational costs. New developments in these areas will pave the way for smarter, more connected communities and industries, ensuring that the transformative promise of 5G and, eventually, 6G becomes a global reality. ■

References

1. "Worldwide Broadband Speed League 2024," *cable.co.uk*, Web: www.cable.co.uk/broadband/speed/worldwide-speed-league/?mc_cid=05b0480aeb&mc_eid=659a6c0250.
2. "Supercharging Small Businesses," *Vodafone*, March 2024, Web: www.vodafone.co.uk/newscentre/app/uploads/2024/02/Supercharging-Small-Businesses-Web-Hi-Res.pdf.
3. "Wireless InSite® 3D Wireless Propagation Software," *Remcom*, Web: https://www.remcom.com/wireless-insite-em-propagation-software.
4. Y. L. C. de Jong, "Uniform Ray Description of Physical Optics Scattering by Finite Locally Periodic Metasurfaces," *IEEE Transactions on Antennas and Propagation*, Vol. 70, No. 4, 2022, pp. 2949–2959.
5. S. Stewart, Y. L. C. de Jong, T. J. Smy and S. Gupta, "Ray-Optical Evaluation of Scattering From Electrically Large Metasurfaces Characterized by Locally Periodic Surface Susceptibilities," *IEEE Transactions on Antennas and Propagation*, Vol. 70, No. 2, 2022, pp. 1265–1278.
6. M. A. S. Tajin, K. Anim and K. R. Dandekar, "Incident Power and Relative Phase Distribution Mapping in Reconfigurable Intelligent Surfaces Using Energy Harvesting," *IEEE Transactions on Antennas and Propagation*, Vol. 71, No. 7, 2023, pp. 6111–6119, Web: https://ieeexplore.ieee.org/document/10105212.
7. K. Anim, M. A. Saleh Tajin, C. E. Amanatides, G. Dion and K. R. Dandekar, "Conductive Fabric-Based Reconfigurable Intelligent Surface," *IEEE International Symposium on Antennas and Propagation and USNC-URSI Radio Science Meeting* (AP-S/URSI), 2022, pp. 1484–1485.

MU-DEL ELECTRONICS
an IRONWAVE Technologies Company
Founded in 1967. Mu-del Electronics excels in the development, design and manufacturing of RF communication products.
MULTICOUPLERS
FREQUENCY CONVERTERS
RF SWITCH DISTRIBUTION SYSTEMS
703.368.8900 • www.mu-del.com

RF BAY
RF Bay, Inc provides online buying capability for customers requiring critical RF components immediately. Provide RF and microwave components in the frequency range from under 1KHz to over 50GHz.
Low Noise Amplifiers
Power Amplifiers
Frequency Dividers/Prescalers
Frequency Doublers/Triplers/Multipliers
301.880.0921 • www.rfbayinc.com

IRONWAVE TECHNOLOGIES
LEADING PROVIDER OF RF AND MICROWAVE, RF OVER FIBER, AND COMMS EXTENSION SOLUTIONS

LUFF RESEARCH
an IRONWAVE Technologies Company
Specializing in the design and manufacture of high performance, high reliability state-of-the-art RF/Microwave Frequency Synthesizers and Phase-Locked Oscillators
OSCILLATORS
SYNTHESIZERS
CUSTOM INTEGRATED MULTI-FREQUENCY SOURCES

SYNTONICS
an IRONWAVE Technologies Company
An engineering driven, mission-focused developer of Communications/ Radar/ related technologies and products.
516.358 2880 • www.LuffResearch.com
410.884.0500 • www.syntonicscorp.com

AMERICAN MICROWAVE
an IRONWAVE Technologies Company
American Microwave Corporation offers a wide variety of Switches, Attenuators, Power dividers, DLVA's and Integrated Assemblies up to 40 GHz.
SOLID STATE SWITCHES
POWER DIVIDERS
DIGITAL VARIABLE ATTENUATORS
INTEGRATED ASSEMBLIES
DETECTOR LOG VIDEO AMPLIFIERS
703.368.8900 • www.americanmic.com

New Bias Tees

We offer a range of in-stock, Bias Tees to address a variety of applications, including test and measurement, research and development, optical communications, satellite communications and more.

In-Stock & Shipped Same-Day

24
SAME-DAY SHIPPING

CUSTOM CABLES

LIVE TECH SUPPORT

fairviewmicrowave.com
+1 (800) 715-4396

Fairview Microwave®
an INFINITE brand

INVITED PAPER

Designing IoT Devices Embedding Antenna Boosters Using Freeware and Low-Cost Equipment

J. Valle*, A. Andújar** and J. Anguera*,**
* *Smart Society Research Group, Universitat Ramon Llull, Barcelona, Spain*
** *Ignion, Barcelona, Spain*

In an ever-evolving technological landscape, the optimization of antennas for enhanced connectivity is of paramount importance. This article introduces an approach to leveraging free tools and low-cost equipment to design an IoT device operating from 863 to 928 MHz using antenna boosters. The design process begins by using a library with pre-simulated impedances of antenna boosters on different ground planes of wireless devices. Then, simulation is carried out to impedance match using free software to synthesize a matching network for an antenna booster, considering the topology and actual components, like inductors and capacitors. The circuit simulation even considers the pad layout for component hosting, simplifying the prototyping. Subsequently, a prototype was built and tested with a low-cost vector network analyzer (VNA). This process demonstrates that freeware and low-cost equipment are viable options for designing wireless devices with embedded antenna boosters.

The rapid increase in demand for wireless connectivity in various applications has emphasized the need to optimize antennas for specific environments. For professional applications, antenna systems are simulated with electromagnetic (EM) software and measured with sophisticated equipment, such as VNAs and anechoic chambers. However, freeware and low-cost tools are proposed for early engineering engagement.[1,2] This alternative approach engages researchers in designing wireless devices embedding antennas and provides a cost-effective and simplified method for antenna design. These designs can be transitioned to professional tools for more accurate device characterization.

To illustrate the simplicity of the design process, a small, non-resonant element will be used in the desired frequency band by modifying the associated matching network.[3] This non-resonant antenna booster element measures 12 × 3 × 2.4 mm^3. It will be integrated into the FR4 board shown in ***Figure 1***.[4]

This design procedure is significantly more straightforward than those based on altering the antenna's geometry.[5] For the antenna booster, only the matching network requires adjustment since an antenna booster can be used for many frequency bands and form factors.[6] This ease of use is thanks to the non-resonant nature of antenna booster circuit design tools based on matching network synthesis.[7] This is a significant advantage as designing a wireless device incorporating an antenna booster can be easily tackled by designing a matching network, which is straightforward, quick and can be entirely addressed by circuit simulation.

Creating a library of devices with different form factors, including antenna boosters, where S-parameters are included over an extensive frequency range, creates the opportunity to simplify the design process. The designer can then select the form factor best suited to the requirements and design

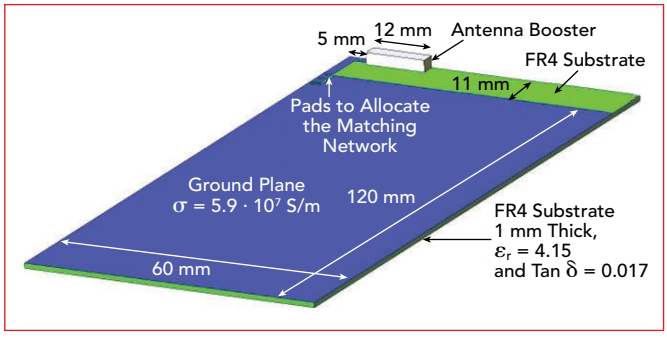

Fig. 1 **Antenna booster on FR4 ground plane.**

PERFORMANCE THAT SEEMS UNREAL

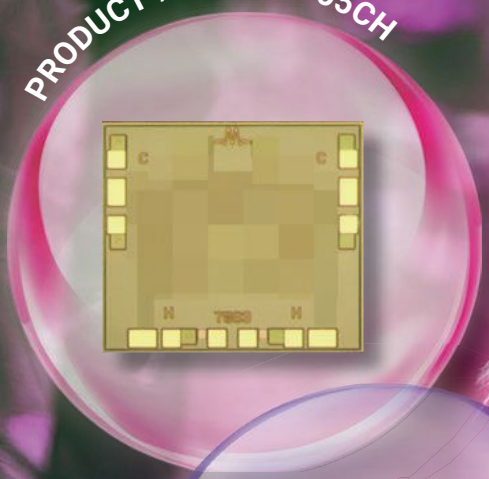

PRODUCT #MDPX-0305CH

PRODUCT #MDPX-00003/4/5/6/7/8PSM

Don't have a **BIG FOOT**print: use MMIC

With the release of the MDPX MMIC diplexer family, Marki Microwave now offers multiple filtering solutions for electronic warfare applications. Marki Microwave's growing portfolio includes bandpass, low-pass and high-pass solutions from 2-18 GHz, diplexers from 3-18 GHz and quadplexers from 4-18 GHz. As RF market trends continue to prioritize SWaP to support high channel density, Marki Microwave's compact MMIC filter designs are enabling the development of next-generation EW systems.

APPLICATIONS

- **Electronic Warfare**
- **SATCOM**
- **Reflectionless Filter Applications**

Marki® microwave

www.markimicrowave.com

RFMW®

Global Distribution Partner

Contact: sales@rfmw.com

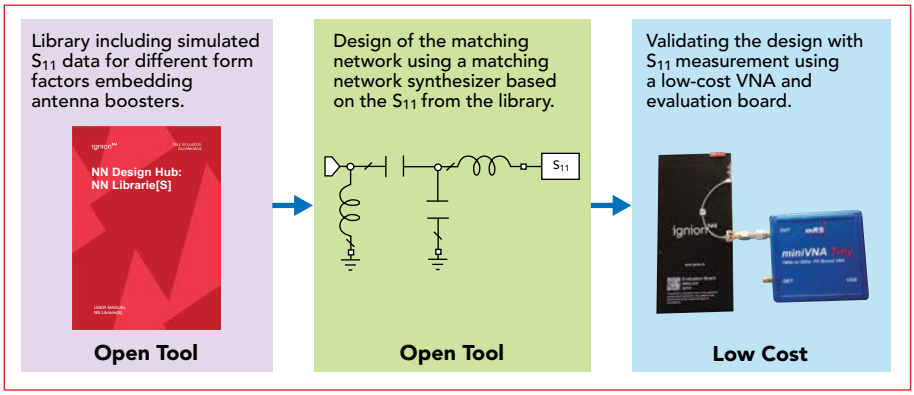

Fig. 2 **Design flow chart.**

the matching network using the library.[8,9] Such a library contains presimulated S_{11} data corresponding to different antenna boosters on PCBs of different sizes.

This article details starting with S-parameter data from a library, designing a matching network with another freeware matching design tool and testing the S-parameter data with a low-cost VNA. Since the library has been extensively covered,[8] this article focuses on using freeware to design the matching network and measure the S_{11} parameter with a low-cost VNA. The design flow chart for this process is shown in ***Figure 2***.

Before selecting a freeware matching network design tool, a comparison analysis has been made between the different synthesis tools. The matching network synthesis program must handle complex frequency-dependent impedances and synthesize matching networks with multiband performance at $f_1 - f_2$ and $f_3 - f_4$ (for example, 824 to 960 MHz and 1710 to 2690 MHz) and the ability to include real inductors and capacitors with finite Q-factors. ***Table 1*** shows programs addressing these needs.

XFdtd Remcom, Optenni-Lab, Cadence AWR Microwave Office and Atyune meet the three criteria in Table 1. The first three software packages offer functionality and are excellent reference tools for professional applications. However, this design uses Atyune because it is an open and easy-to-use tool to synthesize matching networks. It focuses on providing clear and practical guidance to match antennas to specific ground plane dimensions. This software is free to use.

A FREEWARE TOOL FOR MATCHING NETWORK SYNTHESIS

Matching software allows the user to analyze antenna-matching networks. The software will determine parameters like S_{11}, bandwidth, tolerances and matching network efficiency. In addition, these programs can synthesize the matching network for a requirement and specify the components to realize that network.

In this case, the simulations begin with S-parameters from platforms, including antenna boosters, that have been previously simulated. A free library is available from Ignion.[8,9] For example, the device in Figure 1 has been simulated with IE3D, an EM full wave solver. This S_{11} data is available in the library,[8] allowing a designer to synthesize a matching network using the flow diagram of Figure 2.

THE NEED FOR A MATCHING NETWORK

The S_{11} of the circuit in Figure 1 is shown in ***Figure 3***. The S_{11} performance is poor in the desired 863 to 928 MHz frequency region. The goal is to design a matching network with an S_{11} value of less than -6 dB.

Efficient matching is essential to optimize system performance and ensure maximum power transfer between the source and load. A mismatch can result in signal reflec-

smiths interconnect

Cutting-edge Connectivity

Reliable and customizable solutions for mission critical applications

We offer:

Board-Level Components

Radio Frequency Filters

Cable Assemblies & Connectors

Isolators & Circulators

Radio Frequency Converters

Switched Filter Bank & Frequency Synthesizers

more > smithsinterconnect.com

tions and power loss. The results from Figure 3 show S_{11} = -1 dB at 900 MHz. This means that only 20 percent of the available power is delivered to the antenna system, corresponding to 6.8 dB of mismatch loss. The matching network will match impedances to optimize the source and load. The program will synthesize the topology and components, such as inductors and capacitors, for the desired matching network.

BANDWIDTH POTENTIAL

To optimize the matching network design, the potential bandwidth of the antenna impedance must be analyzed. This step is crucial to determine if the design can provide enough bandwidth. Bandwidth potential allows the designer to estimate the bandwidth even if the antenna is not matched. If the potential bandwidth is larger than the target bandwidth, then a simple matching network with one or two components can be designed to meet the bandwidth requirements. It is important to mention that bandwidth potential can be exceeded when using broadband matching networks. For example, a broadband matching network using an LC resonator can theoretically improve the bandwidth by 2.45 at SWR = 3.[19,20,21]

The Atyune tool facilitates the efficient evaluation of bandwidth potential. It allows the exploration of configurations and settings directly affecting it, ensuring that the final design meets the desired bandwidth requirements. In the case of the antenna booster in Figure 1, the operating range is 863 to 928 MHz, resulting in a 65 MHz bandwidth. ***Figure 4*** shows the bandwidth potential curve. At 900 MHz, the value is 175 MHz, equating to 19.4 percent, indicating enough bandwidth with an appropriate matching network.

MATCHING NETWORK DESIGN

Since there is enough bandwidth potential, the program will be used to design a matching network with an S_{11} of less than -6 dB in the 863 to 928 MHz frequency range. This design will be synthesized to limit the system's required components. In this case, the matching network contains two elements, as shown in ***Figure 5***. L1 is a 15 nH inductor with

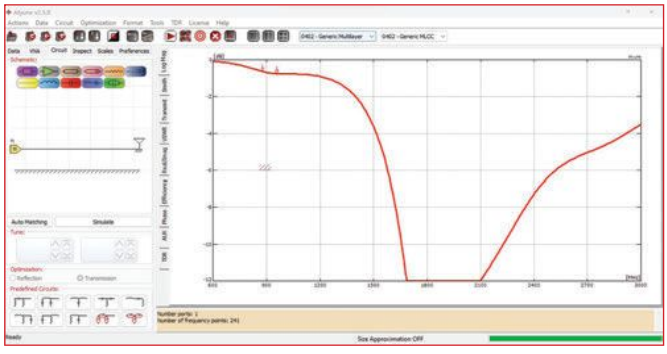

▲ Fig. 3 **Antenna booster S_{11} response using Atyune.**

TABLE 1

MATCHING NETWORK DESIGN PROGRAMS COMPARISON

	Complex Frequency-Dependent Impedances	*Multi-band Matching Networks*	*Real Components*
Atyune[10]	YES	YES	YES
Antune[11]	YES	YES	NO
IMNLab[12]	YES	NO	YES
Matlab[13]	YES	NO	YES
Qorvo MatchCalc[14]	YES	NO	NO
Altium[15]	YES	NO	YES
XFdtd Remcom[16]	YES	YES	YES
Optenni-Lab[17]	YES	YES	YES
AWR Microwave Office[18]	YES	YES	YES

Remtec is the whole package!

Offering exceptional quality, highly innovative, and American-made ceramic solutions for the Microwave & RF industry

High power? High density? Small form factor? Remtec can help develop the best additive *or* subtractive (etched) ceramic circuit for YOUR unique radar, cellular, IoT, or other project.

- Choose from Al203, AIN, BEO, direct-bond copper, thick film, more
- We offer single or integrated components, substrates, packages, multilayer/heterogeneous circuits, more
- ISO 9001:2015 certified; RoHS and ITAR compliant
- Design-build or build-to-print
- Average customer relationship: 15 years
- MADE IN THE USA!

REMTEC

Represented in Western U.S. by **NWN-Inc.com**

remtec.com

PPI Passive Plus
RF & Microwave Components

Medical
Telecommunications
Semiconductor
Military
Broadcast
Industrial Laser

High Power CUSTOM ASSEMBLIES

High-Q Low ESR RF Microwave CAPACITORS

Broadband CAPACITORS

Broadband RESISTORS

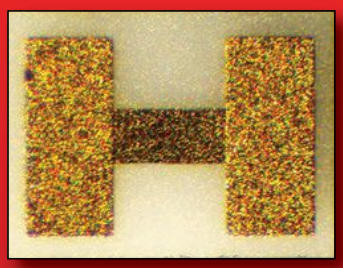

ISO Certified
Quick Deliveries
Competitive Pricing
Inventory Programs
Engineering Support
C.A.P. Engineering Program
Excellent Customer Service

Modelithics®

Contact us today: 631-425-0938 • sales@passiveplus.com • www.PassivePlus.com

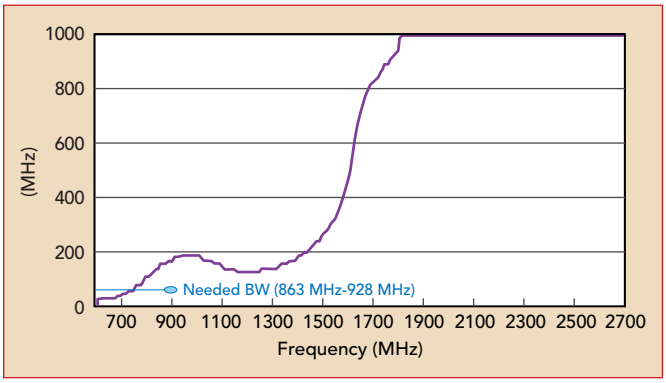

Fig. 4 **Bandwidth potential at SWR = 3 for antenna booster.**

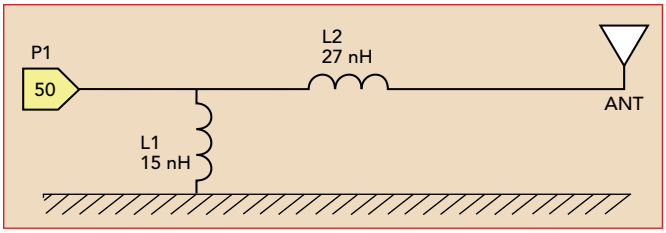

Fig. 5 **Synthesized matching network.**

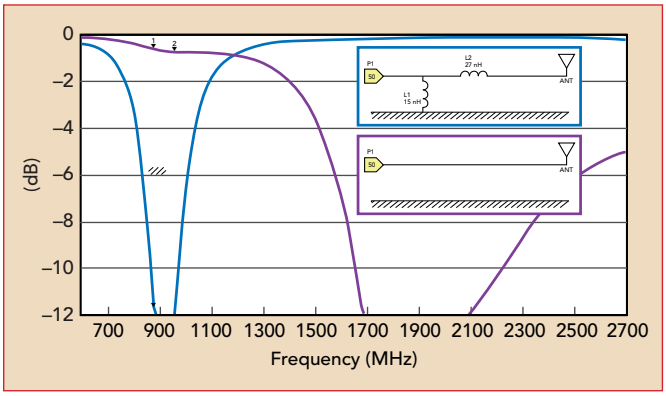

Fig. 6 **Antenna booster S_{11} results with and without matching network.**

a Q of 87 and L2 is a 27 nH inductor with a Q of 89. The program allows real-time adjustments to enable experimentation and optimization.

The simulated results of the antenna booster from Figure 1, with and without the matching network, are shown in ***Figure 6***. The matching network enables an S_{11} value from the antenna of better than -6 dB from 810 to 1000 MHz. This 190 MHz bandwidth easily satisfies the 863 to 928 MHz antenna booster frequency range. The 20.9 percent bandwidth of the booster circuit is also close to the 19.4 percent bandwidth potential shown in Figure 4.

The total matching network efficiency is defined in ***Equation 1*** as:

$$\eta_t = \eta_m \cdot (1 - |S_{11}|^2) \quad (1)$$

Where:

η_t = Total efficiency

η_m = Matching efficiency

This antenna booster's average efficiency is 83 percent over the 863 to 928 MHz frequency range. It should be noted that the total efficiency takes the mismatch and the matching efficiency due to the finite Q of the lumped

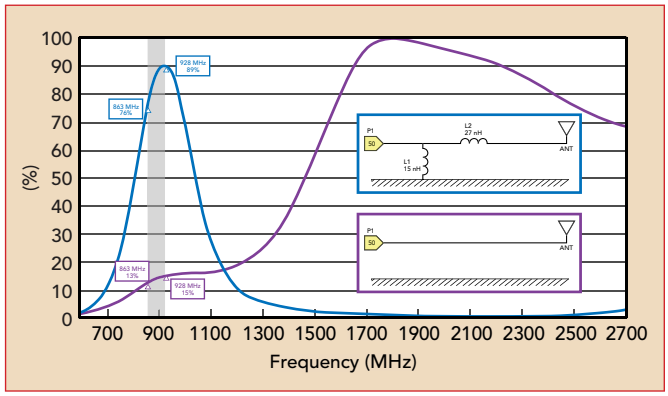

Fig. 7 **Total efficiency with and without the matching network.**

inductors used in the matching network into account. The total efficiency results for the matched and unmatched antenna booster circuits are shown in ***Figure 7***.

MATCHING NETWORK DESIGN CONSIDERING THE PAD LAYOUT

With the bandwidth and efficiency analysis complete, the next step is to build the board. Before fabricating the board, the size of the lumped component pads and their impact on circuit performance must be considered. Each pad can be modeled by a short transmission line and S_{11} can be computed. In this case, the pads form an asymmetric coplanar transmission line. The characteristic impedance and effective permittivity can be easily found.[3]

Figure 8 shows the circuit board layout for this exercise. This layout contains several series and shunt elements to accommodate a variety of circuit configurations. The matching network under consideration requires only Z1 and Z2, so Z3, Z6 and Z7 are shorted, while Z4 and Z5 are left open.

The next step is to add the actual pads to the matching network values. This means modeling each pad as a transmission line and determining the impedance, attenuation, permittivity and length characteristics. From Figure 8, Z1 is the 27 nH inductor (L2), Z2 is the 15 nH inductor (L1) and there is a 2 mm transmission line between Z1 and Z2. Since Z3, Z6 and Z7 are shorted together, they are modeled as a 13 mm transmission line. The matching network with actual pad characteristics is

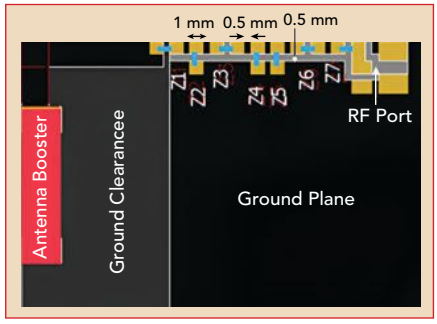

Fig. 8 **Circuit board layout.**

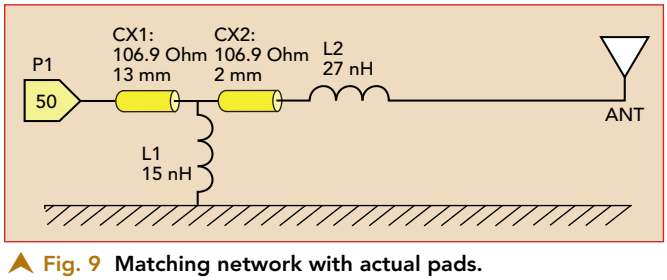

Fig. 9 **Matching network with actual pads.**

Accurate RF Analysis in the Field

Identify interference and signal degradation with ease.

Signal Hound's portfolio of real-time spectrum analyzers and monitoring receivers offers high-performance and reliability at an accessible price. With wide frequency ranges up to 43.5 GHz, ultra-fast sweep speeds up to 200 GHz/sec, and low phase noise, the BB60D, SP145, and SM435C are ideal companions for your remotely located RF data analysis needs.

BB60D
6 GHz Spectrum Analyzer

SP145
14.5 GHz Spectrum Analyzer

SM435C
43.5 GHz Spectrum Analyzer

Signal Hound®

SignalHound.com

Made in the USA

© 2024 Signal Hound. All rights reserved.

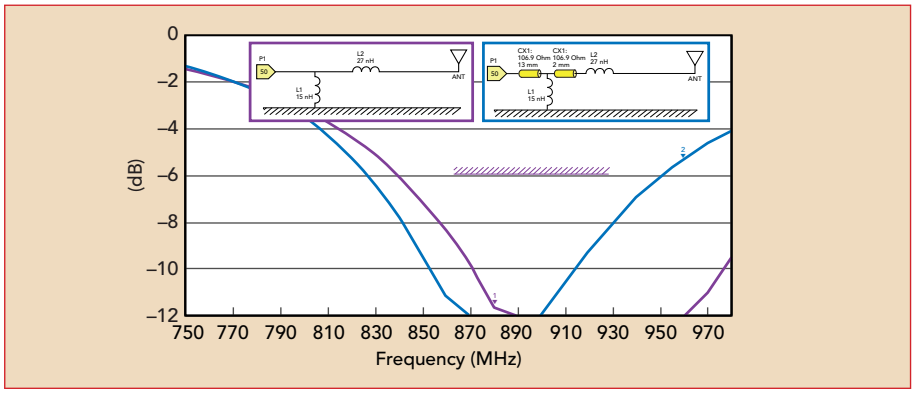

Fig. 10 S_{11} comparison with and without pads.

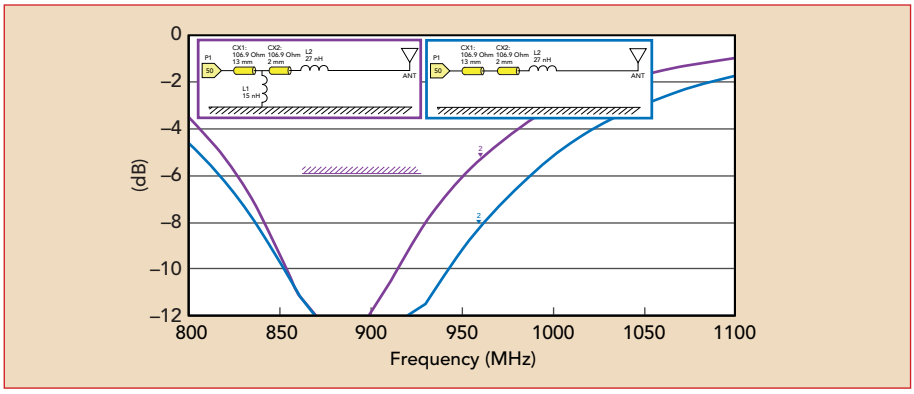

Fig. 11 S_{11} matching network with and without the 15 nH parallel coil.

shown in ***Figure 9***.

With the actual pads included, the matching network is simulated with L1 and L2 values to analyze the impact of the pads. The result is a 133 MHz, or 15.4 percent, bandwidth from 795 to 928 MHz, where S_{11} is less than -6 dB. The frequency shifts to lower frequencies because of the inductance introduced by the 2 mm transmission line. These results are shown in ***Figure 10***.

The next step is to optimize the values L1 and L2 to incorporate the effects of the pad layout. Atyune's AutoMatching feature will update the initial component values to incorporate the effects of the added pads. After adding the pads, the antenna booster meets the S_{11} requirements, so no optimization is needed. In other cases, the optimization tool is useful for fine-tuning values to incorporate layout impacts. The simulation results in a bandwidth of 215 MHz, or 23 percent and the design meets the S_{11} requirements from 825 to 1040 MHz. These results are shown in ***Figure 11***.

After careful analysis, it was determined that the 15 nH parallel inductor could be removed. The impedance of this component at 900 MHz is high enough that removing it does not have a relevant effect. Figure 11 shows that the bandwidth of the matching network improves with the inductor removed.

Figure 12 shows the total efficiency of the final matching network. The average value is 78 percent. This efficiency calculation considers S_{11}, the losses due to the finite Q of the 27 nH inductor and the losses of the layout.

TOLERANCE ANALYSIS

The Atyune program considers component tolerances in the S_{11} analysis. In this case, the component tolerance was set to two percent and the Monte Carlo analysis showed a robust matching network with all S_{11} results over the operating band less than -6 dB. The results are shown in ***Figure 13***.

PROTOTYPING AND MEASUREMENTS

With the analysis and optimization complete, the next step is manufacturing the matching network

ZERO BIAS SCHOTTKY DETECTORS
For 0.01 - 50 GHz

Many Models Available in Stock

> Single unit covers 0.01 - 50 GHz
> Matched input for low VSWR
> Flat frequency response
> High sensitivity (0.5 mV/µW up to 50 GHz)
> Optional output connectors (SMA, BNC, SMC)
> Great for instrumentation and laboratory use

MODEL	FREQ. RANGE	MAX. VSWR	MAXIMUM FLATNESS (± dB)	LOW LEVEL SENSITIVITY (mV / µW)
DZR50024A	10 MHz-50 GHz	1.3:1 (to 18 GHz) 1.6:1 (to 26 GHz): 1.8:1 (to 40 GHz) 2 :1 (to 50 GHz)	± 0.3 (to 18 GHz) ± 0.6 (to 26 GHz) ± 0.8 (to 40 GHz) ± 1.0 (to 50 GHz)	0.5
DZR50024B	10 MHz-50 GHz			0.5
DZR50024C	10 MHz-50 GHz			0.5

*All models have 2.4 mm (M) input connector
*Standard output polarity is negative.
Add letter "P" to end of model number for positive output.
Custom Designs - Write / Call for Quote
Other Products:
Amplifiers, Comb Generators, Limiters, Switches, Integrated Subsystems
Herotek
155 BAYTECH DRIVE, SAN JOSE, CA. 95134--2303
PH: 408-941-8399 . FAX: 408-941-8388
E-Mail: Info@Herotek.com
Web Site: http://www.herotek.com
Visa/MasterCard Accepted

RF-LAMBDA

THE LEADER OF RF BROADBAND SOLUTIONS

EUROPE DEUTSCHLAND

RF SWITCHES

MM / MICROWAVE DC-90GHz

160 CHANNELS
mm/Microwave

0.05-20GHz
Filter Bank Switch Matrix
For Phase Array Radar Application Satellite communication.

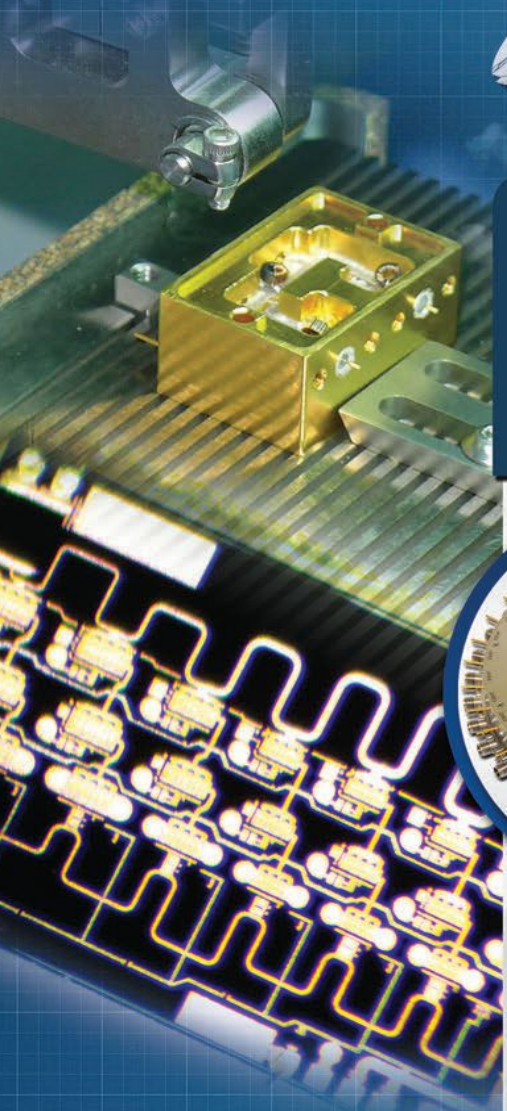

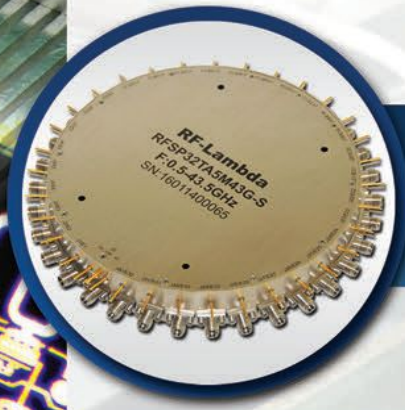

PN: RFSP32TA5M43G
SP32T SWITCH 0.5-43.5GHz

PN: RFSP16TA5M43G
SP16T SWITCH 0.5-43.5GHz

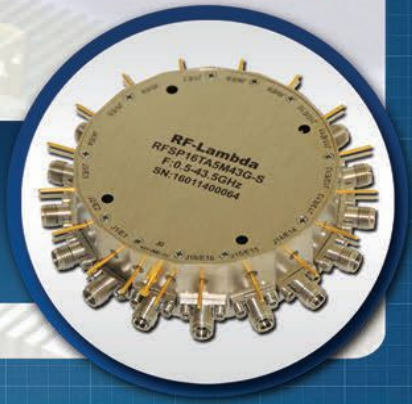

www.rflambda.com
sales@rflambda.com

1-888-976-8880
1-972-767-5998

San Diego, CA, US
Plano, TX, US

Ottawa, ONT, Canada
Frankfurt, Germany

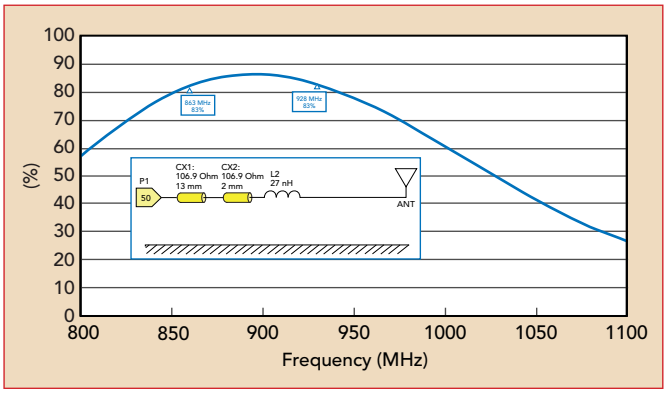

Fig. 12 Matching network efficiency for the final matching network.

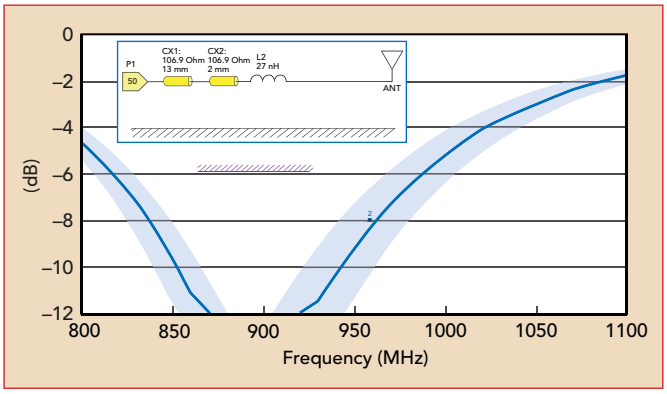

Fig. 13 S_{11} considering the inductor tolerance.

Fig. 14 S_{11} measurement with a low-cost VNA.

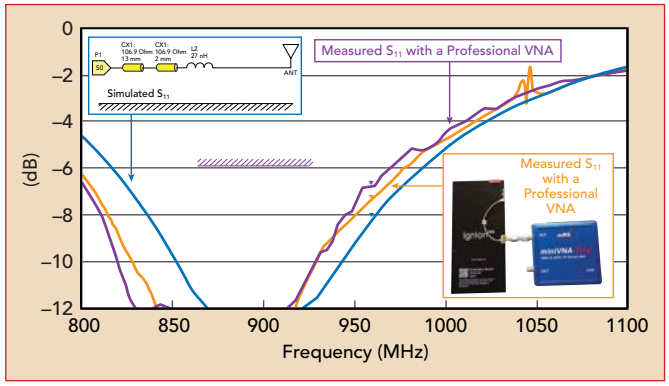

Fig. 15 Measured versus simulated results for the matching network.

Ultra Low Phase Noise **Sapphire** Oscillator

TQSRO-C50

OCXO synthesizer Sapphire Oscillator

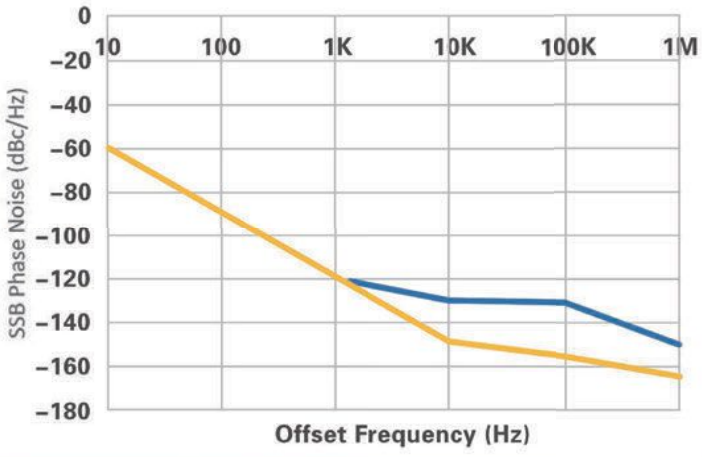

FEATURE

- Frequency Range: 8GHz-12GHz
- Ultra Low Phase Noise (@10GHz) :
  < -146dBc/Hz@10kHz
  < -153dBc/Hz@100kHz
- Frequency Tuning: ±1 ppm
- Size: 125*105*60mm

SHUTAI

Changsha Tianqiong Electronic Technology Co.,Ltd

http: //oscillator.t-timing.com/ en E-mail: sales@ t-timing.com

PERASO

WIRELESS UNLEASHED™

60 GHz Tactical Communications

Secure, Stealthy Wireless Solutions

- Chipsets
- Modules
- Software
- Eval Kits

For addition information please contact sales@perasoinc.com

and checking the actual results versus the simulation. To maximize the matching network's efficiency, the Q of the matching components must be as high as possible. In this case, a 0603 SMD inductor with Q = 89 at 900 MHz has been selected instead of the 0402 version with a Q of approximately 58.

To measure the corresponding S_{11}, the matching network is implemented and the system is connected to a mini VNA. The VNA is calibrated using a standard short/open/load calibration. This setup is shown in ***Figure 14***.

The matching network has also been measured on a professional, lab-grade VNA to complete the investigation. The measurements from both instruments show good agreement, with a measured bandwidth of 19.8 percent. This measured bandwidth compares well with the simulated bandwidth of nearly 23 percent. Both measurement instruments did show a slight frequency shift of 7 percent versus the simulated result. The results are shown in ***Figure 15***.

CONCLUSION

This article presents a novel approach to designing and optimizing IoT devices with embedded antenna boosters. Its premise is that leveraging the Ignion library, freeware and a low-cost VNA provides an accessible, cost-effective pathway for researchers to engage in RF design and wireless device development. Integrating an antenna booster into the ground plane simplifies the design process by focusing on the matching network rather than altering antenna geometry. This approach demonstrates that effective antenna designs operating in the 863 to 928 MHz frequency band are achievable even with basic, affordable tools.

This design method reduces costs and lowers the entry barrier for RF design. This should help promote broader participation and innovation in wireless communications. By adopting this approach, researchers can gain valuable hands-on experience and a deeper understanding of antenna design principles before transitioning to more sophisticated and precise professional tools. ■

References

1. A. Gupta et al., "DIY Antenna Studio: A Cost-Effective Tool for Antenna Analysis [Education Corner]," *IEEE Antennas and Propagation Magazine*, Vol. 63, No. 2, April 2021, pp. 83–88, doi: 10.1109/MAP.2021.3057310.
2. A. Rocha, S. Mota and M. Sousa, "A Demonstrator for Impedance Matching Systems in Transmission Lines With Time and Frequency Simulation [Education Corner]," *IEEE Antennas and Propagation Magazine*, Vol. 61, No. 3, June 2019, pp. 92–103, doi: 10.1109/MAP.2019.2907900.
3. J. Anguera, A. Andújar, J. Leiva and R. Mateos, "Embedded Antennas in Cellular IoT Platforms," *European Conference on Antennas and Propagation*, EuCAP, March 2020, Copenhagen, Denmark.
4. J. Anguera, N. Toporcer and A. Andújar, "Slim Booster Bars for Electronic Devices," May 2018, U.S. Patent 9,960,47.
5. J. Anguera, A. Andújar, G. Mestre, J. Rahola and J. Juntunen, "Design of Multiband Antenna Systems for Wireless Devices Using Antenna Boosters," *IEEE Microwave Magazine*, Vol. 20,

No. 12, Dec. 2019, pp. 102–114, doi: 10.1109/MMM.2019.2941662.
6. J. Anguera, A. Andújar and C. Puente, "Antenna-Less Wireless: A Marriage Between Antenna and Microwave Engineering," *Microwave Journal*, Vol. 60, No.10, October 2017, pp. 22–36.
7. J. Anguera, A. Andújar and C. Puente, "Virtual Antenna™: Easy Design of IoT Devices with Embedded Antennas," *MWEE RF-Microwave*, Sept. 2019.
8. J. Anguera, C. Puente, A. Andújar, R. M. Mateos, D. Vye and M. Lien, "Antenna Library for IoT Devices with Antenna Boosters," *50th European Microwave Conference (EuMC)*, 2021, Utrecht, Netherlands, pp. 1147–1150, doi: 10.23919/EuMC48046.2021.9338246.
9. NN Design Hub: NN Librarie[S], *Ignion*, Web: https://ignion.io/files/UM_Libraries_Generic.pdf.
10. Aytune, Web: https://www.atyune.com.
11. A New Level of RF Network Design, *Aytune*, Web: https://www.antune.net/index.html.
12. IMNLab, Web: https://imnlab.wordpress.com.
13. Matching Network Design - MATLAB & Simulink, *MathWorks España*, Web: https://es.mathworks.com/help/rf/matching-network-design.html.
14. Qorvo MatchCalc RF Impedance Matching Calculator, *Qorvo*, Web: https://www.qorvo.com/design-hub/design-tools/interactive/matchcalc.
15. Z. Peterson, "Antenna Impedance Matching Network Circuit Simulation in Altium Designer," *Altium*, April 5, 2020, Web: https://resources.altium.com/p/antenna-impedance-matching-network-simulation-altium-designer.
16. "Matching Network Design Simulation Software," *Remcom*, Web: https://www.remcom.com/matching-network-design-simulation-software.
17. O. Pekonen, J. Rahola and S. Kosulnikov, "Circuit Synthesis Software for Antenna and RF Optimization," *Optenni Ltd.*, March 7, 2024, Web: https://optenni.com/.
18. AWR Microwave Office, *Cadence*, Web: https://www.cadence.com/en_US/home/tools/system-analysis/rf-microwave-design/awr-microwave-office.html.
19. J. Anguera, C. Puente, C. Borja, G. Font and J. Soler, "A Systematic Method to Design Single-patch Broadband Microstrip Patch Antennas," *Microwave and Optical Technology Letters*, Vol. 31, No. 3, Nov. 2001, pp.185–188.
20. A. Andújar, J. Anguera and C. Puente, "A Systematic Method to Design Broadband Matching Networks," *Conference Proceedings of the Fourth European Conference on Antennas and Propagation*, Barcelona, 2010.
21. A. R. Lopez, "Double-Tuned Impedance Matching," *IEEE Antennas and Propagation Magazine*, Vol. 54, No. 2, April 2012, pp. 109–116, doi: 10.1109/MAP.2012.6230722.

HAROGIC

Extend
RF Boundaries.

REAL-TIME
SPECTRUM ANALYZER
UP TO 40 GHz

info@harogic.com www.harogic.com

Available model

Model	SAE-200	SAN-400	PXE-200	PXN-400	NXE-90
Type	USB	USB	Handheld	Handheld	Networked
Frequency	9 kHz-20 GHz	9 kHz-40 GHz	9 kHz-20 GHz	9 kHz-40 GHz	9 kHz-9.5 GHz
1 GHz phase noise, 10 kHz offset	-100 dBc/Hz	-107 dBc/Hz	-100 dBc/Hz	-107 dBc/Hz	-100 dBc/Hz
1 GHz DANL	-168 dBm	-161 dBm	-168 dBm	-161 dBm	-168 dBm
Sweep speed	1 THz/s	500 GHz/s	900 GHz/s	500 GHz/s	600 GHz/s
Analysis bandwidth			100 MHz		
Starting at	8,498USD	9,498USD	8,998USD	9,998USD	5,498USD

Editor's Note: Part 1 of this tutorial appeared in the October issue of *Microwave Journal*. It addresses extracting DC diode parameters and using Excel to optimize the diode model. Part 2 addresses a similar methodology for AC parameters. Taken together, readers will get a simple, yet powerful tool for optimizing diode models.

Extracting Diode Parameters Using Optimization in Excel Part 2: AC Parameters from Capacitance Measurements

INVITED PAPER

Charles Trantanella
Retired from Custom MMIC, Westford, Mass.

Part 2 of this tutorial builds upon the process for extracting DC diode parameters presented in the October 2024 issue of *Microwave Journal*. This next installment describes extracting pertinent AC diode model parameters from measurements using Excel. This part of the process is concerned with the behavior of the diode in the OFF region, where the voltage across the diode, V_d, causes it to function as a variable capacitor ($V_d < 0$). Of course, the diode is not completely OFF in this region, as there is usually a very small amount of leakage current flowing through the device. However, as will be done here, this leakage can usually be ignored in most RF and microwave applications.

This tutorial discusses the two main types of capacitance versus voltage profiles that diodes can generate, depending on their underlying semiconductor technology. Models are presented for both profiles, followed by an example of each where the pertinent parameters are extracted. Finally, the tutorial will discuss the implementation of these models in a circuit simulation tool.

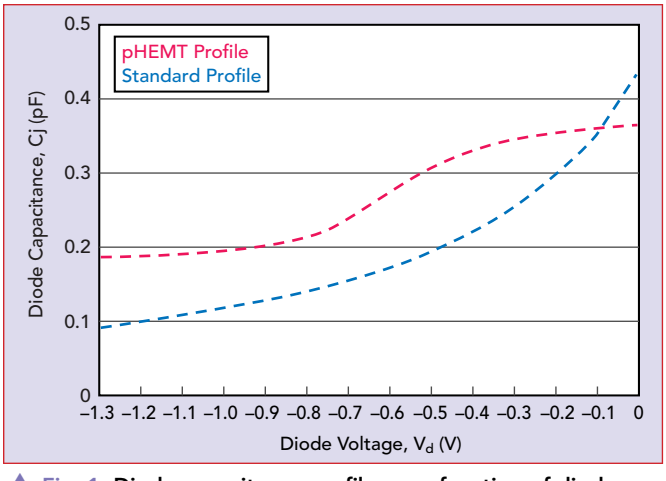

Fig. 1 **Diode capacitance profiles as a function of diode voltage.**

CAPACITANCE VERSUS VOLTAGE PROFILES

The capacitance profile of a diode in the OFF region is usually presented in theory as a zero-bias value ($V_d = 0$) that decreases monotonically as the voltage across the diode becomes more negative. For many types of diodes, from P-N junctions in silicon and GaAs heterojunction bipolar transistors (HBTs) to Schottky field-effect transistor (FET)-connected devices on GaAs and GaN, this profile is very accurate. However, the capacitance profile can take on a much different shape for some diodes, most notably Schottky diodes fabricated with GaAs pHEMT technology. ***Figure 1*** presents a pictorial representation of these two types of profiles.

In Figure 1, the standard profile has a 1/x shape that decreases monotonically as the voltage decreases, where the pHEMT profile takes on an S-curve shape complete with an inflection point. The physics behind these two shapes is somewhat involved, but it suffices to say that many commercial pHEMT foundries ignore the underlying S-curve profile. This results in diode models that follow a standard profile, even though such models are entirely inaccurate.

The standard profile for the diode capacitance, C_j, as a function of diode voltage, V_d, where $V_d < 0$, can be described by the following well-known relationship shown in ***Equation 1***.[1,2]

$$C_j = \frac{C_{j0}}{\left(1 - {}^{V_d}\!/_{V_j}\right)^m} \quad (1)$$

Where:
C_{j0} = diode capacitance at zero voltage
m = grading coefficient
V_j = built-in potential

Unfortunately, no single equation relates the diode capacitance to the diode voltage for the S-curve shape. Instead, to model this behavior, an old FET model known as "Triquint's Own Model" (TOM)[3] is considered. Though initially developed to model three-terminal metal-semi-

Looking for a New Team in New England?

We've Added to Ours!

Bradford RF Sales has been finding new opportunities and helping to grow sales revenue for our principals for over eighteen years. We are seeking several additional microwave/RF companies to represent in the New England territory that align with our current suppliers. Please visit us at ***www.bradfordrfsales.com*** or contact **Mike Crittenden** at ***978.994.9435.***

Bradford RF Sales

Manufacturers' Representatives for New England
58 Beechwood Drive North Andover, MA 01845
www.bradfordrfsales.com

Microwave, RF, and Electronic Products for Military & Commercial Applications

conductor field-effect transistors (MESFETs), the TOM model contains provisions that can accurately describe the S-curve profile of a diode created by shorting the drain and source in a pHEMT FET. Details concerning the TOM model can be found in the paper by McCamant et al.,[3] but in summary, the pertinent results are shown in ***Equations 2*** to ***6***:

$$V_{eff} = \frac{1}{2}(2V_d + DELTA1) \quad (2)$$

$$V_{new} = \frac{1}{2}\left(V_{eff} + V_{to} + \sqrt{(V_{eff} - V_{to})^2 + DELTA2^2}\right) \quad (3)$$

$$V_{max} = F_C * V_{bi} \quad (4)$$

$$V_n = \min(V_{new}, V_{max}) \quad (5)$$

$$C_j = \frac{C_{gs0}}{2\sqrt{1 - \frac{V_n}{V_{bi}}}}\left(1 + \frac{V_{eff} - V_{to}}{\sqrt{(V_{eff} - V_{to})^2 + DELTA2^2}}\right) + C_{gd0} \quad (6)$$

Where:

C_{gd0} = zero-bias gate-to-drain capacitance

C_{gs0} = zero-bias gate-to-source capacitance

DELTA1 = capacitance saturation transition voltage (1/α)

DELTA2 = capacitance threshold transition voltage

F_c = forward-bias depletion capacitance coefficient

V_{bi} = gate diode built-in potential

V_d = voltage across the diode

*V_{eff} = calculated effective voltage

*V_{max} = calculated gate diode capacitance limiting voltage

*V_n = minimum of V_{new} and V_{max}

*V_{new} = calculated new voltage

V_{to} = threshold voltage

The parameters in the list marked with an asterisk are generated by intermediate calculations and are not part of the final TOM parameter set. Also, note that parameter *DELTA1* is sometimes implemented as the reciprocal of another parameter, α, in the TOM model definition.

DIODE MEASUREMENTS, COMPLETE WITH WARNINGS

Unlike the DC I-V measurement described in Part 1 of this tutorial, measuring a diode's OFF capacitance as a function of voltage is not straightforward. Many techniques can be used, from automated systems that determine the capacitance directly to the measurement of S-parameters via a vector network analyzer, which are then processed to determine the capacitance. While each technique has strengths and weaknesses, they all have issues that can creep up and lead to bad measurements. These issues may include:

- Poor calibration of the system; always check your calibration
- Incomplete de-embedding to the diode
- Measuring too small of a device, which allows parasitics to dominate the response
- Not measuring enough voltages, which can obscure the S-curve profile
- Poor layouts of MMIC devices that lead to inaccurate measurements
- Measuring MMIC devices on wafer with the microscope light on.

Of these, a MMIC with a poor layout can be the most frustrating, as overcoming these layout issues may require a separate fabrication run that will cost time and money. Unfortunately, diodes constructed as part of a foundry process control monitor tend to fall into this category and often cannot be used for capacitance extraction. Also, measuring a device with the microscope light on is the same issue described in Part 1, as external light can affect the diode's capacitance. Once the challenges have been conquered and a good set of capacitance values versus diode voltage has been measured, it is time to extract parameters.

EXAMPLE 1: STANDARD PROFILE

In this first example, a diode with a standard capacitance profile typically found in P-N and Schottky diodes fabricated on silicon, GaAs and GaN, with GaAs pHEMT the noted exception, is considered. ***Table 1*** presents the measured capacitance for a GaAs Schottky diode fabricated on an obsolete commercial MESFET process.

The goal is to extract the three parameters in Equation 1, C_{j0}, V_j and m, from this measurement using the Solver function in Excel. This process is identical to that described in Part 1[4] and readers are referred to that article for additional details. To briefly explain the process, four sections are set up in Excel and these sections contain the capacitance parameters, the measured data, the modeled data and the root-mean-square (RMS) error. The following were chosen for seed values: C_{j0} = 0.945 (the measured capacitance at V_d = 0), m = 0.5 (values between 0.3 and 1.0 are good starting points) and V_j = 0.5. The next step is to run Excel Solver with the goal of reducing the RMS error to zero. ***Figure 2*** shows the results of this optimization with values for the desired parameters, C_{j0}, V_j and m, shown in cells C3, C4 and C5, respectively.

Solver has varied all three parameters from the seed values, generating a very low RMS error in cell F5. Note that in cells F8 to F23, the squared error at each voltage is multiplied by 100 to create larger numbers. Solver can fail when the target value is very small, so this problem is avoided by scaling up

TABLE 1

MEASURED STANDARD PROFILE GAAS SCHOTTKY DIODE CAPACITANCE AS A FUNCTION OF VOLTAGE

Voltage Across Diode, V_d [V]	Measured Diode Capacitance, C_j [pF]
0.0	0.945
-0.1	0.786
-0.2	0.663
-0.3	0.565
-0.4	0.485
-0.5	0.422
-0.6	0.371
-0.7	0.330
-0.8	0.297
-0.9	0.271
-1.0	0.250
-1.1	0.234
-1.2	0.220
-1.3	0.210
-1.4	0.201
-1.5	0.195

INSULATED WIRE
INCORPORATED

MAXIMUM POWER!

Insulated Wire's laminated EPTFE dielectric provides industry leading attenuation performance which translates to MAXIMUM power handling capability!

Our range of extremely low loss/phase stable cable designs are available with a range of industry standard high power interfaces and provide performance from -55C to +200C for a diverse range of commercial and military applications including de-frosting, EMC/EMI testing, directed energy and communications systems.

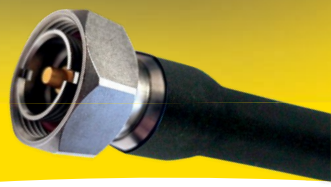

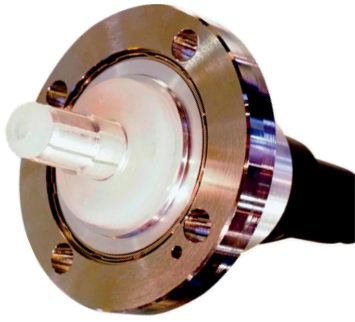

Low loss/phase stable:	2801	1.9KW (c.w) @ 1 GHz, 450W @ 18 GHz
	4806	17KW @ 13.56 MHz, 3.2KW (c.w) @ 1 GHz
	7506	10 kW (c.w) @ 1 GHz 5.5 kW (c.w) @ 2.45 GHz
In the Re-Flex™ family:	RF250	1 kW (c.w) @ 1 GHz

Interconnect options include C, SC, LC, HN, 7/16, 1 5/8" & 3 1/8"EIA flange sizes with different styles available across the range, contact us or your local representative with your requirements!

CALL US TODAY

with your project specs and we'll show you the most reliable way to get connected in the industry.

AS9100 Rev. D & ISO9001:2015 certified.

SCAN THIS CODE
TO FIND OUT HOW YOU CAN GET CONNECTED

We're how the microwave industry **gets connected!**

www.insulatedwire.com
t + 1 631 4724070
e nysales@insulatedwire.com

CERNEX, Inc.
& CernexWave

RF,MICROWAVE & MILLIMETER-WAVE COMPONENTS AND SUB-SYSTEMS UP TO 500GHz
5G Ready

•AMPLIFIERS UP TO 160GHz
• FREQUENCY MULTIPLIERS/ DIVIDERS UP TO 160GHz
• ANTENNAS UP TO 500GHz

• COUPLERS UP TO 220GHz
• ISOLATORS/CIRCULATORS UP TO 160GHz
•FILTERS/DIPLEXERS/SOURCES UP TO 160GHz
•SWITCHES UP TO 160GHz
•PHASE SHIFTERS UP TO 160GHz
•TRANSITIONS/ADAPTERS UP TO 500GHz
•WAVEGUIDE PRODUCTS UP TO 1THz
• TERMINATIONS/LOADS UP TO 325GHz
•MIXERS UP TO 500GHz

•ATTENUATORS UP TO 160GHz
•POWER COMBINERS/DIVIDERS EQUALIZERS
•CABLE ASSEMBLIES/ CONNECTORS UP TO 110GHz
•SUB-SYSTEMS UP TO 110GHz
•DETECTORS UP TO 500GHz
•UMITERS UP TO 160GHz
•BIAS TEE UP TO 110GHz

Add:1710 Zanker Road Suite 103,San Jose, CA 95112
Tel: (408) 541-9226 Fax:(408) 541-9229
www.cernex.com www.cernexwave.com
E mail: sales@cernex .com

the squared error. The final values for these parameters are C_{j0} = 0.954 pF, V_j = 0.632459 V and m = 1.383667. ***Figure 3*** compares measured versus modeled capacitance using these optimized parameters.

Figure 3 shows very good agreement between measured and modeled results over the 1.5 V range. However, a well-known problem with Equation 1 is that as the diode voltage decreases further, the model can deviate noticeably from the measured data. For many diodes, the measured capacitance flattens out at these lower voltages and Equation 1 cannot accurately describe this behavior. Therefore, care must be taken if model accuracy is paramount at lower diode voltages. However, this discrepancy is not an issue in applications such as double-balanced mixers, since the diode ring will clip the diode voltage to levels where Equation 1 is extremely accurate.

	A	B	C	D	E	F	G	H
1								
2		DIODE PARAMETERS						
3		Cj0 [pF] =	0.953694					
4		Vj [V] =	0.632459					
5		m =	1.383667		RMS Error	0.08764764		
6								
7		Voltage	Measured Capacitance [pF]		Modeled Capacitance [pF]	100*Error^2		
8		0	0.945		0.953694427	0.00755931		
9		-0.1	0.786		0.778393313	0.00578617		
10		-0.2	0.663		0.652071883	0.01194237		
11		-0.3	0.565		0.557348011	0.00585529		
12		-0.4	0.485		0.48407064	8.6371E-05		
13		-0.5	0.422		0.425946381	0.00155739		
14		-0.6	0.371		0.378883029	0.00621422		
15		-0.7	0.330		0.340114064	0.01022943		
16		-0.8	0.297		0.307707587	0.01146524		
17		-0.9	0.271		0.28027704	0.00860635		
18		-1	0.250		0.256803605	0.0046289		
19		-1.1	0.234		0.23652327	0.00063669		
20		-1.2	0.220		0.218852794	0.00013161		
21		-1.3	0.210		0.203339875	0.00443573		
22		-1.4	0.201		0.189628808	0.0129304		
23		-1.5	0.195		0.177436326	0.03084826		

Fig. 2 **Standard profile GaAs Schottky diode results.**

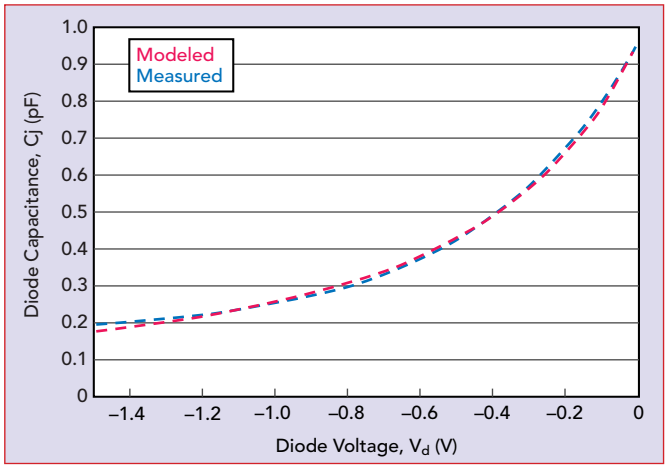

Fig. 3 **Comparison of measured versus modeled diode capacitance using the optimized parameters.**

EXAMPLE 2: S-CURVE PROFILE

This second example will consider the more complicated S-curve capacitance profile. As mentioned earlier, Schottky diodes often generate this profile on many, but not all, GaAs pHEMT processes. ***Table 2*** presents data from a diode fabricated on an obsolete commercial GaAs pHEMT process.

The goal is to use Solver to extract the seven parameters needed for the TOM model: C_{gs0}, C_{gd0}, V_{bi}, V_{to}, *DELTA1*, *DELTA2* and F_c. The process is the same as in Example 1 but with some caveats regarding the seed values. While some parameters, such as V_{to}, can be negative,

TABLE 2
S-CURVE PROFILE GAAS PHEMT SCHOTTKY DIODE RESULTS

Voltage Across Diode, V_d [V]	Measured Diode Capacitance, C_j [pF]
0.0	0.365
-0.1	0.358
-0.2	0.351
-0.3	0.343
-0.4	0.329
-0.5	0.305
-0.6	0.271
-0.7	0.235
-0.8	0.211
-0.9	0.197
-1.0	0.191
-1.1	0.189
-1.2	0.187
-1.3	0.187

MiCable

67GHz

67GHz

67GHz

HIGH PERFORMANCE
SEMI-RIGID CABLE ASSEMBLY
WITH MOVABLE NUT

NEW

- Reliable Structure
- High Performance
- Custom Form
- Phase Match

Frequency	Cable Attenuation	VSWR	Cable Shielding Effectiveness
DC~67GHz	<6.2dB/m@67GHz	<1.35:1@67GHz	<-120dB

VSWR Curve (non-formed)

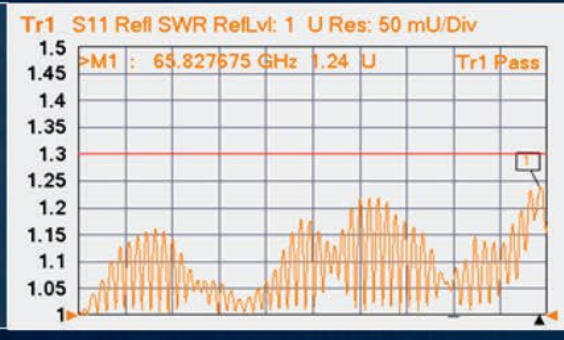

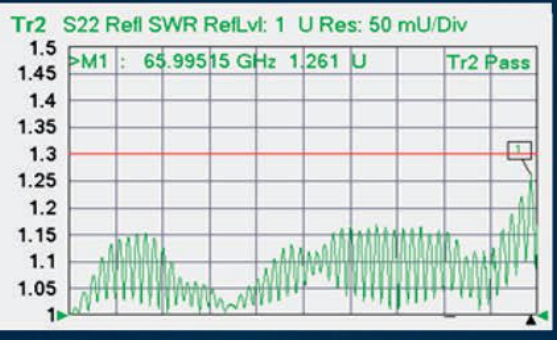

More Information-
Scan the QR Code

MIcable Inc.

www.micable.cn sales@micable.cn +86-591-87382856

the TOM model works best when *DELTA1* and *DELTA2* are positive. Therefore, if the optimization results are negative for these parameters, the optimization process must be rerun with different seed values. In some circumstances, certain combinations of these seven parameters cause convergence problems when used in large signal/harmonic balance circuit simulation tools. If this happens, the situation can be improved by changing the seed values and rerunning Solver to generate new parameter values.

Figure 4 presents the results of running Solver. Extra columns are needed to compute the intermediate parameters V_{eff}, V_{new}, V_{max} and V_n using Equations 2 to 5. Again, the squared error at each voltage is multiplied by 100 to generate larger numbers and a larger RMS error in cell I10, which helps convergence.

Figure 5 shows a comparison of the measured versus modeled capacitance profile. The curves show very good agreement between the measured and modeled results. This agreement would not be possible using the standard capacitance model of Equation 1. As with the standard profile, the TOM model tends to become in-

	DIODE PARAMETERS							
	Cgs0 [pF] =	0.183398						
	Cgd0 [pF] =	0.179459						
	Vbi =	0.119223						
	Vto =	-0.139350						
	DELTA1 =	0.907254						
	DELTA2 =	0.298073						
	Fc =	0.098461						
							RMS Error	0.01532124
	Voltage	Measured Capacitance [pF]	Veff	Vnew	Vmax	Vn	Modeled Capacitance [pF]	100*Error^2
	0	0.365	0.45362708	0.48897787	0.01173877	0.01173877	0.362324153	0.00071602
	-0.1	0.358	0.35362708	0.39518106	0.01173877	0.01173877	0.358679978	4.6237E-05
	-0.2	0.351	0.25362708	0.30375492	0.01173877	0.01173877	0.352982043	0.00039285
	-0.3	0.343	0.15362708	0.2161141	0.01173877	0.01173877	0.343734483	5.3947E-05
	-0.4	0.329	0.05362708	0.13468272	0.01173877	0.01173877	0.328521534	2.2893E-05
	-0.5	0.305	-0.0463729	0.06325736	0.01173877	0.01173877	0.304794036	4.2421E-06
	-0.6	0.271	-0.1463729	0.0062165	0.01173877	0.0062165	0.271427949	1.8314E-05
	-0.7	0.235	-0.2463729	-0.0345093	0.01173877	-0.0345093	0.232923853	0.00043104
	-0.8	0.211	-0.3463729	-0.0614047	0.01173877	-0.0614047	0.211460488	2.1205E-05
	-0.9	0.197	-0.4463729	-0.0789042	0.01173877	-0.0789042	0.199555182	0.0006529
	-1	0.191	-0.5463729	-0.0906138	0.01173877	-0.0906138	0.192813612	0.00032892
	-1.1	0.189	-0.6463729	-0.0987866	0.01173877	-0.0987866	0.188812804	3.5042E-06
	-1.2	0.187	-0.7463729	-0.1047325	0.01173877	-0.1047325	0.186308897	4.7762E-05
	-1.3	0.187	-0.8463729	-0.1092179	0.01173877	-0.1092179	0.184662173	0.00054654

Fig. 4 **S-curve profile GaAs pHEMT Schottky diode results.**

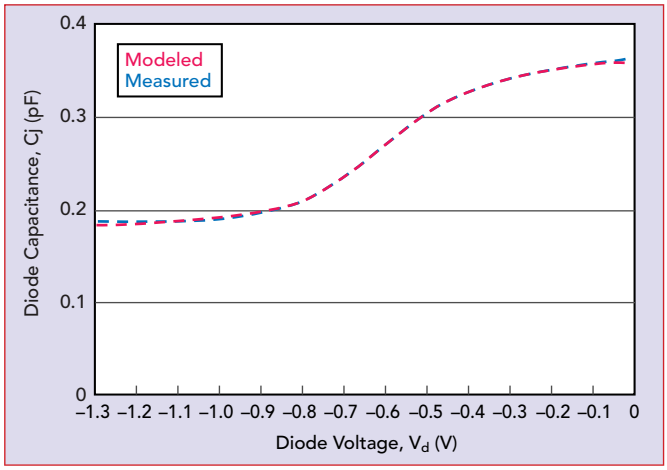

Fig. 5 **Comparison of measured versus modeled diode capacitance using the optimized parameters.**

DUAL or SINGLE LOOP
SYNTHESIZER & PLO MODULES

Features:

- Proprietary digital Integer and Fractional PLL technology
- Lowest digital noise floor available -237 dBc/Hz figure of merit
- Output frequencies from 100 MHz locked crystal to 30 GHz
- Available with reference clean up dual loop, or single loop for very low noise reference
- Parallel fixed band stepping or SPI interface synthesized up to octave bandwidths
- Reference input range 1 MHz to 1.5 GHz
- Dual RF output or reference sample output available
- +12 dBm standard output power +16 dBm available
- Standard module size 2.25 X 2.25 X 0.5 Inches (LxWxH)
- Standard operating temperature -10 to 60 °C, -40 to +85 °C available

Up to 30 GHz*

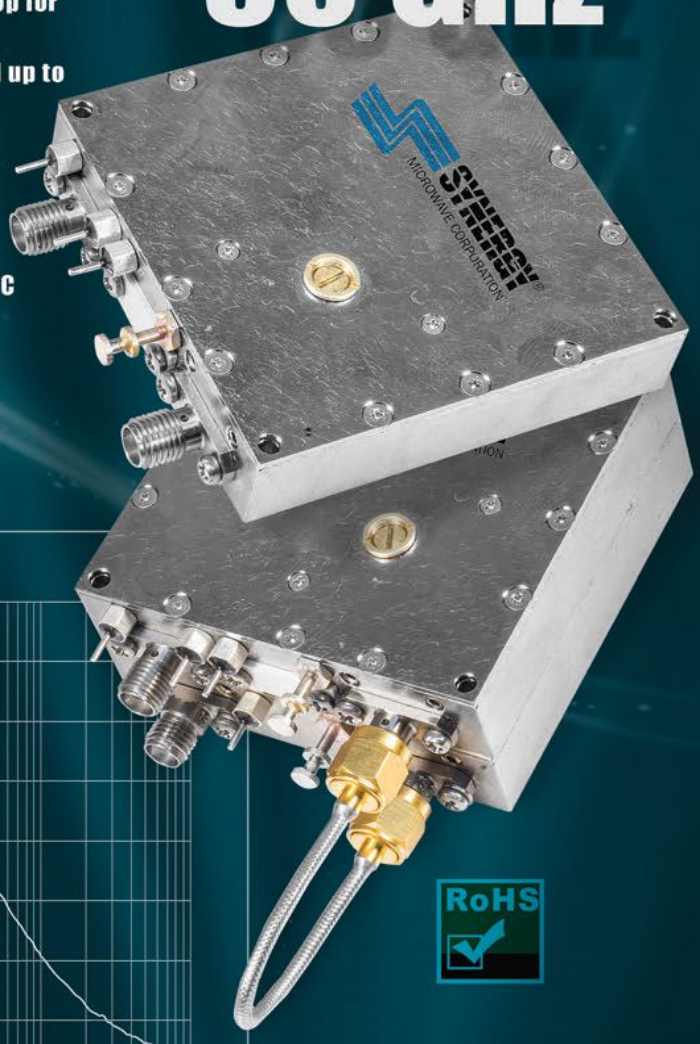

Applications:

- SATCOM, RADAR, MICROWAVE RADIO

* *16 - 30 GHz with added x2 module < 1" in height.*

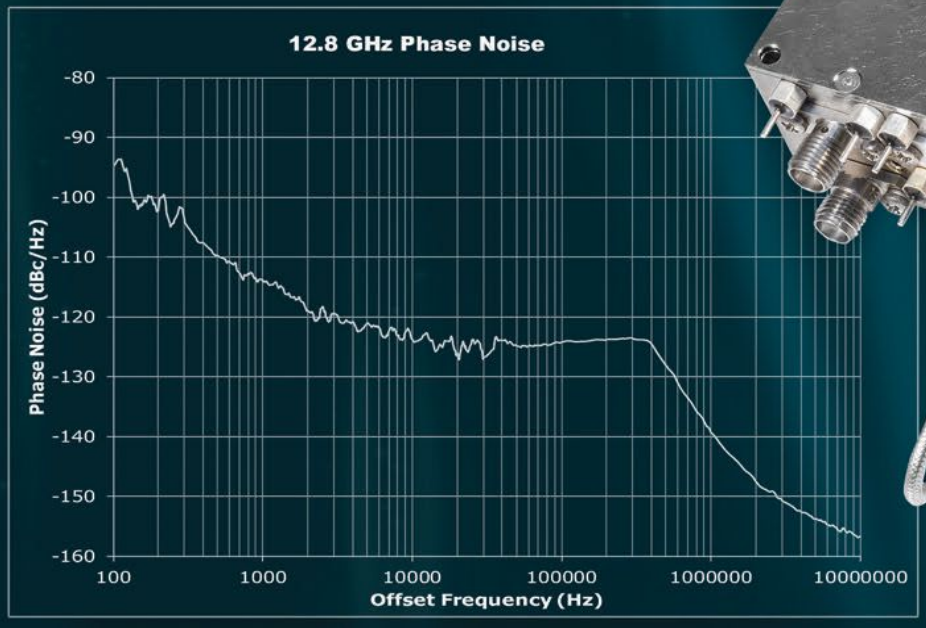

RoHS

Talk To Us About Your Custom Requirements.

SYNERGY® MICROWAVE CORPORATION

Phone: (973) 881-8800 | Fax: (973) 881-8361
E-mail: sales@synergymwave.com
Web: WWW.SYNERGYMWAVE.COM
Mail: 201 McLean Boulevard, Paterson, NJ 07504

accurate as the diode voltage gets lower, though the range of validity is generally greater than the standard model.

MODEL IMPLEMENTATION

The last step in this process is to implement the extracted parameters in a circuit model for simulation. This step is fairly straightforward. For example, Keysight's ADS tool includes the DIODEM model block, which generates the standard capacitance profile and the TOM model block, which produces the S-curve capacitance profile. Additionally, both profiles can be programmed with the DC I-V parameters to complete the model. However, there are two caveats to note. First, some of the extracted model parameters scale with diode size, so they must be scaled for use in a general model where diode size remains a variable. Second, while the TOM model contains the saturation current, I_s, as a variable, the extracted value from Part 1 of this tutorial must be halved when entered into the block. The TOM model assumes two parallel diodes in the FET, one from gate to drain and the other from gate to source. Creating a diode by shorting the drain to the source in the model will cause these two currents to add and generate the correct DC I-V response.

FINAL THOUGHTS

Diode modeling in Excel through the Solver function is a fast and efficient method for determining pertinent parameters. The process described in Parts 1 and 2 of this tutorial allows the engineer to control and understand the process, which is crucial. Proper modeling of the diode will lead to greater accuracy in circuit simulations. For example, the capacitance profile can affect intermodulation distortion in pHEMT diode mixers, so accounting for the S-curve is crucial for determining the third-order intercept point.

Finally, many subtle modeling aspects have not been considered in this tutorial. Among these are the effects of temperature on diode capacitance. If these parameters are important in the application, then techniques described in this tutorial can also be used to extract those parameters. ■

ACKNOWLEDGMENTS

A special thanks to John Mahon of MMIC Works for discussions on the TOM model and to Nick Novaris for checking the Excel calculations.

References

1. R. Goyal, ed., *High-Frequency Analog Integrated Circuit Design*, New York: Wiley-Interscience, 1995, pp. 98–99.
2. P. R. Gray and R. G. Meyer, *Analysis and Design of Analog Integrated Circuits*, New York: John Wiley & Sons, 1993, pp. 37–58.
3. A. J. McCamant, G. D. McCormack and D. H. Smith, "An Improved GaAs MESFET model for SPICE," *IEEE Transactions on Microwave Theory and Techniques*, Vol. 38, No. 6, June 1990, pp. 822–824.
4. C. Trantanella, "Extracting Diode Parameters Using Optimization in Excel Part 1 – DC Parameters from I-V Measurements," *Microwave Journal*, Vol. 67, No. 10, October 2024, pp. 68–76.

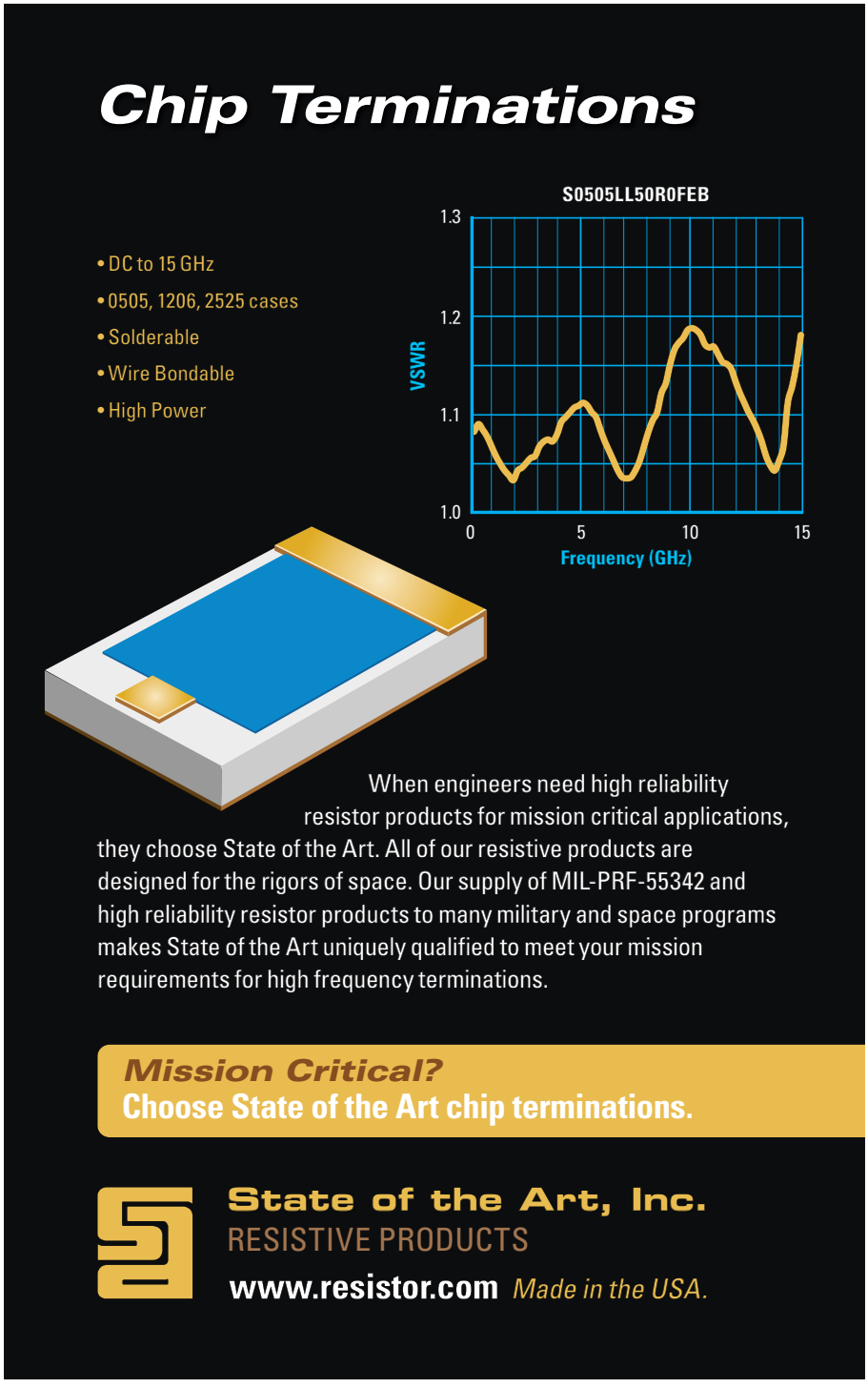

RF-LAMBDA

THE POWER BEYOND EXPECTATIONS

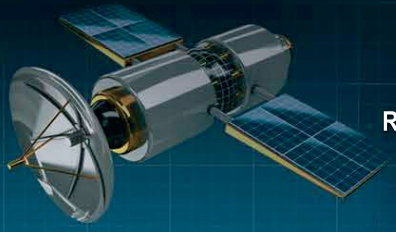

ITAR & ISO9001
Registered Manufacturer
Made in USA

RF T/R MODULES UP TO 70GHz

DREAM? WE REALIZED IT

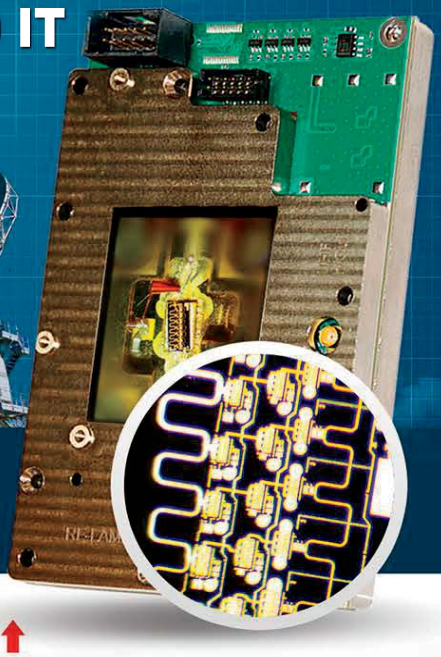

LOW LOSS **NO MORE CONNECTORS**
GaN,GaAs SiGe **DIE BASED BONDING**
SIZE AND **WEIGHT REDUCTION 90%**

HERMETICALLY SEALED
AIRBORNE APPLICATION

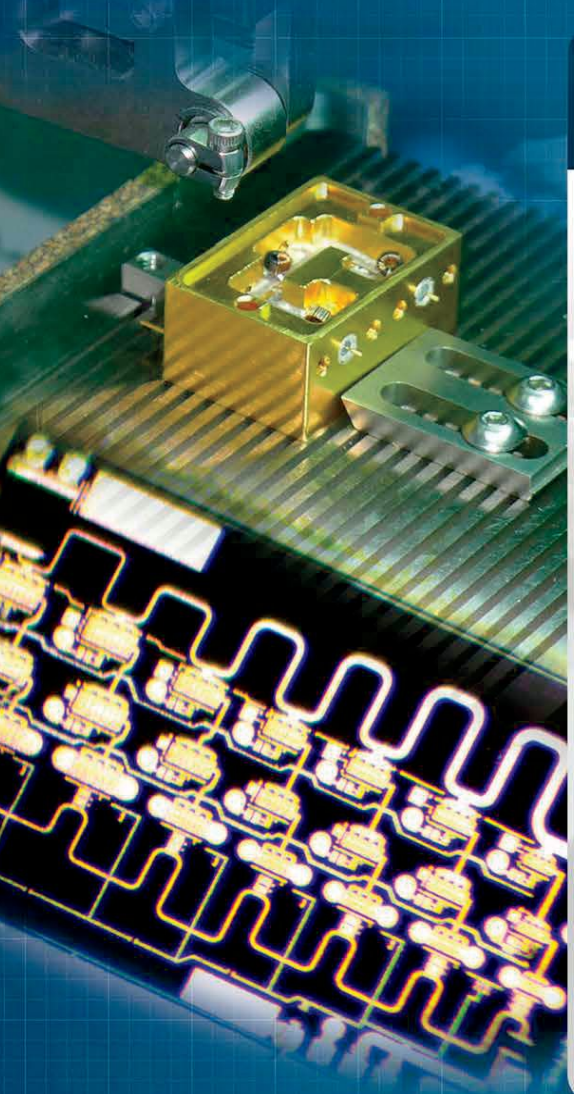

SATCOM TR MODULE
RX 50GHZ TX 22GHZ

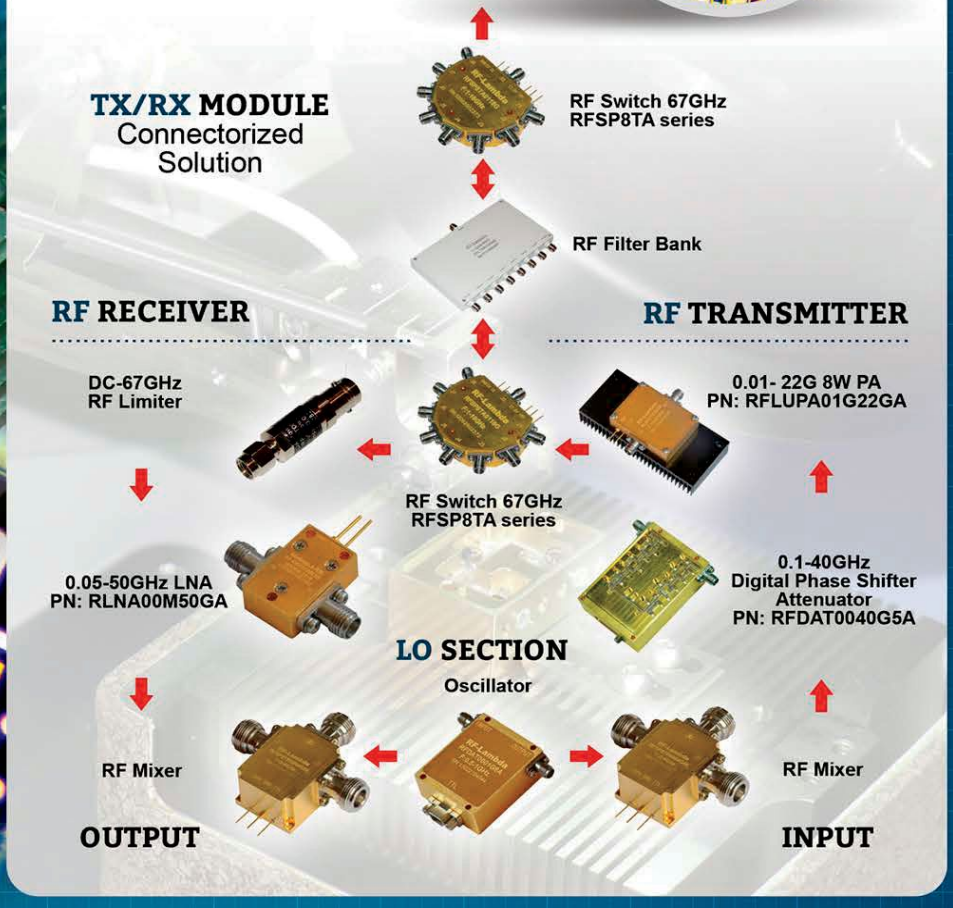

www.rflambda.com
sales@rflambda.com

1-888-976-8880
1-972-767-5998

San Diego, CA, US
Carrollton, TX, US
Ottawa, ONT, Canada
Frankfurt, Germany

INVITED PAPER

Advantages and Applications of GaN Push-Pull Amplifiers

Paramita Maity, Ashish Shinde, Sritama Dutta and Manish Shah
TagoreTech, Arlington Heights, Ill.

Gallium Nitride (GaN) has emerged as the preferred high-power amplifier (HPA) technology due to its superior properties compared to LDMOS technology. GaN enables wider bandwidth and higher efficiency amplifier designs, allowing a single wideband amplifier to replace multiple narrowband amplifiers. This reduces board space without sacrificing performance. While a wideband amplifier design offers advantages in terms of space and cost, its broad bandwidth presents challenges in meeting harmonics requirements.

Push-pull power amplifier (PA) topology is gaining popularity as the architecture of choice for many applications like land mobile radios (LMR) and tactical radios. This topology combines two or more PAs to achieve higher power output, resulting in improved efficiency, lower distortion and reduced power dissipation. This also simplifies thermal management challenges.

This article discusses various wideband GaN amplifier topologies and demonstrates why push-pull topology is the ideal solution for optimal performance in wideband PA designs. It compares the pros and cons of a HPA design using two push-pull PAs combined with a 90-degree hybrid versus two PAs combined with baluns. Additionally, the article addresses the specific requirements of low-power and high-power LMR handsets in terms of efficiency, distortion, power handling and thermal management. The article explains how push-pull amplifiers can reduce overall system size while maintaining these critical parameters. It will also present measured performances of recent designs of low-power and high-power push-pull amplifiers that use existing PAs from TagoreTech to address the challenges faced in LMR handset applications.

HPA TECHNOLOGIES

GaN and LDMOS are two of the most common semiconductor process technologies for PA design. With an ever-increasing demand to reduce the size, weight, power and cost (SWaP-C), GaN is rapidly replacing LDMOS in many new PA designs. This is, in part, because LDMOS transistors are typically built on a silicon substrate, while some advanced designs may use silicon-on-insulator substrates.

Due to its material properties, GaN offers several advantages over silicon. ***Table 1*** highlights the basic material properties of both GaN and silicon. The properties listed in Table 1 show that GaN devices have much higher power density due to a higher break-

TABLE 1
COMPARISON OF GAN AND SILICON TECHNOLOGY

Property	GaN	Silicon
Energy Band Gap (eV)	3.4	1.1
Critical Electric Field (MV/cm)	3 to 4	0.3
Charge Density	Higher	Lower
Thermal Conductivity (W/cm·K)	1.3 to 1.5	1.5 to 1.6
Electron Mobility ($cm^2/V·s$)	1000 to 2000	1400
Thermal Stability	High	Moderate
Saturation Velocity (cm/s)	2×10^7	1×10^7
Breakdown Voltage	High	Moderate
Cost of Fabrication	Higher for SiC substrate Moderate for silicon substrate	Lower due to mature technology

TABLE 2
COMPARISON OF BROADBAND AMPLIFIER TOPOLOGIES

Topology	Bandwidth	Efficiency	Linearity	Design Complexity
Lossy Matched Amplifier	Moderate	Low	Moderate	High
Feedback Amplifier	Moderate	Moderate	High	Moderate
Distributed Amplifiers	High	High	Moderate	High
Push-Pull Amplifiers	Moderate to High	High	High	Moderate to High

down voltage, saturation velocity and charge density. This higher power density enables GaN devices to be significantly smaller for the same output power, reducing all device capacitances compared to existing LDMOS technology. Lower input and output capacitances facilitate the realization of broadband matching networks. Additionally, higher voltage operation increases the load line impedance for a desired output power, further aiding in the realization of broadband output matching. These factors make GaN an excellent choice for PAs, RF components and functions in other demanding electronic systems where performance and reliability are critical.

BROADBAND PA TOPOLOGIES AND TRADE-OFFS

Broadband PAs are essential components across a wide range of applications, enabling effective communication, enhancing signal quality and ensuring reliability in various fields, from telecommunications to consumer electronics and beyond. The performance of these PAs enables them to handle a broad frequency range, making them versatile components in modern communication systems. Several broadband PA topologies are available, each with its advantages and disadvantages. Some important topologies include:

Lossy Matched Amplifier or Multistage Lumped Element Matching: This topology employs multistage input and output matching networks with lumped elements like resistors, capacitors and inductors to achieve wider bandwidth.

Feedback Amplifier: Negative feedback is applied to extend the bandwidth. Both shunt and series feedback configurations have been used in this context, but shunt feedback generally yields the best results.

Distributed Amplifiers: This topology uses the concept of "additive amplification" with multiple transistors and offers ultra-broadband operation that can extend from DC up to the cutoff frequency of the active devices.

Push-Pull Amplifiers: A push-pull amplifier configuration uses two active devices to address the positive and negative cycles of an input signal. This design improves efficiency and reduces distortion by canceling even-order harmonics, making it particularly effective in audio and RF applications. By alternating the conduction between the two devices, push-pull amplifiers can deliver high output power while maintaining good linearity and thermal performance. Complementary operation, reduced distortion and improved thermal stability contribute to the overall bandwidth improvement of push-pull amplifiers.

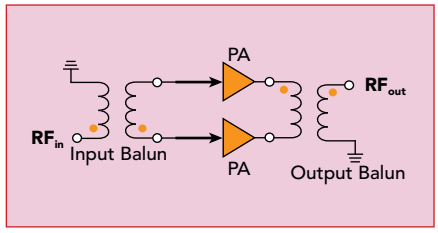

Fig. 1 **Push-pull PA block diagram.**

Table 2 summarizes the comparison of different broadband PA topologies. Distributed amplifiers typically offer the maximum bandwidth among the four types of PA topologies listed. This makes them suitable for applications requiring very wide frequency coverage. Push-pull amplifiers and feedback amplifiers can also provide extended bandwidth but generally do not reach the same levels of bandwidth as distributed amplifiers.

When considering distortion, efficiency and other factors like bandwidth, both push-pull and distributed amplifiers have their strengths. However, push-pull amplifiers stand out in terms of efficiency, ease of design, reduced distortion, better heat management and lower costs. This makes them an excellent option for high-power applications, such as tactical radio and LMR systems.

GaN push-pull PAs have distinct advantages over other technologies due to the properties of GaN. This amplifier topology/technology choice delivers better efficiency, wider bandwidth, higher power density and improved thermal performance. Overall, these benefits make GaN push-pull amplifiers an appealing option for various applications, including telecommunications, aerospace and defense systems.

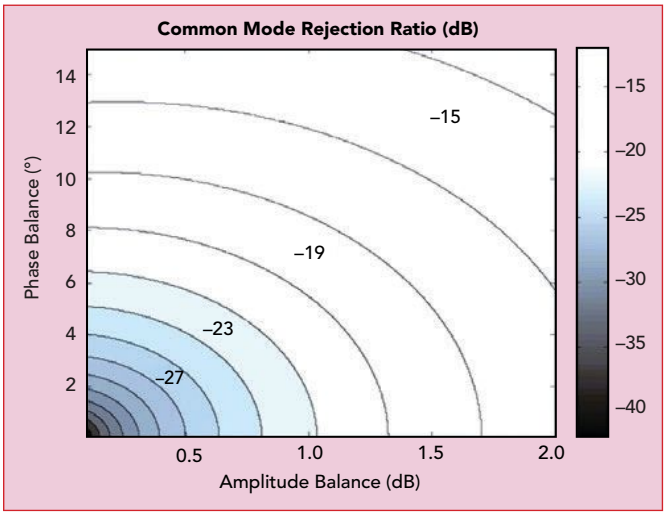

Fig. 2 **CMRR versus amplitude and phase imbalance.**

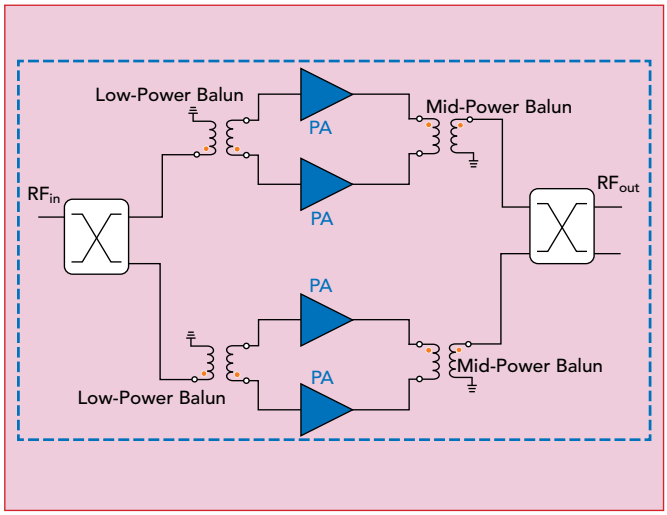

Fig. 3 **Push-pull PA using hybrid 90° couplers.**

PUSH-PULL DESIGN APPROACH

The push-pull design approach uses two transistor or HEMT-based devices to amplify an input signal. In this setup, one device handles the positive half of the waveform while the other manages the negative half. ***Figure 1*** shows the basic building block of a push-pull PA.

The key components of a push-pull PA are:

Input Stage: The input signal is typically differential, coming from a source that can produce balanced outputs. A balun converts the single-ended unbalanced signal into two equal but opposite phase-balanced signals that drive the two active devices.

Active Devices: Two active FETs or HEMTs are arranged in a push-pull configuration. Each device handles one half of the input waveform. One amplifies the positive half, while the other amplifies the negative half.

Balun: A balun is located at the input and output of the PA. At the input, the balun translates the single-ended signal into a differential signal. At the output, it translates the differential signal back into a single-ended signal. The balun can also be designed to provide impedance transformation for the desired bandwidth. It helps in minimizing common-mode noise and ensures that the power is evenly distributed between the two devices.

Output Stage: The outputs of the two transistors are combined at the output stage. The balun ensures that the combined output is in phase and delivers the amplified signal to the load.

Feedback Mechanism (optional): Feedback can be implemented to improve linearity and reduce distortion. It may be applied from the output back to the input stage, stabilizing the overall gain.

The input signal enters the amplifier, where the balun converts it

TABLE 3

COMPARISON OF PUSH-PULL CONFIGURATIONS

Parameters	*Single High-Power PA*	*Two Smaller PAs in Push-Pull*
Design Simplicity	Less complex design	More complex design
Footprint	Potentially smaller footprint	Potentially larger size
Bandwidth	Faces challenges	Typically, better
Efficiency	Faces challenges	Improved efficiency
Harmonic Control	Faces challenges	Improved harmonic performance

TABLE 4

COMPARISON OF SINGLE PA AND PUSH-PULL AMPLIFIER WITH 90° HYBRIDS

Parameters	*Single High-Power PA*	*Two PAs with 90° Hybrid*
Design Complexity	Less complex design	More complex design
Footprint	Smaller	Larger size
Bandwidth	Low	High
Efficiency	Faces challenges	Improved efficiency
Harmonic Control	Faces challenges	Improved harmonic performance
Output Return Loss	Often sacrificed to improve PAE and P_{out}	Enhanced return loss
Cost	High-power devices and LPF components are expensive.	Potentially lower cost from smaller PAs. Additional components may increase total cost, depending on specific components and system design.
Filtering Needs	Requires significant LPF stages, increasing cost and loss.	Lower filtering needs due to better harmonic.

into two balanced signals. The two active devices amplify their respective halves of the signal. The amplified outputs are fed into the balun, which combines them into a single unbalanced output. The output is delivered to the load (e.g., an antenna), providing high power with low distortion. The architecture of a push-pull PA using a balun effectively combines the benefits of balanced operation and push-pull design, resulting in high efficiency, low distortion and broader bandwidth.

CRITICAL BALUN PARAMETERS

The design/selection of the balun is one of the most critical factors in the design of push-pull PAs. Several factors need to be considered when designing or selecting the correct balun for the amplifier design:

Operational Bandwidth: The bandwidth where the balun must meet the specified requirements.

Insertion Loss: A critical parameter that directly impacts the overall efficiency of the amplifier. Higher insertion loss also limits the power handling capability of the balun and may make thermal management challenging.

Amplitude and Phase Imbalance: Directly impacts the achievable common-mode rejection ratio (CMRR) of the balun.

Impedance Transformation Ratio: The desired ratio between the input and output impedances.

Power Handling: The maximum power the balun can handle without exceeding its specified limits.

A CMRR of 20 to 25 dB is commonly achievable in a balun over a wide bandwidth. ***Figure 2*** shows a chart of CMRR versus phase and amplitude imbalance. This chart shows that a balun must have less than 0.5 dB of amplitude imbalance and 5 degrees of phase imbalance to achieve 25 dB CMRR. These imbalance values need to be measured at the even-order harmonic frequencies.

The maximum power requirements of the amplifier drive the maximum power handling requirements of the baluns. Higher power baluns that are used on the PA output will typically be larger due to thermal management considerations. This is a critical factor when designing baluns.

HIGH-POWER BROADBAND PA DESIGN

For broadband high-power applications, a single high-power device may be used to design a single-ended PA to meet specifications. However, using a single high-power

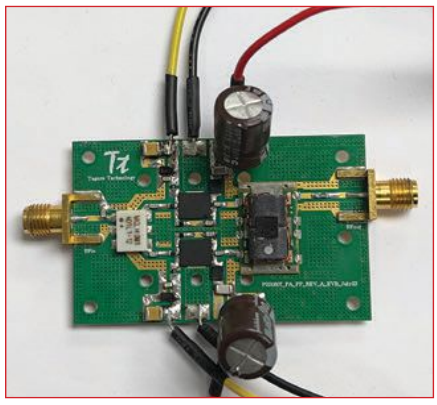

▲ Fig. 4 15 W push-pull PA module.

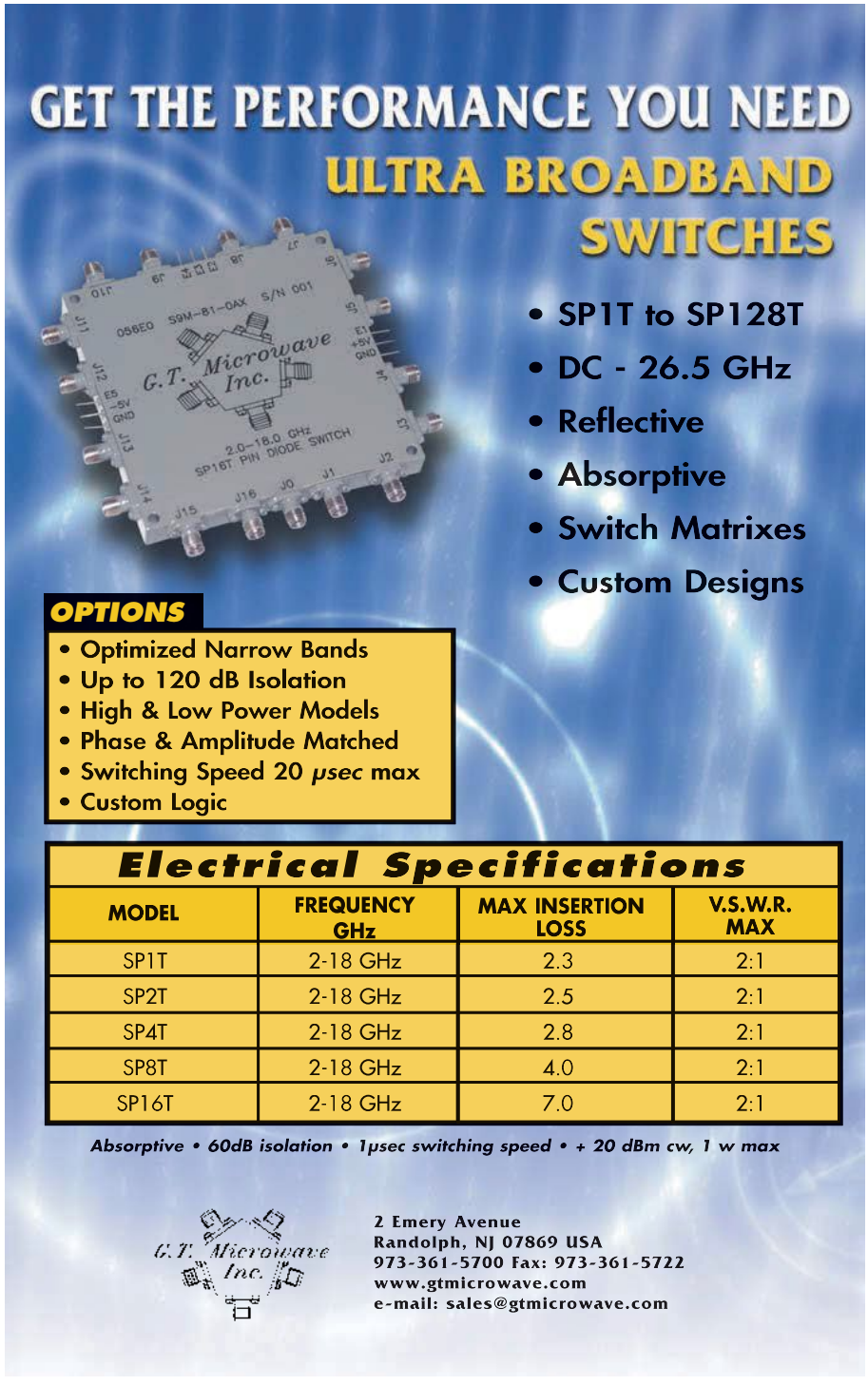

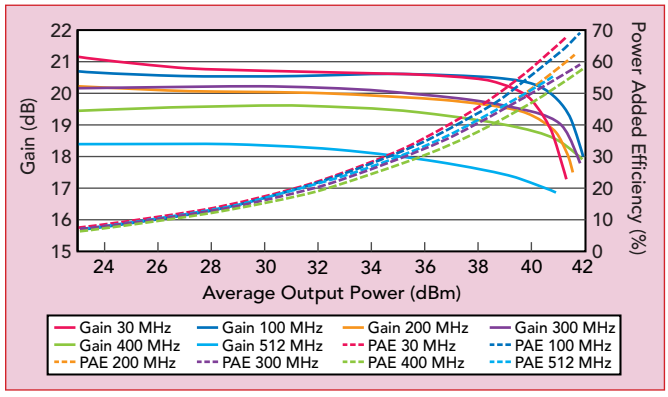

Fig. 5 15 W PA module gain and PAE.

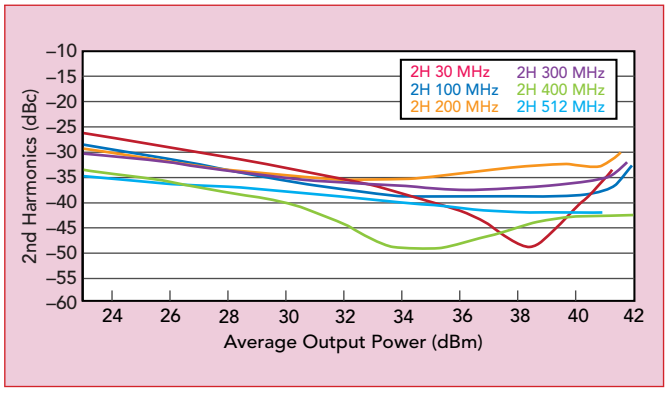

Fig. 6 15 W PA module second-order harmonics.

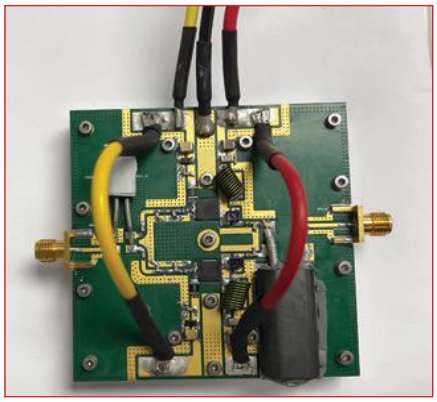

Fig. 7 65 W push-pull PA module.

device presents challenges with bandwidth, PAE, harmonics, thermal management and cost. To minimize harmonics, lowpass filters (LPFs) are needed to suppress the harmonics generated by the PA. LPF components must support the appropriate power levels, which may increase their size and the space required on the PCB. This adds to the loss and cost of the overall design. Additionally, achieving better PAE and output power with a single PA often requires sacrificing output return loss. Standard designs using a single high-power PA also typically achieve poor second harmonic levels.

Alternatively, using two smaller PAs in a push-pull topology and combining them with a 90-degree hybrid, as shown in ***Figure 3***, can yield higher P_{out}, improved PAE, better harmonic performance and excellent input and output return loss due to the inherent characteristics of the hybrid. This approach enhances overall performance and addresses the efficiency issues associated with single high-power device designs. This topology also simplifies thermal management efforts since power dissipation is distributed across four active devices rather than one in the single-device HPA. One of the drawbacks of this push-pull topology is cost, as it requires additional baluns and hybrid combiners at the input and output.

Table 3 summarizes the comparison of a single PA configuration versus two small push-pull PAs. ***Table 4*** summarizes the comparison of a single HPA versus two push-pull PAs combined with a 90-degree hybrid.

Overall, the push-pull topology with 90-degree hybrids offers a more efficient and higher performing solution for high-power broadband PA design despite the increased design complexity and potential for higher costs.

PUSH-PULL AMPLIFIER REFERENCE DESIGNS

To illustrate the practical application of the push-pull PA design approach, this section presents 15 W and 65 W push-pull PA module reference designs.

15 W Push-Pull PA Module

Figure 4 shows a 15 W push-pull amplifier design using TagoreTech's TA9310E GaN-on-SiC power transistors and baluns. This amplifier is designed to operate from 30 to 512 MHz. The two GaN HEMTs are biased at an 18 V drain supply with a total quiescent current of 80 mA. The input side of the module uses a balun rated at 1 W, while the output uses a balun from Mini-Circuits rated at 15 W.

The push-pull design effectively minimizes second-order harmonics to -35 dBc without sacrificing output power or PAE. The desired levels of power and PAE can be achieved by operating the push-pull amplifier at drain voltages below the maximum rating for the GaN PA. The reduction of second-order harmonics makes this design particularly advantageous for tactical radio applications, especially within the 30 to 512 MHz frequency band. The GaN power transistors shown in Figure 4 are mounted on an evaluation board developed by TagoreTech. This module delivers an average power output of approximately 15 W. ***Figure 5*** shows the measured gain and PAE versus output power for the 15 W PA module. ***Figure 6*** shows the performance of the second-order harmonics versus the output power of the 15 W amplifier module.

65 W Push-Pull PA Module

Figure 7 showcases a 65 W push-pull amplifier design developed us-

TABLE 5

65 W PUSH-PULL PA MEASURED DATA

Function/Parameters	Measured Data			
	VHF	UHF1	UHF2	800 MHz
Operating Voltage	50 V 100 mA (50 mA+50 mA)			
Test Frequency (MHz)	136 to 175	380 to 450	450 to 520	760 to 870
P_{avg} (dBm)	48 to 48.5	48.6 to 48.8	48.4 to 48.6	48
PAE at P_{sat} (Percent)	58 to 61	57 to 61	52 to 57	42 to 45
Second Harmonic (dBc) at P_{sat}	-25	-25	-26	-30

SIX DAYS ■ THREE CONFERENCES ■ ONE EXHIBITION

EUROPE'S PREMIER MICROWAVE, RF, WIRELESS AND RADAR EVENT

EUROPEAN MICROWAVE WEEK
JAARBEURS UTRECHT
THE NETHERLANDS
21-26 SEPTEMBER 2025
www.eumweek.com
WAVES OF INNOVATION

EUROPEAN MICROWAVE WEEK 2025

SAVE THE DATE

JAARBEURS UTRECHT, THE NETHERLANDS
21 - 26 SEPTEMBER 2025

THE 28TH EUROPEAN MICROWAVE WEEK COMBINES THREE CONFERENCES:

- The European Microwave Conference (EuMC)
- The European Microwave Integrated Circuits Conference (EuMIC)
- The European Radar Conference (EuRAD)

PLUS:

- Workshops, Short Courses, Focussed/Special Sessions
- Defence, Security and Space Forum, 6G Forum, Automotive Forum
- Student Activities

ALSO: THE EUROPEAN MICROWAVE EXHIBITION

23 - 25 September 2025

EuMA European Microwave Association

Official Publication: Microwave Journal

Organised by: horizon house

Supported by: IET The Institution of Engineering and Technology

Co-sponsored by: MTT-S

Co-sponsored by: IEEE

EuMIC 2025
The 20th European Microwave Integrated Circuits Conference

55TH EUROPEAN MICROWAVE CONFERENCE 2025
The 55th European Microwave Conference

EuRAD 2025
The 22nd European Radar Conference

Co-sponsored by: GAAS, Electron Devices Society

Co-sponsored by: IEEE AP-S Antennas and Propagation Society, EurAAP, APMC 2025

Co-sponsored by: IEEE AP-S Antennas and Propagation Society, EurAAP

INTERESTED IN EXHIBITING?
CALL +44(0) 20 7596 8742 OR VISIT WWW.EUMWEEK.COM

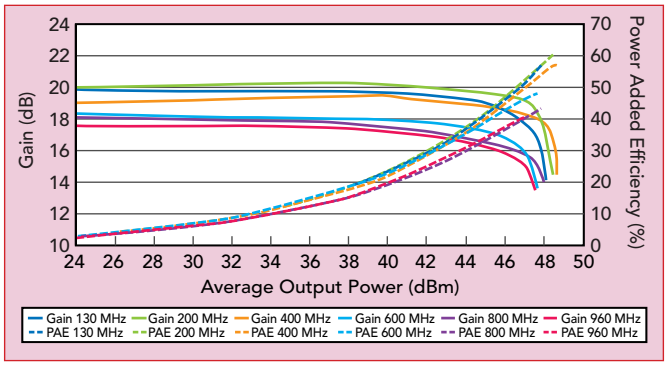

Fig. 8 65 W PA module gain and PAE.

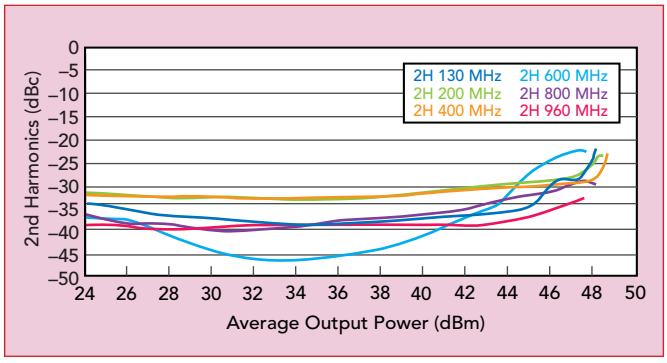

Fig. 9 65 W PA module second-order harmonics.

ing two of TagoreTech's TA9410E 40 W GaN-on-SiC power transistors in conjunction with an in-house coaxial balun design. This amplifier is designed to operate from 135 to 870 MHz, driven by a 50 V drain supply. For optimal performance, a balun rated at 4 to 5 W is utilized on the input side, while a balun rated at 75 W is employed at the output.

The amplifier's push-pull topology effectively reduces second-order harmonics to -30 dBc. This ensures that output power and PAE are not compromised. Operating at a maximum voltage of 50 V, this design meets the high-power requirements essential for dash-mount or vehicular LMR/PMR radio applications.

The suppression of second-order harmonics makes this amplifier particularly suitable for LMR applications, especially across very high frequencies (VHF), ultra-high frequency 1 (UHF1), UHF2 and the 800 MHz band. ***Table 5*** shows a summary of the 65 W push-pull amplifier performance in these bands. The evaluation board in Figure 7 delivers an average power output of 63 to 70 W in the LMR frequency range. ***Figure 8*** shows the measured gain and PAE versus output power for the 65 W PA module. ***Figure 9*** shows the performance of the second-order harmonics versus the output power of the 65 W amplifier module.

SUMMARY

This article has explored the advantages of push-pull amplifier topology, particularly when combined with GaN technology, for wideband PA design. By pairing two or more amplifiers, push-pull amplifiers effectively address the challenges of achieving high power output, wide bandwidth and low distortion in broadband PA designs. GaN technology offers superior properties such as wide bandwidth, high efficiency, superior thermal conductivity and high breakdown voltage, making it an ideal choice for these applications.

The article has compared push-pull configurations to PA designs using a single device. This analysis has highlighted the superior harmonic performance, efficiency and thermal distribution of the push-pull architecture. Despite the increased design complexity and potentially higher component count, push-pull configurations provide significant advantages in bandwidth, efficiency and harmonic control.

Combining push-pull topology with GaN technology results in high performance, wideband amplifiers that meet stringent requirements for efficiency, distortion, power handling and thermal management. This makes them a compelling choice for RF applications where performance, size and cost are critical. ■

EDI CON ONLINE

EDUCATIONAL DAYS

Now Available On Demand

4 FOCUSED TRACKS WITH FREE SEMINARS ON:

PCB/Interconnect/ EMC-EMI

•

5G-6G/Wi-Fi/IoT

•

Signal Integrity/Power Integrity

•

Radar/Automotive/SATCOM

Platinum Sponsors

KEYSIGHT

COMSOL

samtec

Organized by

horizon house®

Official Publications

Microwave Journal

Signal Integrity Journal

EDICONONLINE.COM

Vector Network Analyzer for Embedded OEM Applications

LA Techniques Ltd
Surbiton, U.K.
AAI Robotics Ltd
Cambridge, U.K.

The LA19-14-06 instrument is a compact vector network analyzer (VNA) module designed to be embedded into original equipment manufacturer (OEM) applications. It is a turnkey solution that enables fast and flexible microwave vector measurements within an embedded system. The module is provided with extensive cross-platform software and programming examples are available in multiple languages. The instrument features a novel calibration store feature with a patent application that aids temperature measurement stability over time.

VECTOR NETWORK ANALYZERS

VNAs are increasingly employed in medical and industrial processes, requiring microwave reflection and transmission measurements. Recent examples of novel VNA applications include detecting total dissolved solids in steam boilers, detecting corrosion under insulation in steel pipes, detecting positive margins in breast cancer surgery and detecting biomarkers in assessing traumatic brain injury. These novel, dedicated applications are challenging to serve using traditional desktop or handheld VNAs mainly because of cost, size and frequency and practicality of calibration.

LA Techniques Ltd has developed an OEM VNA module to address these challenges. With this development, the company plans to enable the potential of VNAs to be fully realized in embedded applications. Using the module can significantly reduce the time-to-market, development and production costs of any new embedded application involving RF vector measurements.

The OEM VNA module operates from 300 kHz to 6.4 GHz. The compact module measures only 117 × 69 × 19 mm. It provides a measurement speed down to 100 µs per complex reflection coefficient measurement point, a low distortion test signal with 10 Hz setting resolution and up to 10,001 measurement points. It features a unique calibration store that significantly reduces temperature drift of reflection measurements and reduces the number of calibrations required over time. Optionally, the VNA module can also measure complex transmission coefficients.

FAST AND FLEXIBLE SOFTWARE SUPPORT

Extensive cross-platform software support for the new OEM VNA is provided. A user interface and SCPI control are available to prototype and develop new applications rapidly. Programming examples are available in the C++, C and Python programming languages to facilitate the transition of new applications into production. Out-of-the-box, the software can be run on Windows, Linux, macOS and Raspberry Pi. It can be made available for other embedded platforms on request. ***Figure 1*** illustrates a possible remote access arrangement.

CALIBRATION TEMPERATURE DRIFT COMPENSATION

VNA calibration is used to remove inherent errors introduced by imperfections in the VNA as well as test fixtures and cables between the VNA and the DUT. In addition, there will be a temperature dependence, mainly due to variations in the characteristics of circuit components within the VNA. In the case of reflection measurements, these imperfections can be conveniently

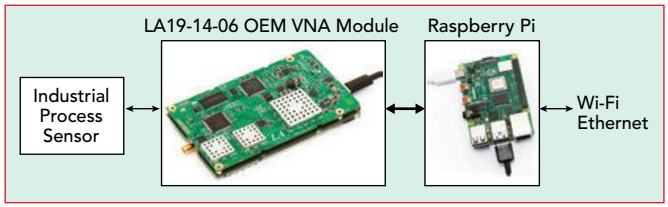

Fig. 1 **OEM VNA module can be paired with a Raspberry Pi.**

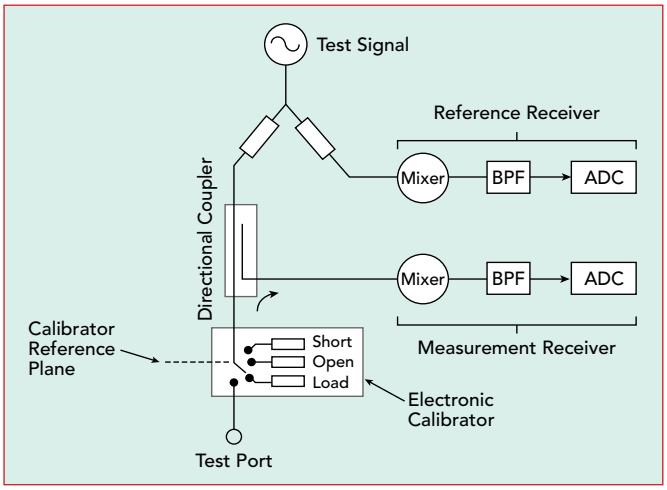

Fig. 2 **OEM VNA module circuit with built-in electronic calibrator.**

modeled by three error terms: e11 (directivity), e22 (source match) and e121 (frequency tracking). Conventionally, these errors can be corrected by calibrating immediately before use.

The OEM VNA module will likely be used over a wide range of ambient temperatures. In many applications, it will not be practical to perform a calibration before use to reduce the effect of temperature drift. The LA19-14-06 OEM VNA module employs an internal electronic calibrator, a new technique to reduce drift and improve the quality of reflection measurements by refreshing the external calibration. The arrangement used is shown in ***Figure 2***.

STORING AND REFRESHING A CALIBRATION

Once a conventional calibration using an external calibration kit is complete, the user can make the calibration resilient to temperature drift by immediately measuring the calibrator's internal short, open and load (SOL) standards and storing these measurements in non-volatile memory. New algorithms developed by LA Techniques Ltd can then use these measurements to remove the effect of any temperature drift later in the measurements by refreshing the calibration, which computes a new set of error terms e11, e22 and e121. The ability to instantly compute a new set of error terms makes the feature unique and potentially transparent to the use of the module.

The measurements of the calibrator's embedded SOL standards are not meaningful by themselves. They cannot be used directly for a conventional reflection measurement calibration. The advantage of the novel calibration store/refresh technique is that, with the new mathematical processing developed,

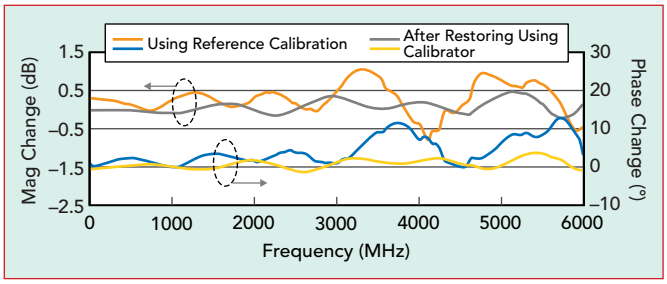

Fig. 3 **Measured S11 magnitude and phase deviation (ΔT = -22°C)**

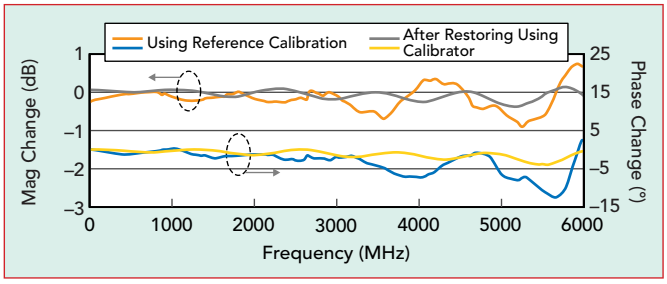

Fig. 4 **Measured S11 magnitude and phase deviation (ΔT = +15°C).**

the internal standards do not have to be known or fabricated accurately to be later used to remove the effects of temperature drift from a conventional reflection measurement calibration.

The advantage of using the embedded electronic calibrator can be seen by measuring a device with a suitable reflection coefficient and observing how the measurement varies as the VNA temperature varies. A mismatched device with a nominal linear reflection coefficient of 0.25 (12 dB return loss) was chosen for this test. The VNA was calibrated with an external calibration kit when the VNA case temperature was 32°C. The DUT was then measured at 32°C, 10°C and 47°C. ***Figure 3*** shows the results with and without the temperature stabilization algorithm at a temperature change of -22°C and ***Figure 4*** shows the results at a temperature change of +15°C.

CONCLUSION

A new, compact OEM VNA module has been described with a module that includes an embedded electronic calibrator. This module, together with a novel algorithm, can minimize the effect of temperature drift. This provides clear benefits in reducing measurement errors caused by large changes in the operating temperature of the VNA, without the need for an operator to perform a new calibration. The low-cost module is supplied with fast and flexible software options, making it ideally suited for many dedicated OEM and embedded applications.

LA Techniques Ltd
Surbiton, U.K.
www.latechniques.net

AAI Robotics Ltd
Cambridge, U.K.
www.aairobotics.com

20 GHz 3U VPX Module Speeds EW and Radar Design Times

Analog Devices, Inc.
Wilmington, Mass.

System requirements are driving demand for compact electronic products with enhanced capabilities and shorter design cycles. The ADSY1100-series RF system-on-module (SoM) assemblies from Analog Devices, Inc. combine an RF tuner, sensors and a field-programmable gate array (FPGA) in a 3U VPX module aligned to the Sensor Open Systems Architecture™ (SOSA™) standard. The RF SoMs are available with swappable RF front-end mezzanine cards to provide a selection of frequency ranges from 10 MHz to 55 GHz. The small size, weight and power (SWaP) of these multifunction modules, coupled with selectable frequency ranges, help designers of advanced electronic systems in communications, electronic test and measurement, electronic warfare (EW) and radar systems to speed these devices to the production line. ***Figure 1*** shows an ADSY1100-series RF SoM housed in 3U VPX enclosures with backplane connectors aligned to the SOSA™ standard.

Fig. 1 **ADSY1100-series RF SoM.**

The ADSY1100-series RF SoMs pack an RF/microwave tuner, Apollo MxFE® 20 GSPS high speed digitizer, microprocessor and a large FPGA into a single 1 in. pitch 3U VPX assembly. The system shown in Figure 1 features a slot profile for the backplane connectors aligned according to the SOSA™ standard. Within the compact VPX housing, the mezzanine cards connect to the heart of each digitizer, an Apollo MxFE™ model AD9084 signal converter housed in a ball grid array package. To sample signals from the RF tuner mezzanine cards, each AD9084 incorporates four 16-bit digital-to-analog converters capable of sample rates to 28 GSPS and four 12-bit analog-to-digital converters running at speeds up to 20 GSPS.

Marrying high dynamic range and wideband digitization with up to 10 GHz of instantaneous bandwidth with advanced processing capabilities in a reduced SWaP format, the AD9084 within each ADSY1100-series SoM feeds a Virtex™ UltraScale+™ VU11P FPGA from AMD connected to a Zynq™ UltraScale+ ZU4EG multiprocessor system-on-chip (MPSoC) device with 64-bit microprocessor capability from AMD Xilinx. These devices and the AD9084 signal converter are on the ADSY1100 Digitizer Base Card within each ADSY1100 VPX unit. The base card also houses optical transceivers, clock conditioning, power distribution and

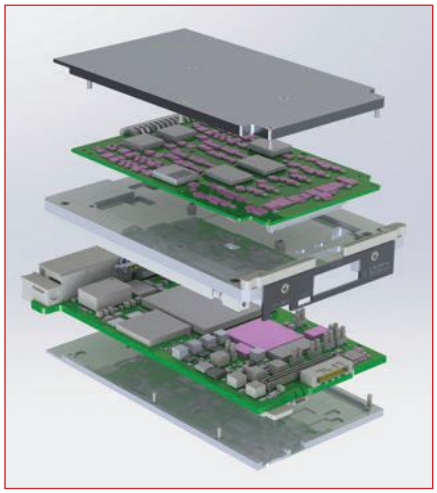

Fig. 2 **Rendering of the ADSY1100-series VPX module.**

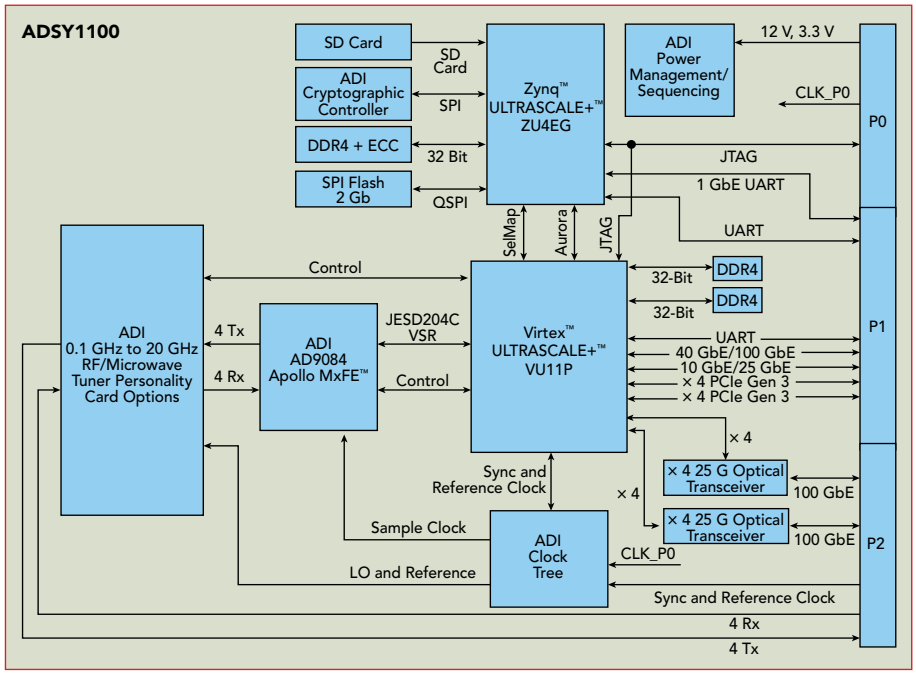

Fig. 3 **ADSY1100 functional block diagram.**

onboard memory. Multiple circuit cards fit within each ADSY1100-series VPX module, including a base card and an RF mezzanine card. ***Figure 2*** shows a rendering of the components and the layout of the ADSY1100-series SoM.

The ADSY1100-series 3U VPX modules are well-suited for various applications, including wideband instrumentation, communications, radar and EW systems. This design is especially suitable for applications requiring reduced SWaP. The multiple-channel RF SoMs can be optimized and quickly deployed for a targeted frequency range by choosing swappable RF front-end mezzanine cards.

CHOOSING AN RF CARD

RF mezzanine cards are available for direct sampling in the 0.01 to 8.5 GHz and 0.1 to 18 GHz frequency ranges. They are also available for frequency tuning from 0.1 to 20 GHz and tuning input signals as high as 55 GHz. Each tuner card provides four receive and four transmit channels and operates on +3.3 VDC and +12 VDC power supplies.

All ADSY1100-series SoMs offer an array of control interfaces, including 1, 10 and 40 Gb Ethernet, two-channel 100 Gb optical Ethernet and eight PCIe Gen. 3 connectivity lanes. Captured data can be stored within internal memory or transferred at high speed by the 100 Gb optical Ethernet port. The digitizers are protected against overvoltage transients and ESD, although ESD precautions should always be taken, given the high density of function and performance. ***Figure 3*** is a block diagram of the ADSY1100-series SoM showing these functions and interfaces.

THEORY OF OPERATION

The ADSY1100 Digitizer Base Card houses the AD9084, Virtex UltraScale+ FPGA and Zynq UltraScale+ MPSoC, as well as optical transceivers, onboard memory, a power distribution network, clock conditioning and more. The P0 and P1 backplane connectors connect directly to the ADSY1100 Digitizer Base Card to provide a 12 V power source, clock sources, auxiliary power, UART, JTAG, PCIe Gen3 data plane, 40/100 Gb Ethernet data plane, 10/25 Gb Ethernet data plane, 1 Gb Ethernet SGMII control plane, Aurora expansion plane and more. An onboard phase-locked loop/synthesizer accepts a low frequency reference clock. It synthesizes two 20 GHz output signals with low phase noise that serve as the sample clock for the AD9084 and the LO for some attached Tuner Personality Cards (TPCs).

A family of TPCs mates to the ADSY1100 Digitizer Base Card to enable optimized performance based on user case. Typical TPC functions include variable gain and attenuation, RF filtering, optional RF frequency conversion and switched paths. Among these, the 0.01 to 8.5 GHz personality card employs a simple RF chain to operate in the first Nyquist zone. However, a 0.1 to 18 GHz personality card implements a switchable filter bank for a higher frequency range to operate in the first and second Nyquist zones. A 0.1 to 20 GHz personality card uses an integrated up-converter and down-converter to operate in the first Nyquist zone for a different high frequency option. A pass-through personality card that omits the front-end signal chain to enable direct signal flow into the base card is also available. Detected and synthesized signals arrive on the ADSY1100 Digitizer Base Card via RF/microwave connectors delivered from the TPC.

Data is offloaded from the ADSY1100 Digitizer Base Card through a 2× 100 Gb Ethernet optical transceiver, which feeds P2A and P2B connectors or by storing the digitized data to onboard memory and subsequently querying the memory from the SGMII interface.

VENDORVIEW

Analog Devices, Inc.
Wilmington, Mass.
www.analog.com/adsy1100

Millimeter Wave Filters Shrink EW and Radar Systems

Benchmark Lark Technology
Tempe, Ariz.

Military electronic systems rely on rugged filters to separate desired and undesired signals. As systems and components shrink to meet reduced size, weight and power (SWaP) requirements, filters must also shrink as they extend into Ku-/Ka-Band and mmWave frequency ranges. With short wavelengths, mmWave filters are smaller than their lower frequency counterparts.

Filters for electronic warfare (EW) and radar applications present design and fabrication challenges at mmWave frequencies. Benchmark Lark Technology's mmWave bandpass filters demonstrate that careful selection of circuit materials and manufacturing processes can reduce mmWave SWaP. With low loss passbands through 40 GHz and high out-of-band rejection, the filters fit in small SMT packages. Though small, the filters meet demanding EW and radar performance requirements in harsh operating environments with wide temperature ranges.

High frequency filters are essential for spectrum management in EW and radar systems. The need for filters grows as spectrum usage extends into mmWave frequencies. Because of shorter mmWave wavelengths, critical components like bandpass filters must be small and often require more fabrication time. Close spacing of filter transmission lines can create unwanted electromagnetic coupling and pose challenges for manufacturing processes requiring tight component tolerances.

Printed circuit board (PCB)-based bandpass filters, like SMT filters, enable miniaturization in single-layer and multilayer configurations. They support reduced SWaP

Fig. 1 **mmW-STL filters feature temperature-stable stripline circuits.**

trends in defense systems and equipment. EW and radar systems often need narrow passbands with high selectivity. Increasing system frequencies limit signal power levels and passband loss becomes an essential performance parameter. In addition, more than 30 dB rejection of unwanted signals outside the passband frequency is required in those systems. Radar applications may also require extended power-handling capabilities for high-power pulsed signals and thermal stability to maintain consistent electrical performance at these power levels.

Careful transmission line layout contributes to tightly controlled electrical characteristics despite the shrinking size of mmWave circuits. Transmission lines include microstrip, stripline and substrate-integrated-waveguide (SIW) technologies. High frequency PCB designers are familiar with microstrip and stripline transmission lines, but perhaps less so for mmWave frequencies. SIW circuits are well suited for closely-spaced transmission lines typical of mmWave circuits. SIW filters fabricated on suitable circuit materials can consistently perform in hostile environments, like those with varying operating temperatures and humidity.

Miniature SIW bandpass filters manufactured with PCB processes can produce consistent and repeatable unit-to-unit performance. Producing SIW filters on low loss substrate materials can reduce non-recurring engineering costs and the time required to transform a prototype into a production unit. Microstrip, stripline and coplanar-waveguide technologies also support mmWave filter responses and circuit miniaturization. These technologies must be fabricated on high-quality dielectric materials with high conductivity plating to achieve the required filter responses at mmWave frequencies.

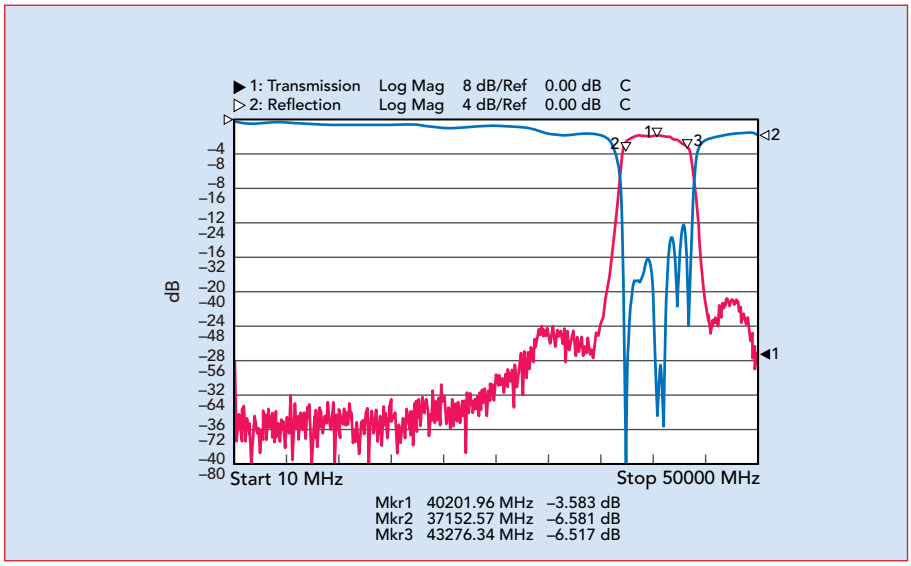

Fig. 2 **Transmission and reflection plots for a 40 GHz mmW-STL filter.**

EW AND RADAR FILTERS

High frequency EW and radar bandpass filter requirements include well-defined, often narrow, passbands with low passband insertion and return loss. High selectivity and minimal center frequency loss ensure the filter will not obscure passband signals of interest. Filter rejection levels, characterized by the lower and upper stopbands, characterize unwanted signal suppression in the filter's operating frequency range. Power-handling capabilities determine the maximum input power level before signal distortion. The maximum input power rating will be CW or pulsed depending upon the application.

Filter circuit topology and circuit material choices complicate bandpass and other filter responses at mmWave frequencies. Smaller mmWave circuit dimensions can stress manufacturing process capabilities, lowering yields and achieving tight dimensional tolerances to enhance production yields raises the manufacturing cost per filter. Circuit material choices also impact filter manufacturing yield, especially at mmWave frequencies. Material parameters like dielectric constant or dissipation factor consistency across the material impact filter consistency, repeatability and performance.

EXPLORING EXAMPLES

Through careful design and thoughtful choice of circuit materials, Benchmark Lark Technology has developed several mmWave filter families that provide the performance needed for EW and radar systems and are small enough to enable system miniaturization. The mmW-STL and mmW-FH mmWave bandpass filters are available in SMT formats for PCB mounting. Both have customizable passbands from 5 to 40 GHz and operating temperatures from -40°C to +85°C.

The mmW-STL bandpass filters in ***Figure 1*** have impressive capabilities in SMT housings. Their performance and size rely on stripline circuits fabricated on advanced substrate materials with a proprietary blend of soft thermoplastic substrates and rigid thermoset materials. This combination of materials provides the electrical and mechanical char-

Fig. 3 **mmW-FH SIW filter.**

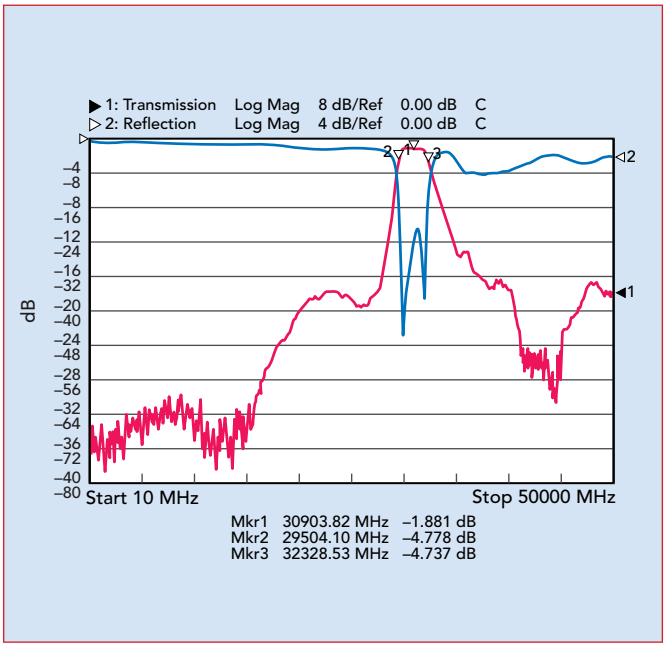

▲ Fig. 4 **Transmission and reflection responses of a mmW-FH filter.**

acteristics needed for rugged, high performance mmWave SMT filters. Because the stripline filter circuits can be fabricated with standard PCB manufacturing processes, mmW-STL bandpass filters can be quickly transformed from design to production. They can be modified for 10 to 25 percent custom passbands from 5 to 40 GHz.

For example, an mmW-STL bandpass filter with a 40.2 GHz center frequency and 6124 MHz (15.2 percent bandwidth) 3 dB passband was designed for a 0.275 × 0.080 × 0.025 in. package. ***Figure 2*** shows the transmission and reflection measurements. The loss is 3.58 dB at the center frequency and the passband return loss is greater than 10 dB. Unwanted, out-of-band signals are rejected by more than 40 dB.

An mmW-FH SIW filter with soft thermoplastic substrates and rigid thermoset materials was fabricated with a 2824 MHz 3 dB passband centered at 30.9 GHz (9.1 percent bandwidth). ***Figure 3*** shows this device in a 0.360 × 0.120 × 0.070 in. package. Loss at center frequency is 1.8 dB, while return loss is better than 10 dB. ***Figure 4*** shows transmission and reflection measurements of the mmW-FH SIW filter.

Both mmWave filter series are customizable to electrical and mechanical requirements. Well-equipped test capabilities for design and production support the manufacturing processes that enable quick prototype-to-production transition. When SWaP is a concern for mmWave frequencies, filters can be quickly developed for the most demanding defense-related applications, including EW and radar systems.

Benchmark Lark Technology
Tempe, Ariz.
www.bench.com/lark

Join the 2025 IEEE AP-S iWAT at Cocoa Beach, FL, Feb. 19-21, 2025. Registration site is open LIVE LINK.

The International Workshop on Antenna Technology (iWAT) is an annual forum for the exchange of information on the research and development in innovative antenna technologies. It especially focuses on small antennas and applications of advanced and artificial materials to the antenna design. At iWAT, all the oral presentations are delivered by invited prominent researchers and professors. iWAT has a particular focus on posters by which authors have the opportunity to interact with leading researchers in their fields. iWAT2025 is a continuation of a series of annual international antenna workshops held in Singapore (2005), White Plaines, USA (2006), Cambridge, UK (2007), Chiba, Japan (2008), Santa Monica, USA (2009), Lisbon, Portugal (2010), Hong Kong, PRC (2011), Tucson, USA (2012), Karlsruhe, Germany (2013), Sydney, Australia (2014), Seoul, Republic of Korea (2015), Cocoa Beach, Florida, USA (2016), Athens, Greece (2017), Nanjing, China (2018), Miami, USA (2019), Bucharest, Romania (2020), Dublin, Ireland (2022), Aalborg, Denmark (2023), and Sendai, Japan (2024).

The workshop is technically sponsored by IEEE AP-S and financially sponsored by IEEE Orlando Section.

On the conference website, you can find the technical program, travel information, and hotel reservation link. In addition, sponsorship and exhibition opportunities are available. Please contact the conference general chair.

Media Sponsor

Microwave Journal

SCAN ME

FOR FULL CONFERENCE DETAILS VISIT

https://attend.ieee.org/iwat-2025/

IEEE AP-S

EUROPE'S PREMIER
MICROWAVE, RF, WIRELESS
AND RADAR EVENT

EUROPEAN
MICROWAVE WEEK
JAARBEURS UTRECHT
THE NETHERLANDS
21-26 SEPTEMBER 2025
www.eumweek.com
WAVES OF INNOVATION

THE EUROPEAN MICROWAVE EXHIBITION

JAARBEURS UTRECHT, THE NETHERLANDS
23 - 25 SEPTEMBER 2025

- 10,000 sqm of gross exhibition space
- Around 5,000 attendees
- 1,700 - 2,000 Conference delegates
- In excess of 300 international exhibitors (including Asia and US as well as Europe)

INTERESTED IN EXHIBITING?

Please contact one of our International Sales Team:

Richard Vaughan,
International Sales Manager
rvaughan@horizonhouse.co.uk

Gaston Traboulsi, France
gtraboulsi@horizonhouse.com

Mike Hallman, USA
mhallman@horizonhouse.com

Victoria and Norbert Hufmann, Germany, Austria & Switzerland
victoria@hufmann.info
norbert@hufmann.info

Katsuhiro Ishii, Japan
amskatsu@dream.com

Young-Seoh Chinn, Korea
corres1@jesmedia.com

CALL +44(0) 20 7596 8742 OR VISIT WWW.EUMWEEK.COM

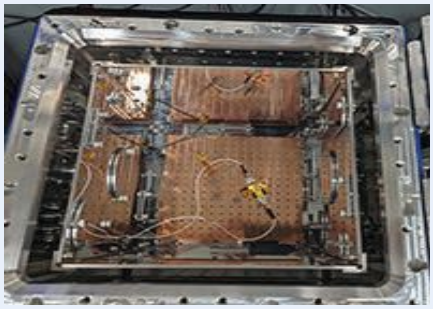

Chamber Enables 110 GHz 4K Testing

Eravant's in-house cold vacuum (CVAC) test chamber supports component testing at frequencies from DC to 110 GHz using 1.0 mm coaxial feedthrough connectors. Other feedthrough connector types include SMA, 2.92, 2.4 and 1.85 mm. Component tests are performed at temperatures down to 4K (-269°C) using a two-stage Gifford-McMahon cryocooler providing 1 W of second stage cooling power down to 4.2K. The cryocooler's second stage is attached to an OFHC cold plate that is surrounded by a mirror-finished radiation shield connected to the first stage. Shield temperatures as low as 60K can be achieved to minimize the heat contribution from internal radiation. The chamber is equipped with silicon diode temperature sensors and a vacuum pressure transducer that feeds digital temperature and vacuum controllers. The controllers include communication interfaces that enable fully-automated testing and provide data logging capabilities.

Vacuum levels as low as 10^{-8} Torr are possible for low-power components. Achievable temperatures and vacuum levels depend on the component heat dissipation and the number of signal feedthroughs. With an array of KF-50, KF-40, KF-25 and KF-16 access ports, the chamber provides a test volume of 7.5 x 7.5 x 7.5 in. Eravant uses the CVAC chamber to develop components for military and space applications that demand reliable low temperature performance and zero low pressure outgassing. Eravant offers CVAC chamber access along with an array of advanced test equipment to support S-parameter, conversion gain, phase noise, noise figure and device linearity measurements.

Eravant is dedicated to making mmWave technology accessible and affordable for developers of new applications. Our decades-long record of innovation and efficient production enables us to help customers test their ideas quickly and transition more directly toward commercialization.

VENDORVIEW

Eravant (formerly Sage Millimeter Inc.)
Torrance, Calif.
www.eravant.com

High-Power SSPA Produces 600 W

Exodus Advanced Communications has developed a high-power solid-state gated amplifier for pulsed radar applications. This amplifier targets TWT-based field applications. The AMP2088-GC uses gating control for 15 nsec (typical) rise and fall times with typical RF delays of 200 to 250 nsec, making it ideal for data acquisition. Although ideal for radar applications, it may also be used for electronic warfare applications and general radiated susceptibility requirements such as EMI-Lab/RS103. The AMP2088-GC amplifier covers the 500 to 1000 MHz P-Band instantaneously while providing outstanding band flatness. The amplifier produces a minimum output of 500 W and exceeds 600 W for much of the band. The amplifier incorporates a class A/AB design that produces 57 dB minimum gain, less than -20 dBc harmonics at rated output and -60 dBc spurious with a 3 dB peak-to-peak power gain flatness. The AMP2088-GC is rack-mountable or may be used on a bench. The solid-state power amplifier (SSPA) noise output is better than -140 dBm/Hz, enabling excellent measurement resolution. The high-power amplifier (HPA) has type N-female connectors for the RF input/output and an optional RF sampling port.

The HPA provides extensive control and monitoring, including optional calibrated power monitoring. Monitoring is via the color display or remote control. The color touchscreen shows forward and reflected power, real-time VSWR, system voltages and currents, operating temperature of the PA modules and heat sinks and internal system temperature. Gain control of more than 20 dB is accessible using the screen or remote interface.

The Exodus product lines use LDMOS, GaN HEMT and GaAs technology, many manufactured internally. In addition to HPAs, Exodus designs low noise amplifiers, modules and multi-band systems from 10 kHz to > 75 GHz.

VENDORVIEW

Exodus Advanced Communications
Las Vegas, Nev.
exoduscomm.com

LEARNING CENTER

Presented by: Microwave Journal

NOW

12/10

Recent Advances in Broadband RF Amplifiers: Beyond Distributed Amps

Sponsored by:

Marki microwave

microwavejournal.com

Now On Demand

Advancing Safety and Reliability in Automotive Radar with Specialized PCB Materials

Sponsored by:

ROGERS CORPORATION

microwavejournal.com/events/2295

Innovations in Satellite Communications & Emerging ESA Technologies

Sponsored by:

RFMW qorvo all around you

microwavejournal.com/events/2293

ONLINE PANEL

New Technologies Driving Military Radar

Sponsored by:

FORTIFY ROHDE&SCHWARZ ALTAIR mercury CAES by Honeywell

microwavejournal.com/events/2296

Test Methodologies for RF/Microwave Transceiver Systems

Sponsored by:

RIGOL

microwavejournal.com/events/2294

FEATURED eBooks

mwjournal.com/ebooks

MAKING WAVES

ADI's SOI Switches

In this video, ADI introduces their latest high-power RF silicon on insulator (SOI) switch technology, tailored to meet the increasing power demands in the aerospace, defense and instrumentation market segments.

Analog Devices Inc.
www.analog.com/en/resources/media-center/videos/6355241554112.html

High-Power Combiners for ISM RF Energy Applications up to 16 kW

Check out this new Mini-Circuits video on their expanded family of high-power splitters and combiners for ISM RF and microwave energy applications.

Mini-Circuits
www.youtube.com/watch?v=9ZDIl-YMJ6g&t=2s

New 2024 RF Product Guide

Insulated Wire Inc. announced the availability of their 2024 High Power Microwave Products catalog. The new 15-page brochure features products for a broad range of both defense and commercial markets.

Insulated Wire Inc.
www.insulatedwire.com

Model Rap Blog

In the latest blog post in the Model Rap Blog series, "Push Higher Frequencies with Lumped-Element Filters," see how it is possible to extend beyond a few GHz and successfully design bandpass filters with center frequencies in the X-/Ku-Band range thanks to Modelithics models for surface-mount components.

Modelithics
www.modelithics.com

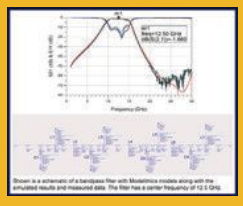

Website Upgrade

MPG launched a powerful new interface on their website to simplify your search for RF and microwave products. Whether you are selecting filters or switches, the revamped UI will streamline your experience like never before.

MPG
https://wizards.mpgdover.com/

M5i.63xx Arbitrary Waveform Generators

Spectrum Instrumentation released a video highlighting their new AWGs in PCIe format, offering a combination of 10 GSPS output speed, 2.5 GHz bandwidth, 16-bit vertical resolution and 8 GS of onboard memory.

Spectrum Instrumentation
www.youtube.com/watch?v=GtJeM17LP3o

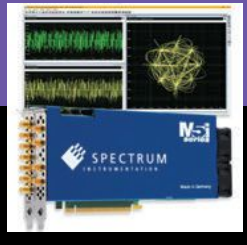

NEW PRODUCTS

FOR MORE NEW PRODUCTS, VISIT WWW.MWJOURNAL.COM/BUYERSGUIDE
FEATURING VENDORVIEW STOREFRONTS

DEVICES/ COMPONENTS/MODULES

Directional Couplers

VENDORVIEW

KRYTAR, Inc. announced two new directional couplers operating in the wideband frequency range of 1.7 to 20.0 GHz (L- through K-Bands) offering nominal coupling of 20 dB and 30 dB. These new couplers offer the ultimate solution for emerging designs and test and measurement applications, including wireless communications, radar and satellite communications. Model 101720020 offers superior performance ratings, including nominal coupling (with respect to output) of 20 dB, ±1.8 dB.
KRYTAR, Inc.
www.krytar.com

Waveguide Switch

High reliability for your RF and microwave requirements, the WR90 Waveguide Switch performs from 8.2 to 12.4 GHz with a VSWR of 1.10:1 maximum, insertion loss of 0.07 dB maximum and isolation of 80 dB minimum.
Logus Microwave
www.logus.com

Splitter/Combiner

VENDORVIEW

Mini-Circuits' model COM-G90G9316K+ is an eight-way, 0/180-degree power splitter/combiner capable of handling as much as 20 kW CW power as a splitter or combiner from 900 to 930 MHz. It features 0.1 dB typical insertion loss above the 9 dB division loss with ± 0.1 dB typical amplitude unbalance and ± 1 degree typical phase unbalance. The 50 Ω non-isolating differential power combiner has low 1.10:1 typical VSWR at the WR975 waveguide sum port and has eight 7/16 DIN female connectors.
Mini-Circuits
www.minicircuits.com

Trimmer Capacitors

Complementing Passive Plus Inc.'s comprehensive range of high Q variable capacitors (air tubular, sapphire, zirconia, PTFE and air plate trimmers) are the film trim and 3 mm trimmer capacitors. Also known as a trimmer capacitor, these are designed for fine adjustments or calibration in RF circuits, providing the ability to vary capacitance, allowing precise tuning and optimization of electronic circuits in LC filters, radio transmitters and receivers, quartz oscillators, low noise amplifiers and NMR coil systems.
Passive Plus Inc.
www.passiveplus.com

Subrack Components

Pixus Technologies now offers an expanded line of subrack components. This includes new subrack depths and heights in both the version-mount and horizontal-mount orientations for boards plugging into a 19 in. rack-mountable enclosure. Pixus provides all of the piece parts for a subrack and options for a fully assembled enclosure. Examples include card guides, horizontal rails, subrack sidewalls, threaded inserts and components geared for IEEE mount and Eurocard mechanicals (standard 3U, 6U and related sizes). The company offers several customized sizes and design styles.
Pixus Technologies
www.pixustechnologies.com

Digital Programmable Attenuator

VENDORVIEW

Quantic PMI Model PDVAN-8018-60-8-OPT25D-BM is an 8-bit digital programmable attenuator that operates over the frequency range of 8 to 18 GHz. This model offers low loss of 3.6 dB typically and an attenuation range of 60 dB. This model handles input power levels up to +25 dBm CW and signal levels up to +30 dBm CW without damage. The attenuation flatness over frequency is less than ±1.6 dB at full attenuation. Switching speed is < 800 ns. Housing is 2.0 × 1.8 × 0.5 in. and has SMA connectors.
Quantic PMI
www.quanticpmi.com

Optical Wavelength Transceiver

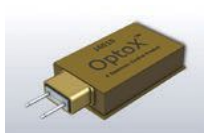

Spectrum Control introduces OptoXtreme™ 16010 quad 10G multi-mode optical wavelength (850 nm) transceiver that effectively addresses the high speed requirements of emerging defense systems, including avionics, radar, missile-detection and counter-measure and reconnaissance video surveillance. Featuring a proprietary pluggable optical connector interface and ball grid array (BGA) base layer contacts in a fully hermetic enclosure, the SMT optical transceivers are designed for reliable, high speed, mission-critical digital data transfer in harsh environments. OptoXtreme operates at 20 Mbps to 10 Gbps per channel.
Spectrum Control
www.spectrumcontrol.com

Inductors

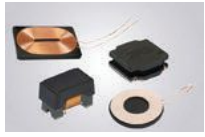

Vishay Intertechnology, Inc. announced a significant expansion of its inductor product lines, adding a broad array of new products designed to provide customers with enhanced options for achieving specific cost/performance ratios in their designs. The broadened portfolio will simplify the sourcing process for Vishay's customers, offering a wider range of device options at various price points. This expansion includes new product offerings that cater to applications requiring higher inductance — by an order of magnitude — and higher voltage inductors. Additionally, Vishay has introduced more size variations, ensuring that customers can find suitable inductors for any available PCB space, no matter how small.
Vishay Intertechnology, Inc.
www.vishay.com

16-Way Combiners/Dividers

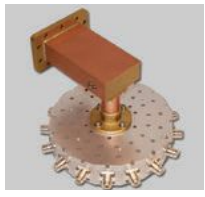

Werlatone Model D9706 is a 16-way in-phase connectorized combiner/divider. It covers the full 2700 to 3500 MHz band and is rated at 2000 W CW. Model D9706 is a non-isolated combiner and operates with less than 0.35 dB of insertion loss. Choose your specific connector configurations from a list of options. Werlatone RF combiners handle the most stringent operating conditions for military and commercial applications.
Werlatone
www.werlatone.com

CABLES & CONNECTORS

Non-Magnetic Connectors

Amphenol RF announced non-magnetic offerings with new SMPM PCB designs. These new connectors are available in the straight jack configuration, featuring either full detent or smooth bore retention. They are specifically engineered with non-ferrous metals and alloys. Non-magnetic RF interconnects are essential for applications such as medical equipment, quantum computing components and military/aerospace technology where the presence of magnetic material in the components may cause interference. These 50 Ω non-magnetic SMPM jacks offer reliable electrical performance up to 26.5 GHz and are engineered with gold-plated, beryllium copper bodies.
Amphenol RF
www.amphenol.com

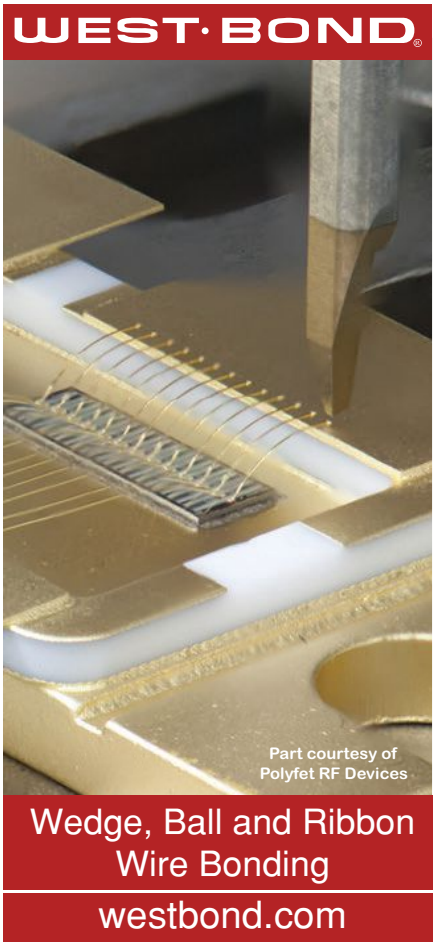

High Precision Armored Test Cable

VENDORVIEW

MIcable's AT110 series armored precision test cable uses low loss, phase and amplitude stable cable, coupled with multi-layer composite armor protection. It has excellent mechanical properties in reliable structure, water and oil proof, abrasion, compression and torsion resistance and good durability, as well as excellent electrical performance in low VSWR, low loss, high shielding effectiveness and stable amplitude and phase, especially in the room temperature range (-10°C ~ +30°C), the phase change rate is less than 100 ppm. It is your ideal choice for the testing of 110 GHz products in laboratory and production line.
MIcable
www.micable.cn

Cable Assemblies

VENDORVIEW

Pasternack has launched its semi-rigid and conformable cable assembly options. These new additions provide enhanced flexibility, performance and customization for a wide range of RF systems and applications. The new cable assemblies include a variety of sizes — 0.047 in., 0.086 in., 0.141 in. and 0.250 in. — in both semi-rigid and conformable cables, offering versatile solutions for signal routing. Customers can select from multiple connector types, including 1.85 mm, 2.4 mm, 2.92 mm, 3.5 mm, SMP, SMPM, SSMC, SMA and TNC.
Pasternack
www.pasternack.com

Test Cables

VENDORVIEW

The P1dB PinPoint™ high performance test cables are built to last, with excellent performance to 125°C, along with a flex life of > 50K cycles. These cables have exceptional phase stability across the entire band, along with best-in-class insertion loss and VSWR performance during flexure and bending. They are available in four different lengths: 24 in., 36 in., 48 in. and 68 in. assemblies and in a variety of interfaces. Available now at RFMW.
RFMW
www.rfmw.com

AMPLIFIERS

Solid-State X-Band Pulse Amplifier

VENDORVIEW

Exodus Advanced Communications' AMP4022DBP-LC-2KW pulse amplifier is designed for pulse/HIRF, EMC/EMI MIL-STD 461/464 and radar applications. Providing superb pulse fidelity and up to 100 usec pulse widths. Duty cycles to 6 percent with a minimum 63 dB gain. Available monitoring parameters for forward/reflected power in watts and dBm, VSWR, voltage, current, temperature sensing for outstanding reliability and ruggedness for compact integrations.
Exodus Advanced Communications
www.exoduscomm.com

Driver Amplifier

The QPA9822 is a wideband, high gain and high linearity driver amplifier. It provides 39 dB gain at 3.5 GHz and achieves a P1dB of 28 dBm. The amplifier is designed to handle wideband 5G NR instantaneous signal bandwidths, making it perfectly suited for mMIMO applications. The QPA9822 is internally matched to over the entire operating frequency band of 3.3 to 4.2 GHz and incorporates a fast enable/disable function through the VEN pin. QPA9822 also has external bias control capability for linearity optimization.
Qorvo
www.qorvo.com

Power Amplifiers

VENDORVIEW

Richardson RFPD Inc., an Arrow Electronics company, announced a featured lineup of Ka-Band, GaN-on-SiC MMIC power amplifiers from United Monolithic Semiconductors (UMS). Offered in die and plastic QFN packaging, the devices are available in a variety of power levels to support Ka-Band satcom uplink and 5G FR2 bands n257, n258, n259 (partial), n260 and n261. UMS' proprietary GH15 GaN process is optimized up to 42 GHz and delivers high power, high PAE and high linearity. It is ideal for transmitting modulated waveforms.
Richardson RFPD Inc.
www.richardsonrfpd.com

New**Products**

Broadband Power Amplifier

Model ABP0250-02-5037 is a three-stage GaN-transistor-based power amplifier module operating in the frequency range from 50 to 2500 MHz with 5 W of output power at a 4 dB gain compression point. It offers 50 dB of linear gain with excellent gain flatness. The unit operates with a single +28 V DC power supply. The package size of the amplifier is 4.0 × 2.0 × 0.875 in.
Wenteq
www.wenteq.com

Wideband Low Noise Amplifier

Z-Communications Inc. announced the AWB0022M wideband low noise amplifier spanning frequencies from DC to 22 GHz. The AWB0022M is a new product line introduction to the low noise amplifier space for applications varying from test and measurement, lab bench and prototyping, to potential OEMs. The AWB0022M low noise amplifier is a continuation of ZCOMM's product line in the RF frequency chain and compliments the company's existing frequency sources, such as the SS-G22645LX wide band frequency synthesizer (45 MHz to 22 GHz).
Z-Communications Inc.
www.zcomm.com

ANTENNAS

Gooseneck Omni Antennas

VENDORVIEW

Fairview Microwave announced the launch of its new gooseneck omni antennas. They are designed to deliver unmatched flexibility and durability for a wide range of applications. The new flexible omni antennas feature a gooseneck-shaped mounting base that allows them to be bent and repositioned at any angle, offering users exceptional adaptability in optimizing signal reception and transmission. Engineered to meet the demands of various environments, the gooseneck omni antennas are available across a wide range of frequencies and radiation patterns.
Fairview Microwave
www.fairviewmicrowave.com

Duck Antennas

L-com has just added a new line of rubber duck antennas. These omnidirectional antennas are compact and flexible for easy installation and adjustment, suitable for low-power applications and cost-effective. They come in three main frequency bands: 2.4 GHz, 433 MHz and 916 MHz. The 2.4 GHz antennas are commonly used to extend the range of Wi-Fi routers, improve the signal strength of Bluetooth devices and enhance the function of cordless telephones.
L-com
www.l-com.com

TEST & MEASUREMENT

Cryogenic and Vacuum Test Services

VENDORVIEW

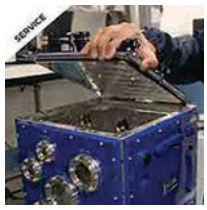

Eravant offers cryogenic and vacuum component testing services using a custom-built cryogenic test chamber. Available feedthroughs include coaxial connectors operating up to 110 GHz. A 1 W cryo-cooler drops the device under test temperature to as low as 4.2 K while a turbomolecular vacuum pump reaches pressures as low as 10^{-8} Torr.
Eravant
www.eravant.com

MICRO-ADS

TRANSIENT IMMUNITY TESTERS

The Avtech AVRQ series of high-voltage, high-speed pulsers is ideal for testing the common-mode transient immunity (CMTI) of next-generation optocouplers, isolated gate drivers, and other semiconductors.

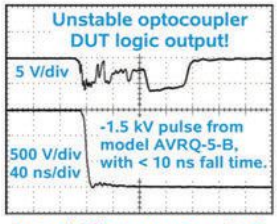

Avtech Electrosystems Ltd.
http://www.avtechpulse.com/
AVTECH
Nanosecond Electronics Since 1975

LOW NOISE AMPLIFIERS
WWW.SATELLINK.COM

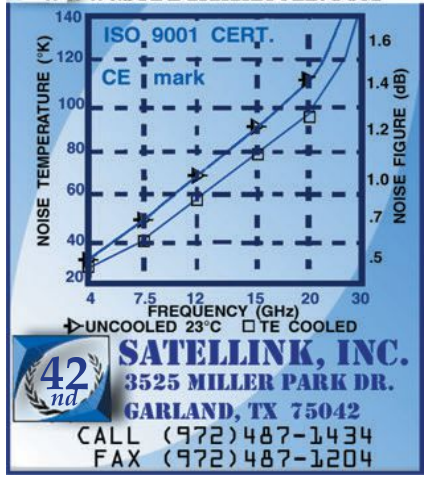

42nd
SATELLINK, INC.
3525 MILLER PARK DR.
GARLAND, TX 75042
CALL (972)487-1434
FAX (972)487-1204

REVOLUTIONARY HERMETIC SMP CONNECTORS

These SMPs meet the requirements of MIL-STD-348, but utilize unique housing interface features, which significantly improves reliability and production assembly yields. Proprietary techniques are used to independently control plating thickness on pin and housing.

For use with Aluminum, Kovar and other package materials

SHP
SPECIAL HERMETIC PRODUCTS, INC.
PO BOX 269 – WILTON – NH – 03086
(603) 654-2002 – Fax (603) 654-2533
E-mail: sales@shp-seals.com
Web: www.shp-seals.com

RF Amplifiers, Isolators and Circulators from 20MHz to 40GHz

- Super low noise RF amplifiers
- Broadband low noise amplifiers
- Input PIN diode protected low noise amplifiers
- General purpose gain block amplifiers
- High power RF amplifiers and broadband power amplifiers

- RF isolators and circulators
- High power coaxial and waveguide terminations
- High power coaxial attenuators
- PIN diode power limiters
- Active up and down converters

Wenteq Microwave Corporation
138 W Pomona Ave, Monrovia, CA 91016
Phone: (626) 305-6666, Fax: (626) 602-3101
Email: sales@wenteq.com, Website: www.wenteq.com

Reviewed by: Ajay Poddar

Bookend

Electromechanical Coupling Theory, Methodology and Applications for High-Performance Microwave Equipment

By Baoyan Duan and Shuxin Zhang

The subjects covered in "Electromechanical Coupling Theory, Methodology and Applications for High-Performance Microwave Equipment" are intriguing for those interested in high performance microwave equipment. This book provides readers with a comprehensive understanding of the theoretical model of field coupling between the mechanical displacement field, electromagnetic (EM) field and temperature field. These topics are not extensively covered in books available on the market. The authors, a team of university researchers, emphasize the application of electromechanical coupling theory in the broadest definition of terms, such as EM interaction and coupling for high performance microwave equipment. The book reports 11 chapters, discussing the background of EM coupling and coupling models, EM coupling-based evaluation and measurement, CAD tools for coupling analysis and design of electronic equipment and development trends of coupling dynamics. The book covers a broad range of topics and provides readers with a deeper insight into the design and development of electronic equipment. It is an excellent resource for anyone interested in designing high performance electronic equipment.

Overall, the content explores the influence mechanism of mechanical factors on electrical performance. It proposes EM coupling test methods, evaluation methods and multidisciplinary optimization design methods based on field coupling theory and influence mechanism. Moreover, the book develops a comprehensive design software platform that integrates EM, mechanics and thermodynamics to solve the bottleneck problem that restricts the improvement of electronic equipment performance, affecting the development of electronic equipment in the next generation.

This book caters to an extensive range of buyers, covering a broad spectrum of expertise. It is an excellent resource for students and professionals working in the engineering field, from those just starting as junior design engineers to experienced technical expert scientists. The book is highly informative and packed with valuable insights and information that can benefit individuals with varying levels of expertise.

ISBN 13: 978-1-119-90439-7
Pages: 336
To order this book, contact:
Wiley (December 2022)
https://www.wiley.com/en-us

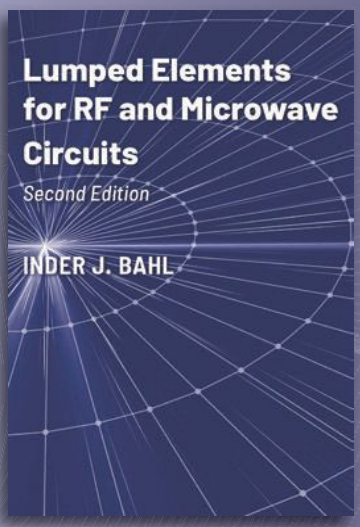

- Presents a comprehensive text on lumped elements useful in the design of RF, microwave and millimeter wave components and circuits;
- Revised version has a more balanced treatment between standalone lumped elements and their circuits using MICs, MMICs and RFICs technologies;
- Provides detailed information on a broader range of RFICs not included in the 1st Edition;
- Features extensive formulas for lumped elements, design trade-offs, and updated and current list of references;
- Discusses fundamentals, equations, modeling, examples, references, and overall procedures to design, test, and produce microwave components.

Lumped Elements for RF and Microwave Circuits, Second Edition

Inder J. Bahl

ISBN 9781630819323 · 2023
Hardcover · 600 pp

$189 / £164

Sign up for our newsletter for 15% OFF your first purchase.

Find out more by scanning the QR code or visiting us at artechhouse.com

ARTECH HOUSE
BOSTON | LONDON

30th ANNIVERSARY

DESIGNCON® 2025

WHERE THE CHIP MEETS THE BOARD

Host Sponsor: Amphenol

JANUARY 28–30, 2025

Santa Clara Convention Center
Santa Clara, California

The Nation's Largest Event for Chip, Board & Systems Design Engineers

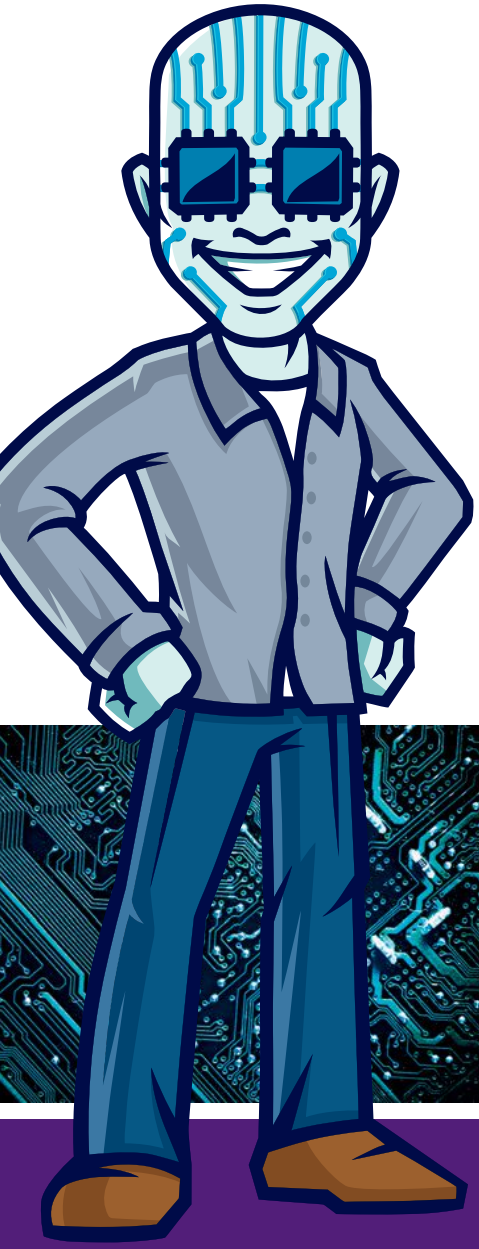

Created by engineers for engineers, DesignCon celebrates its 30th anniversary bringing together designers, technologists, and innovators from the high-speed communications and semiconductors communities for three jampacked days of education, exhibits and networking.

EXPO

- Over 170 exhibits
- Daily keynotes open to all attendees
- Free education at Chiphead Theater and panels
- 30th anniversary Welcome Reception

EDUCATION

- 14 track conference with technical sessions and tutorials
- Drive World conference focused on EV and autonomous electronics and intelligence
- Over 240 expert speakers

informa markets

Register at:

DesignCon.com

Use code **MJH25** when registering for **15% off any conference pass** or a **free expo pass**

Advertising**Index**

Advertiser	Page No.
3H Communication Systems	35
Aaronia AG	COV 3
Analog Devices	41
Artech House	102
Avtech Electrosystems	101
B&Z Technologies, LLC	11
Bradford RF Sales	71
Cernex, Inc.	74
Ciao Wireless, Inc.	28
Coilcraft	19
COMSOL, Inc.	15
DesignCon 2025	103
EDI CON Online	87
Empower RF Systems, Inc.	30
ERAVANT	23
EuMW 2025	85, 95
Exceed Microwave	38
Exodus Advanced Communications, Corp.	49
Fairview Microwave	55
G.T. Microwave Inc.	83
GGB Industries, Inc.	3
Harogic Technologies	69
Herotek, Inc.	64
IEEE WAMICON 2025	42
iNRCORE	53
Insulated Wire, Inc.	73
Ironwave Technologies	54
iWAT 2025	94
KRATOS Microwave USA / CTT	24
KRYTAR	68
KVG Quartz Crystal Technology GmbH	38
LadyBug Technologies LLC	46
Marki Microwave, Inc.	57
MECA Electronics, Inc.	22
Menlo Micro	47
MIcable Electronic Technology Group	39, 75
Micro Lambda Wireless, Inc.	51
Microwave Journal	40, 97
Microwave Products Group (a Dover Company)	52
Miller MMIC	COV 2, 21
Millimeter Wave Products Inc.	43
Mini-Circuits	4-5, 16, 32, 105
Networks International Corporation	6
Norden Millimeter Inc.	58
Nxbeam	25
Passive Plus	61
Pasternack	8
Peraso, Inc.	67
Q-Tech Corporation	86
QML Inc.	40
Quantic M Wave	34
Reactel, Incorporated	31
Remcom	45
Remtec	60
RF-Lambda	9, 27, 65, 79
RFMW	13, 57
Saetta Labs	26
Safran Electronics & Defense	76
Satellink, Inc.	101
Sigatek LLC	50
Signal Hound	63
Smiths Interconnect	59
Special Hermetic Products, Inc.	101
Spectrum Control	7
State of the Art, Inc.	78
Synergy Microwave Corporation	37, 77
Tecdia, Inc.	48
Tianqiong Electronic	66
Weinschel Associates	20
Wenteq Microwave Corporation	101
Werlatone, Inc.	COV 4
West Bond Inc.	100

Sales Representatives

Eastern and Central Time Zones
Michael Hallman
Associate Publisher
(NJ, Mid-Atlantic, Southeast, Midwest, TX)
Tel: (301) 371-8830
Cell: (781) 363-0338
mhallman@mwjournal.com

Carl Sheffres
Northeastern Reg. Sales Mgr.
(New England, New York, Eastern Canada)
Tel: (781) 619-1949
csheffres@mwjournal.com

Pacific and Mountain Time Zones
Brian Landy
Western Reg. Sales Mgr.
(CA, AZ, OR, WA, ID, NV, UT, NM, CO, WY, MT, ND, SD, NE & Western Canada)
Tel: (831) 426-4143
Cell: (831) 713-9085
blandy@mwjournal.com

International Sales
Carl Sheffres
Tel: (781) 619-1949
csheffres@mwjournal.com

Germany, Austria, and Switzerland (German-speaking)
Victoria and Norbert Hufmann
victoria@hufmann.info
norbert@hufmann.info

Korea
Jaeho Chinn
JES MEDIA, INC.
Tel: +82 2 481-3411
corres1@jesmedia.com

China
Shanghai
Linda Li
ACT International
Tel: +86 136 7154 0807
lindal@actintl.com.hk

Wuhan
Phoebe Yin
ACT International
Tel: +86 134 7707 0600
phoebey@actintl.com.hk

Shenzhen
Annie Liu
ACT International
Tel: +135 9024 6961
anniel@actintl.com.hk

Beijing
Cecily Bian
ACT International
Tel: +86 135 5262 1310
cecilyb@actintl.com.hk

Hong Kong
Floyd Chun
ACT International
Tel: +852 28386298
floydc@actintl.com.hk

Taiwan, Singapore
Simon Lee
ACT International
Tel: +852 2838 6298
simonlee@actintl.com.hk

Japan
Katsuhiro Ishii
Ace Media Service Inc.
Tel: +81 3 5691 3335
amskatsu@dream.com

Submitting ad material?
Visit: www.adshuttle.com/mwj
(866) 774-5784
outside the U.S. call
+1-414-566-6940

Ed Kiessling
(781) 619-1963
ekiessling@mwjournal.com

ISM RF & MW ENERGY

2.4 GHz Building Blocks

Flexible, Scalable Capabilities up to 6 kW

LEARN MORE

Signal Generator/Controller

ISC-2425-25+

Key Features:

- 30 to +25 dBm (0.1 dB steps)
- Frequency from 2.4 to 2.5 GHz (1 kHz steps)
- Closed loop and feed forward RF power control modes
- User-friendly GUI and full API

300W SSPA

ZHL-2425-250X+

Key Features:

- 300W output power
- Supports CW & pulsed signals
- 42 dB gain
- 60% efficiency
- Built-in monitoring and protection

4-Way Splitter with Phase & Amplitude Control

SPL-2G42G50W4+

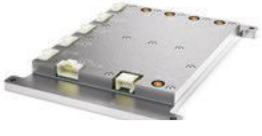

Key Features:

- 2.4 to 2.5 GHz
- Drive up to 4 amplifier stages from 1 ISC-2425-25+ controller
- Precise control of amplitude and phase on each path

Coming soon

High Power 4-Way Combiner

COM-2G42G51K0+

Key Features:

- 1.2 kW power handling (sum port)
- 0.1 dB insertion loss
- 0.15 dB amplitude unbalance
- 1° phase unbalance
- 4x N-Type to 7/16 DIN

Mini-Circuits

Microsembly: A Fully Equipped Partner

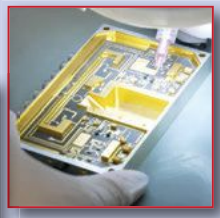

Microsembly, founded in 2019 and based in Merrimack, N.H., brings together prototyping, manufacturing, and testing capabilities in a 20,000-square-foot facility equipped with ISO 14644-1-compliant Class 7 and Class 8 cleanrooms. The company is positioned to serve two main types of customers: smaller and medium-sized RF and microwave designers and suppliers looking to fulfill specific, high performance requirements and larger manufacturers who need to maintain tight delivery schedules without compromising quality. In both cases, Microsembly provides scalable, flexible support that allows clients to manage fluctuating demands without extensive capital investments.

For both customer groups, the prototyping stage at Microsembly emphasizes design for manufacturability (DFM), integrating practical manufacturing insights into the design process. For smaller companies, Microsembly can refine designs to avoid costly production rework processes, while larger manufacturers can leverage the company's DFM insights to validate product iterations before going to production volumes. Their cleanroom environments support contamination-sensitive processes like die attach, critical for high frequency RF and optical components, helping clients achieve high reliability.

Once a design is validated, Microsembly's manufacturing capabilities offer a range of specialized techniques suited to high performance RF and microwave applications. Microsembly's manufacturing processes include eutectic and epoxy die attach, wire and ribbon bonding and the direct attachment of beam lead diodes for minimized parasitics in high frequency circuits.

Additional manufacturing capabilities at Microsembly include custom coil fabrication and feedthrough soldering, which allow for tailored solutions and unique design need if specific RF and magnetic properties are required. In addition, Microsembly performs encapsulation and wafer processing to add protection and durability to components that may need to operate in rigorous and harsh environments.

These processes enable Microsembly to support complex builds and component integrations, allowing clients to effectively add significant manufacturing capacity without needing to expand in-house facilities.

Microsembly has test capabilities to 110 GHz. This enables validation of RF, microwave and mmWave chips, components and assemblies across a full range of electrical and mechanical performance metrics. For smaller suppliers, these capabilities eliminate the need for costly, in-house, high frequency testing equipment. Small and large suppliers can benefit from Microsembly's testing suite that covers RF and EMI/EMC performance, mechanical stress and environmental conditions for a range of devices from basic active and passive components to complex, fully integrated microwave assemblies like up-converters and transceivers.

Manufacturers can also benefit from Microsembly's expertise by augmenting their quality control and inspection needs. Quality control is built into each phase of production. This includes rigorous in-process inspections and certifications including ISO-9001, ITAR registration, ANSI/ESD S20.20 and IPC-A-610, along with J-STD-001 (Space Addendum).

Through its prototyping, manufacturing, inspection and testing services, the company reinforces a commitment to precision. This enables Microsembly products to meet the most stringent client requirements before reaching the field. In addition to these manufacturing services, the company also offers inventory services as part of a flexible, on-demand partner relationship. Microsembly offers a unique set of value propositions for the industry. Smaller RF and microwave suppliers can benefit from a contract relationship that allows them to scale performance, quality and throughput. Larger manufacturers can use Microsembly as an extension to fill specific design, production and testing gaps. For customers of any size, Microsembly stands ready to manage manufacturing and supply chain demands with their expertise and service capabilities.

www.microsembly.com

SPECTRAN® V6

BEYOND REALTIME

Setting **the Mobile Benchmark**

The ULTIMATE Real-Time Spectrum Analyzer TABLET

HIGH-END SPECTRUM ANALYZER

- 9 kHz up to 140 GHz
- Optional Tx (Generator)
- 490 MHz Bandwidth
- 3 THz/s Sweep Speed
- 16-Bit ADC
- -170dBm/Hz | 4dB NF
- GPS & Time Server
- Incl. RTSA-Software

PREMIUM PC POWER

- AMD 8-Core 8845HS CPU
- 64 GB LPDDR5 RAM
- 64 TB Highspeed SSD
- 2x M.2 2280 & 3x M.2 2242
- Lots of I/Os incl. USB4, SD & HDMI
- Inbuilt SIM, opt. WiFi, Bluetooth, 5G
- SFP+ 10G Ethernet, SATA, RS232
- Windows or Linux

RUGGED FORM FACTOR

- 15.6" 1500 NIT Full HD Touchscreen
- Rugged Aluminum Casing
- Front and Back Cameras
- Optional Handle and Back Stand
- Removable Battery

MADE IN GERMANY

www.aaroniausa.com
ubuy@aaroniausa.com
+1 (214) 935-9800

www.aaronia.com
mail@aaronia.de
+49 6556 900 310

AARONIA AG®
WWW.AARONIA.COM

WERLATONE

A STEP AHEAD

SOLUTIONS FOR EVERY MILITARY PLATFORM

COMMUNICATIONS | EW | RADAR

DC TO X-BAND

INTEGRATED SUB-ASSEMBLIES

BEAMFORMERS

WAVEGUIDE SOLUTIONS

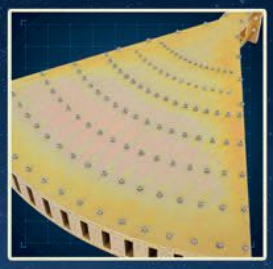

E-PLANE COMBINERS

FIXED | AIRBORNE | GROUND MOBILE | SHIPBOARD

WE OFFER A VARIETY OF POWER LEVELS RANGING FROM 10 W CW TO 20 KW CW.
WERLATONE'S HIGH POWER, MISMATCH TOLERANT® SOLUTIONS
ARE DESIGNED TO OPERATE IN EXTREME LOAD MISMATCH CONDITIONS.

BRING US YOUR CHALLENGE | WWW.WERLATONE.COM

WERLATONE

LEARN MORE

REVIEW BOARD MWJ APPROVED

exclusive Digital Content >>>

Nonlinear Algorithm for Small-Signal GaN HEMT Modeling

Ziyue Ding, Haiyi Cai, Jincan Zhang, Yuhao Ren and Jinchan Wang
Henan University of Science and Technology, Luoyang, China

A nonlinear dynamic adaptive inertia weights-particle swarm optimization (DAIW-PSO) algorithm is described for GaN high electron mobility transistors (HEMTs) small-signal model intrinsic parameter extraction and optimization. Experimental results show that the DAIW-PSO algorithm addresses the problem that the PSO algorithm tends to converge too early and fall into a local optimum. It accurately extracts and optimizes the intrinsic parameters in the frequency range of 0.5 to 20.5 GHz.

The electronic information industry is rapidly changing, closely coupled with the thriving development of semiconductor devices.[1-3] With the advantages of wide bandwidth, high electron mobility, high voltage resistance and the ability to operate reliably at high temperatures, GaN HEMTs are widely used in high-power and high frequency circuits.[4-11] Accurate modeling of GaN HEMTs is necessary to enable device and circuit design, where the accuracy of large-signal modeling depends largely on the small-signal model.[12,13] It is therefore important to conduct small-signal modeling and to accurately extract and optimize the small-signal model parameters.[14,15]

Since 2000, representative GaN HEMT small-signal models and parameter extraction methods have been proposed.[16,17] At present, the parameter extraction methods for GaN HEMT small-signal models include mainly direct extraction[18-20] and numerical optimization.[21-23] To extract the GaN HEMT small-signal model parameters quickly and accurately, this article employs the direct extraction method to extract the parasitic parameters. Then, it uses an improved PSO algorithm to extract and optimize the intrinsic parameters.[24] The PSO algorithm has many advantages, such as being easy to implement with few adjustable parameters and it is often applied in many fields.[26,27] However, the standard PSO algorithm has the problem of converging too early and easily falling into a local optimum.[28,29]

To address this, Clerc and Kennedy[30] proposed using the constraint factor λ to control the algorithm's convergence speed. This strategy improves the performance of the standard PSO algorithm to a certain extent, but it is still easy to fall into a local optimum in highly complex and high-latitude optimization problems. To better improve the algorithm's tendency to converge too early and fall into a local optimum, a nonlinear DAIW-PSO algorithm is described in this article to extract and optimize the intrinsic

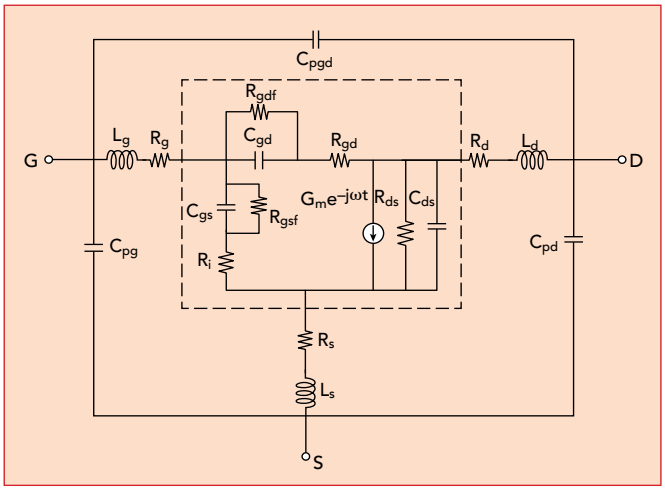

Fig. 1 **GaN HEMT small-signal model equivalent circuit.**

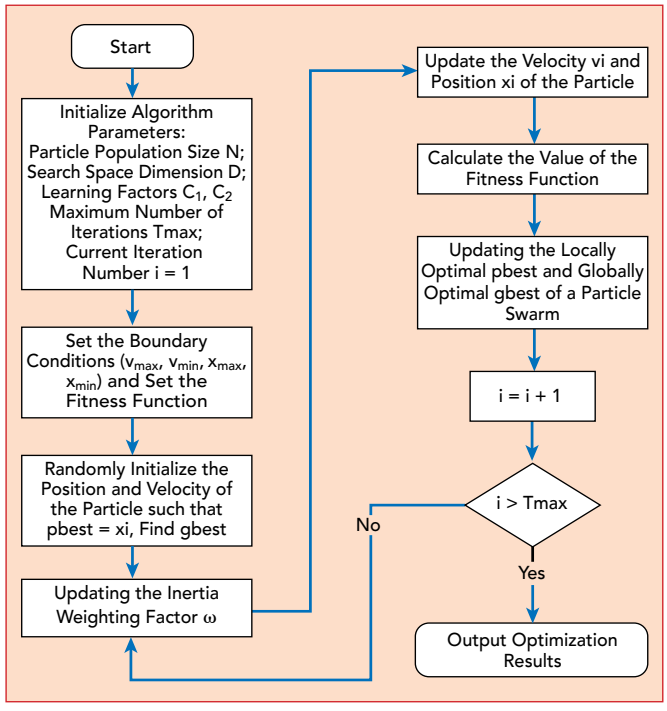

Fig. 2 **DAIW-PSO optimization of intrinsic parameters algorithm flow chart.**

parameters of a GaN HEMT small-signal model.[31]

SMALL-SIGNAL MODEL

The GaN HEMT small-signal equivalent circuit model is divided into two parts, as shown in ***Figure 1***. In this diagram, the intrinsic circuit model is inside the dashed box and the parasitic circuit model is outside the box. The parasitic components include mainly parasitic capacitances (C_{pg}, C_{pd}, C_{pgd}), parasitic inductances (L_g, L_d, L_s) and parasitic resistances (R_g, R_d, R_s). The intrinsic components include mainly gate-source capacitance (C_{gs}), gate-drain capacitance (C_{gd}), drain-source capacitance (C_{gs}), intrinsic resistance (R_i), drain-source resistance (R_{ds}), gate-drain resistance (R_{gd}), transconductance (G_m), time-delay constant (τ), gate-drain differential conductance (G_{gdf}) and drain-source differential conductance (G_{gsf}).

SMALL-SIGNAL MODEL PARAMETER EXTRACTION

Parasitic Parameter Extraction

The values of parasitic capacitances, parasitic inductances and parasitic resistances are extracted separately. The parasitic capacitances are extracted at the cutoff condition where V_{GS} = -3 V, V_{DS} = 0 V or V_{GS} = -2.75 V, V_{DS} = 0 V and the low frequency state.[32] Under this condition, parasitic resistances and parasitic inductances can be neglected and the device exhibits mainly capacitive characteristics, allowing the parasitic capacitances to be extracted.

After stripping the effect of parasitic capacitances, parasitic inductances are extracted under unbiased conditions (V_{GS} = 0 V, V_{DS} = 0 V). After removing the effects of parasitic capacitances and parasitic inductances, the parasitic resistances are then extracted using the reverse cutoff method with V_{GS} = - 2.5 V and V_{DS} = 0 V. This extraction technique does not rely on positive biasing of the Schottky gate junction, which eliminates gate degradation induced by large gate currents.

DAIW-PSO Algorithm

The PSO algorithm randomly defines massless and volumeless particles to determine the optimal solution. Each particle has two vectors: velocity and position. In the iterative process, each particle updates the local optimal value (p_{best}) according to the fitness function and the particle swarm finds the global optimal value (g_{best}) according to all the local optimal values. The particles continuously adjust speed and position according to their own experiences and the experience of the swarm. The particles update their velocities and positions in the iterative process described by ***Equation 1*** and ***Equation 2***:

$$v_i^{t+1} = \omega v_i^t + c_1 r_1 \left[p_i^t - x_i^t \right] + c_2 r_2 \left[g_i^t - x_i^t \right] \quad (1)$$

$$x_i^{t+1} = x_i^t + v_i^{t+1} \quad (2)$$

Where:

v_i^t is the velocity of the particle

x_i^t is the position of the particle

p_i^t is the local optimum

g_i^t is the global optimum

c_1 and c_2 are the learning factors

r_1 and r_2 are random numbers, usually in the range of [0 to 1]

ω is the inertia weight factor, typically taking values in the range of 0.4 to 0.9.

The inertia weight factor is very important in regulating the global and local searches. When the value of ω is large, the swarm can perform the broadest search in the determined range. When the value of ω is small, the swarm can perform a fine local search in a small, determined range. The inertia weight factor of the standard PSO algorithm is fixed, so the algorithm cannot balance the global search and local search well, suffering from the problems of converging too early and easily falling into a local optimum.

Shi and Eberhart[33] proposed a PSO algorithm with linearly decreasing inertia weights to improve the algorithm's search capability. However, the trajectory of the particle swarm in the actual optimization process is complicated, so the linearly decreasing inertia weights cannot reflect the actual optimization

search process. Considering this problem, this article uses nonlinear dynamic adaptive inertia weights to improve the PSO algorithm to produce the DAIW-PSO algorithm.

Evolutionary dispersion is used in the DAIW-PSO algorithm to describe changes in the overall fitness values during population evolution. The standard deviation of the fitness value between the population of generation (t) and the population of generation (t-1) is defined as the evolutionary dispersion k(t).[31] This is shown in ***Equation 3***:

$$\begin{cases} k(t) = 1 & t = 1 \\ k(t) = \dfrac{fitness(t)}{fitness(t-1)} & t > 1 \end{cases} \quad (3)$$

The sigmoid function *S(x)* shows a good balance between linear and nonlinear and is a very good threshold function,[31] as shown in ***Equation 4***:

$$S(x) = \frac{1}{1 + exp(-x)} \quad (4)$$

The DAIW factor is obtained by jointly evolving the discretization and sigmoid functions.[31] Its inertia weight factor is given in ***Equation 5***:

$$\omega(t) = \omega_{max} + (\omega_{min} - \omega_{max}) \frac{1}{1 + exp\left[-10b\left(\dfrac{2t}{k(t)T_{max}}\right) - 1\right]} \quad (5)$$

Where:

ω_{max} is the maximum inertia weight factor (usually taking the value of 0.9)

ω_{min} is the minimum inertia weight factor (usually taking the value of 0.4)

t is the number of contemporary iterations

T_{max} is the maximum number of iterations

b is the damping factor to adjust the smoothing degree of k(t).

The DAIW-PSO algorithm is used to extract the intrinsic parameter parts of the device model. Its specific flow is shown in ***Figure 2***.

Intrinsic Parameter Extraction

After stripping the effect of parasitic parameters by de-embedding, the intrinsic parameters are extracted and optimized under specific bias conditions using the DAIW-PSO algorithm using ***Equation 6*** through ***Equation 9***.

$$Y_{gs} = Y_{int,11} + Y_{int,12} = \frac{j\omega C_{gs} R_{gsf}}{R_{gsf} + R_i + j\omega R_i C_{gs} R_{gsf}} \quad (6)$$

$$Y_{gd} = -Y_{int,12} = \frac{1 + j\omega C_{gd} R_{gdf}}{R_{gdf} + R_{gd} + j\omega R_{gd} C_{gd} R_{gdf}} \quad (7)$$

$$Y_{ds} = Y_{int,22} + Y_{int,12} = \frac{1}{R_{ds}} + j\omega C_{ds} \quad (8)$$

$$Y_{gm} = Y_{int,21} - Y_{int,12} = \frac{R_{gsf} G_m e^{-j\omega\tau}}{R_{gsf} + R_i + j\tau C_{gs} R_{gsf}} \quad (9)$$

Where:

$Y_{int,11}$, $Y_{int,12}$, $Y_{int,21}$ and $Y_{int,22}$ are the Y-parameters of the intrinsic circuit model

Y_{gs} is the gate-source admittance

Y_{gd} is the gate-drain admittance

Y_{ds} is the drain-source admittance

Y_{gm} is the intrinsic conductance.

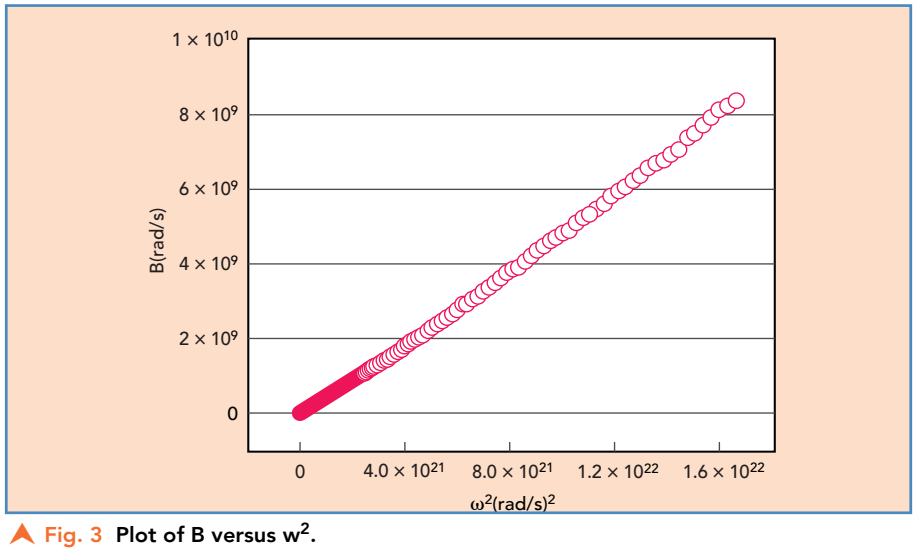

Fig. 3 **Plot of B versus w^2.**

From this, ***Equation 10*** through ***Equation 12*** are derived.

$$B_1 = \frac{1}{C_{gs} R_{gsf}^2} + \omega^2 C_{gs} \quad (10)$$

$$B_2 = \omega \mathrm{Im} g Y_{ds} = \omega^2 C_{ds} \quad (11)$$

$$B_3 = \omega \frac{Y_{gd}^2}{\mathrm{Im}\, Y_{gd}} = \frac{1}{C_{gd} R_{gsf^2}} + \omega^2 C_{gd} \quad (12)$$

The value of C_{gs} is found from the slope of Equation 10, which is plotted in ***Figure 3*** and R_{gsf} is found from its intercept. The values of C_{ds} and C_{gd} are found from the slopes of Equations 11 and 12, respectively.

The R_{ds}, τ and G_m values are found from ***Equation 13*** through ***Equation 15***.

$$R_{ds} = \frac{1}{\mathrm{Real}(Y_{int,22} + Y_{int,12})} = \frac{1}{\mathrm{Real}(Y_{ds})} \quad (13)$$

$$\tau = \frac{tan^{-1}\left(\dfrac{-\mathrm{Imag}(Y_{int,21} - Y_{int,12})}{Real(Y_{int,21} - Y_{int,12})}\right)}{\omega} \quad (14)$$

$$G_m = -\frac{\mathrm{Imag}(Y_{int,21} - Y_{int,12})}{sin(\omega\tau)} = \frac{\mathrm{Real}(Y_{int,21} - Y_{int,12})}{cos(\omega\tau)} \quad (15)$$

The R_{gd}, C_{gd} and R_iC_{gs} values are derived from the slopes of the real part of ***Equation 16*** and ***Equation 17*** to obtain the values of R_{gd} and R_i, R_{gdf} is derived from the intercept of the real part of Equation 16.

$$B_4 = \omega \cdot \frac{|Y_{gd}|^2}{\mathrm{Imag}(Y_{gd})} = \frac{R_{gd} + R_{gdf}}{R_{gdf} C_{gd}} + \omega^2 R_{gd} C_{gd} + j\omega \quad (16)$$

$$B_5 = \omega^2 R_i C_{gs} + j\omega \quad (17)$$

EXPERIMENTAL RESULTS

A GaN HEMT device is used to verify the small-signal model in the frequency range of 0.5 to 20.5 GHz. The device is calibrated with an off-wafer precision short/open/load standard. A Keysight E3631A power supply is used to provide the DC bias voltage and S-parameters are measured with a Keysight N522A vector network analyzer. The GaN HEMT 19-parameter small-signal model is constructed in Keysight

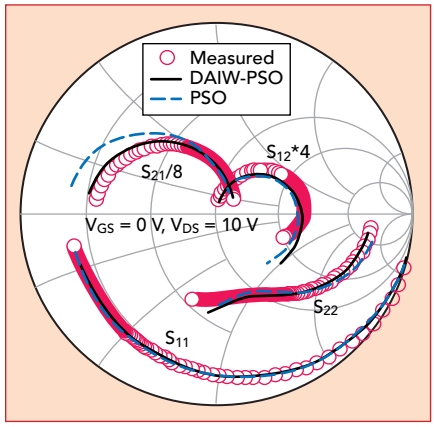

Fig. 4 S-parameter modeled results for V_{GS} = 0 V, V_{DS} = 10 V.

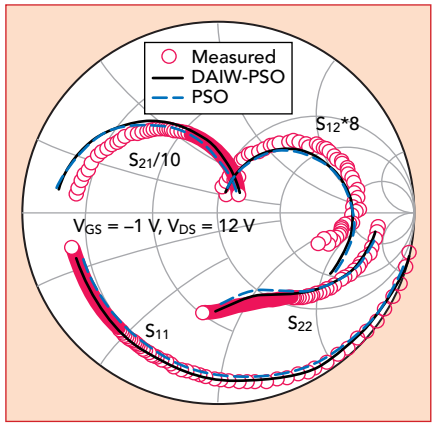

Fig. 5 S-parameter modeled results for V_{GS} = – 1 V, V_{DS} = 12 V.

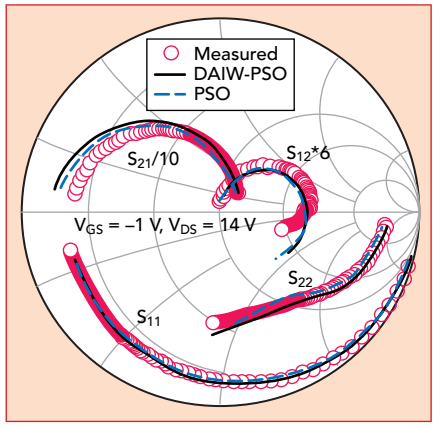

Fig. 6 S-parameter modeled results for V_{GS} = – 1 V, V_{DS} = 14 V.

ADS software for parametric simulation. The optimization algorithm is constructed in MATLAB software to extract and optimize the intrinsic parameters.

After extracting the values of parasitic and intrinsic parameters, the S-parameters are obtained by substituting the parameter values into the small-signal ADS model. For a more intuitive view of the performance of the PSO and DAIW-PSO algorithms in parameter optimization, the modeled and measured results are compared in the Smith charts in ***Figure 4*** through ***Figure 6***. Under the three bias conditions, the parameters extracted using the DAIW-PSO algorithm are modeled with small errors and close to the measured results.

Error analysis of the developed model is derived from ***Equation 18***:

$$\text{Error}ij = \frac{1}{N}\sum_{k=1}^{N}\frac{\left|\left|S_{ij}^{meas}(f_k)\right| - \left|S_{ij}^{model}(f_k)\right|\right|}{\left|\max\left(S_{ij}^{model}(f_k)\right)\right|}, \quad i,j = 1,2 \tag{18}$$

Where:

N denotes the number of measurement points selected in the scanning frequency range

$S_{ij}^{meas}(f_k)$ denotes the actual measured S-parameters

$S_{ij}^{model}(f_k)$ denotes the S-parameter values obtained from the simulation of the small-signal model established in this work.

Table 1 shows the errors of the GaN HEMT S-parameters. The S-parameters obtained from the simulation using the parameters extracted by the DAIW-PSO algorithm show smaller errors and better optimization results than the PSO algorithm alone.

CONCLUSION

To accurately characterize the small-signal properties of a GaN HEMT device, the DAIW-PSO algorithm is used to extract and optimize the intrinsic parameters. The DAIW-PSO algorithm combines the evolutionary discretization k(t) and the sigmoid function to obtain nonlinear dynamic adaptive inertia weight factors to optimize the standard PSO algorithm. The DAIW-PSO algorithm significantly improves upon the performance of the standard PSO algorithm, which converges too early and easily falls into a local optimum.

Experimental results show that S-parameter modeling using the parameters extracted by the DAIW-PSO algorithm are very close to measurements in the 0.5 to 20.5 GHz range, which validates its accuracy and effectiveness. The DAIW-PSO algorithm also facilitates extracting and optimizing the GaN HEMT small-signal model parameters. ■

ACKNOWLEDGMENTS

This work was supported by the Foundation of the Department of Science and Technology of Henan Province (Grant No. 232102211066).

References

1. J. Zhang, X. Hou, M. Liu, S. Yang, B. Liu, J. Wang and J. Zhang, "Hybrid Small-Signal Modeling of GaN HEMTs Based on Improved Genetic Algorithm," *Microelectronics Journal*, Vol. 127, September 2022.
2. S. Husain, A. Khusro, M. Hashmi, G. Nauryzbayev and M. A. Chaudhary, "Demonstration of CAD Deployability for GPR Based Small-Signal Modelling of GaN HEMT," *IEEE International Symposium on Circuits and Systems*, May 2021.
3. A. Majumdar, S. Chatterjee, S. Chatterjee, S. S. Chaudhari and D. R. Poddar, "An Ambient Temperature Dependent Small Signal Model of GAN HEMT Using Method of Curve Fitting," *International Journal of RF and Microwave Computer-Aided Engineering*, Vol. 30, No. 12, December 2020.
4. J. Zhang, S. Wang, M. Liu, B. Liu and J. Wang, "An Improved GaN P-HEMT Small-Signal Equivalent Circuit with its Parameter Extraction," *Microelectronics Journal*, Vol. 112, June 2021.
5. Z. Hu, Q. Zhang, K. Ma, R. He and F. Feng, "An Improved Compact Large-Signal GaN HEMT Model for Switch Ap-

TABLE 1

GAN HEMT S-PARAMETER ERRORS

Bias Point	V_{GS} = 0 V, V_{DS} = 10 V		VGS = –1 V, V_{DS} =12 V		V_{GS} = – 1 V, V_{DS} = 14 V	
Algorithm	PSO Error (percent)	DAIW-PSO Error (percent)	PSO Error (percent)	DAIW-PSO Error (percent)	PSO Error (percent)	DAIW-PSO Error (percent)
S_{11}	1.5	0.7	3.3	0.8	1.8	0.8
S_{12}	4.1	3.1	3.2	4.2	3.3	4.5
S_{21}	4.1	0.9	1.9	1.7	3.8	2.2
S_{22}	3.7	3.2	5.0	3.7	4.2	3.0
$Error_{avg}$	3.3	2.0	3.4	2.6	3.3	2.6

plication," *IEEE Transactions on Electron Devices*, Vol. 69, No. 6, June 2022, pp. 3061–3067.
6. Y. S. Chauhan, A. Pampori, R. Dangi, P. Kushwaha, E. Yadav and S. Sinha, "A Turnkey Large-Signal Model for Amplifier Design in 5G Spectra using AlGaN/GaN HEMTs," *IEEE Electron Devices Technology & Manufacturing Conference*, March 2022, pp. 354–356.
7. A. Jadhav, T. Ozawa, A. Baratov, J. T. Asubar, M. Kuzuhara, A. Wakejima, S. Yamashita, M. Deki, S. Nitta, Y. Honda, H. Amano, S. Roy and B. Sarkar, "Modified Small Signal Circuit of AlGaN/GaN MOS-HEMTs Using Rational Functions," *IEEE Transactions on Electron Devices*, Vol. 68, No. 12, December 2021, pp. 6059–6064.
8. A. Khusro, S. Husain, M. S. Hashmi, A. Q. Ansari and S. Arzykulov, "A Generic and Efficient Globalized Kernel Mapping-Based Small-Signal Behavioral Modeling for GaN HEMT," *IEEE Access*, Vol. 8, October 2020, pp. 195046–195061.
9. A. Jarndal, M. A. Alim, A. Raffo and G. Crupi, "2-mm-Gate-Periphery GaN High Electron Mobility Transistors on SiC and Si Substrates: A Comparative Analysis from a Small-Signal Standpoint," *International Journal of RF and Microwave Computer-Aided Engineering*, Vol. 31, No. 6, June 2021.
10. J. Kim, "A New GaN HEMT Small-Signal Model Considering Source via Effects for 5G Millimeter-Wave Power Amplifier Design," *Applied Sciences*, Vol. 11, No. 19, 11(19), September 2021.
11. Y. Chen, Y. Xu, Y. Luo, C. Wang, Z. Wen, B. Yan and R. Xu, "A Reliable and Efficient Small-Signal Parameter Extraction Method for GaN HEMTs," *International Journal Numerical Modelling – Electronic Networks, Devices and Fields*, Vol. 33, No. 3, May/June 2020.
12. M. Al Sabbagh, M. C. E. Yagoub and J. Park, "New Small-Signal Extraction Method Applied to GaN HEMTs on Different Substrates," *International Journal of RF and Microwave Computer-Aided Engineering*, Vol. 30, No. 9, September 2020.
13. H. Cai, J. Zhang, M. Liu, S. Yang, S. Wang, B. Liu and J. Zhang, "Adaptive Particle Swarm Optimization Based Hybrid Small-Signal Modeling of GaN HEMT," *Microelectronics Journal*, Vol. 137, July 2023.
14. A. Jarndal, "On Modeling of Substrate Loading in GaN HEMT Using Grey Wolf Algorithm," *Journal of Computational Electronics*, Vol. 19, No. 2, February 2020, pp. 576–590.
15. A. Jarndal and A. S. Hussein, "On Reliable Modeling of Substrate/Buffer Loading Effects in a Gallium Nitride High-Electron-Mobility Transistor on Silicon Substrate," *Journal of Computational Electronics*, Vol. 20, No. 1, February 2021, pp. 503–514.
16. A. Jarndal and G. Kompa, "A New Small-Signal Modeling Approach Applied to GaN Devices," *IEEE Transactions on Microwave Theory and Techniques*, Vol. 53, No. 11, November 2005, pp. 3440–3448.
17. E. Chigaeva, W. Walthes, D. Wiegner, M. Grozing, F. Schaich, N. Wieser, M. Berroth, O. Breitschadel, L. Kley, B. Kuhn, F. Scholz, H. Schweizer, O. Ambacher and J. Hilsenbeck, "Determination of Small-Signal Parameters of GaN-Based HEMTs," *IEEE/ Cornell Conference on High Performance Devices*, August 2000.
18. Z. Wen, Y. Xu, C. Wang, X. Zhao and R. Xu, "An Efficient Parameter Extraction Method for GaN HEMT Small-Signal Equivalent Circuit Model," *International Journal of Numerical Modelling of Electronic Networks, Devices and Fields*, Vol. 30, No. 1, January/February 2017.
19. S. Husain, A. Jarndal, M. Hashmi and F. M. Ghannouchi, "Accurate, Efficient and Reliable Small-Signal Modeling Approaches for GaN HEMTs," *IEEE Access*, Vol.11, September 2023, pp. 106833–106846.
20. L. Zhai, H. Cai, S. Wang, J. Zhang and S. Yang, "A Reliable Parameter Extraction Method for the Augmented GAN High Electron Mobility Transistor Small-Signal Model," *International Journal of RF and Microwave Computer-Aided Engineering*, Vol. 32, No. 8, August 2022.
21. Y. Liu, F. Cao, X. Xiong, J. Huang and W. Deng, "Parameter Extraction for Small-Signal Model of GaN HEMTS on SiC Substrates Based on Modified Firefly Algorithm," *International Journal of RF and Microwave Computer-Aided Engineering*, Vol. 32, No. 12, December 2022.
22. A. Majumder, S. Chatterjee, S. Chatterjee, S. Sinha Chaudhari and D. R. Poddar, "Optimization of Small-Signal Model of GaN HEMT by Using Evolutionary Algorithms," *IEEE Microwave Wireless Components Letters*, Vol. 27, No. 4, April 2017, pp. 362–364.
23. A. Majumdar, S. Chatterjee, S. Bose, S. Chatterjee, S. S. Chaudhari and D. R. Poddar, "Differential Evolution Based Small Signal Modeling of GaN HEMT," *International Journal of RF and Microwave Computer-Aided Engineering*, Vol. 29, No. 6, June 2019.
24. R. Eberhart and J. Kennedy, "A New Optimizer Using Particle Swarm Theory," *Proceedings of the Sixth International Symposium on Micro Machine and Human Science*, October 1995.
25. T. Zong, J. Li and G. Lu, "Identification of Hammerstein–Wiener Systems with State-Space Subsystems Based on the Improved PSO and GSA Algorithm," *Circuits Systems and Signal Processing*, Vol. 42, No. 5, December 2022, pp. 2755–2781.
26 D. Subramoney and C. N. Nyirenda, "Multi-Swarm PSO Algorithm for Static Workflow Scheduling in Cloud-Fog Environments," *IEEE Access*, Vol. 10, November 2022, pp. 117199–117214.
27. S. Chen, C. Zhang and J. Yi, "Time-Optimal Trajectory Planning for Woodworking Manipulators Using an Improved PSO Algorithm," *Applied Sciences*, Vol. 13, No. 18, September 2023.
28. Q. Zheng, B. -W. Feng, Z. -Y. Liu and H. -C. Chang, "Application of Improved Particle Swarm Optimization Algorithm in Hull Form Optimization," *Journal of Marine Science and Engineering*, Vol. 9, No. 9, September 2021.
29. X. Jinwei, J. Chengpeng, C. Zhizhao and X. Wendong, "Improved Particle Swarm Optimization Algorithm with Fireworks Search," *41st Chinese Control Conference*, July 2022.
30. M. Clerc and J. Kennedy, "The Particle Swarm - Explosion, Stability, and Convergence in a Multidimensional Complex Space," *IEEE Transactions on Evolutionary Computation*, Vol. 6, No. 1, February 2002, pp. 58–73.
31. S. Wang and G. Liu, "A Nonlinear Dynamic Adaptive Inertial Weight Particle Swarm Optimization," *Computer Simulation*, Vol. 38, No. 4, 2021.
32. B. L. Ooi and J. Y. Ma, "Consistent and Reliable MESFET Parasitic Capacitance Extraction Method," *IEEE Proceedings - Microwaves Antennas and Propagation*, Vol. 151, No. 1, March 2004, pp. 81–84.
33. Y. Shi and R. Eberhart, "A Modified Particle Swarm Optimizer," *IEEE International Conference on Evolutionary Computation Proceedings/IEEE World Congress on Computational Intelligence*, May 1998.

exclusive Digital Content

REVIEW BOARD MWJ APPROVED

CPW-Fed Microstrip Antenna Design Uses Machine Learning Approach

Sonmati Verma, Rajiv Kumar Singh and Neelam Srivstava
Institute of Engineering & Technology, Lucknow, India

Pinku Ranjan
ABV-Indian Institute of Information Technology and Management, Gwalior, India

A compact, wideband coplanar waveguide (CPW)-fed microstrip patch antenna fabricated on an FR4 substrate is developed for high data wireless applications. The flower-shaped antenna, featuring circular slots and a 50 Ohm line, exhibits a 2490 MHz impedance bandwidth (3.96 to 6.45 GHz) and 2.5 dBi gain enhanced by a circular parasitic component for dual-band flexibility. It is cost-effective, compact and easy to fabricate, making it suitable for high data rate wireless applications. The design, validated by artificial neural networks (ANNs), k-nearest neighbor (KNN), decision tree and random forest machine learning algorithms, demonstrates good matching characteristics and radiation performance in prototype tests.

In response to the growing demand for high data rates in short-range indoor applications, wireless communication system antennas, particularly those utilizing parasitic element antennas with split-ring resonators, are gaining traction. These antennas offer wide bandwidth, favorable radiation patterns and multifunctionality, making them highly suitable for a range of practical applications. A broadband effect can be achieved by inserting a rectangular-shaped parasitic element into a CPW-fed ground plane. For example, a broadband high gain mushroom-shaped parasitic patch-loaded microstrip patch antenna was reported by Cao et al.[1] In another work, a circularly polarized dual-band single-layer antenna was developed using a crescent-shaped parasitic patch.[2] Without the crescent-shaped patch, the antenna resonated at 2.4 and 5.4 GHz. Its bandwidth was increased from 5.2 to 5.8 GHz by loading with the parasitic element; however, the size increased dramatically. W. J. Yang et al.[3] demonstrated a centered parasitic patch antenna to enhance its bandwidth by up to 80 percent.

Recently, CPW-fed antennas have gained popularity for diverse applications. A recent design, described by Ding et al.[4] incorporates an open-loop parasitic patch on the substrate for broad bandwidth and sustained gain, albeit with a large size. Likewise, a penta-band planar dipole antenna with a

CPW feed is described by Chen et al.[5] and Abkenar and Rezaei.[6] Despite their advantages, these antennas have had limited adoption due to their intricate geometries and lack of flexibility.

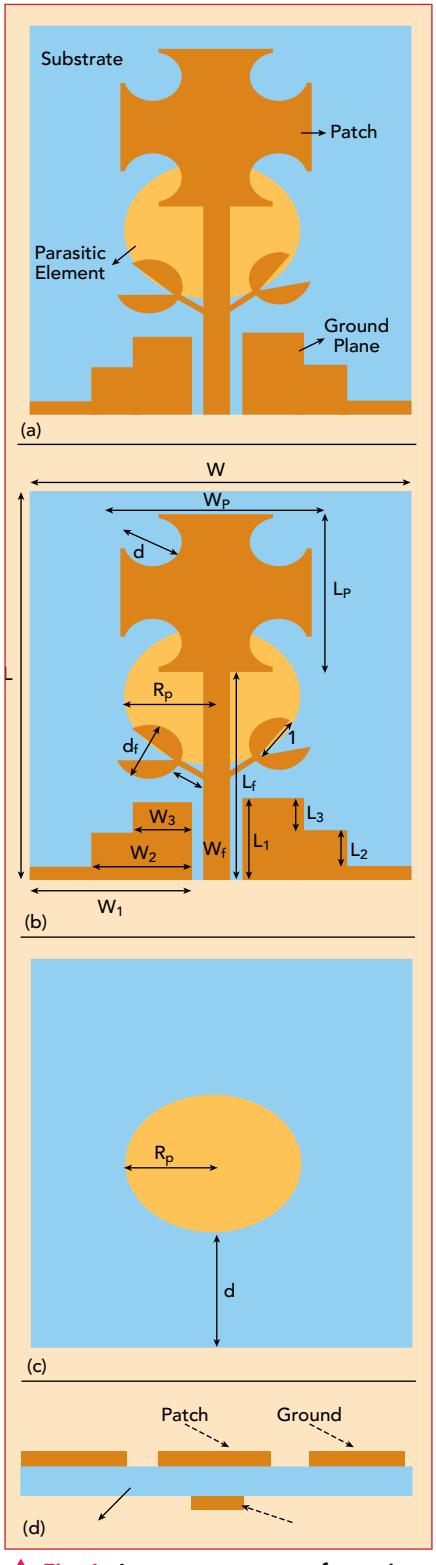

Fig. 1 **Antenna geometry: front view (a), front view parameters (b), back view parameters (c) and side view (d).**

This article describes a flower-shaped CPW-fed patch antenna with a parasitic element that increases bandwidth. The antenna's tiny size and flexibility to fine-tune its frequency, bandwidth and directivity make it ideal for small devices.[7,8] This adjustability makes it highly adaptable and suitable for diverse applications with varying environmental dynamics or performance demands. Smart machine learning (ML) techniques like ANN, KNN, random forest and decision tree[9-11] are employed for optimization, overcoming the limitations of traditional time-consuming and computationally intensive methods.

ANTENNA STRUCTURE

The modified flower-shaped antenna shown in various views in ***Figure 1*** is constructed from 0.8 mm thick FR4 with ε_r = 4.4 and tan δ = 0.2. A circular parasitic element with a radius R_p = 5.5 mm at d = 6.58 mm is deposited onto the substrate's bottom surface. The square radiating patch is modified with four circular slots of diameter d_c = 2.5 mm. The coplanar CPW feedline is a simple planar structure that provides wide bandwidth. Square and rectangular slots are used to change the dimensions of the ground plane, L_g and W_g, to improve impedance matching. ***Table 1*** lists the antenna's optimized dimensions. The compactness of this radiator is realized with the CPW ground plane and slots. Two identical branches at 45-degree angles are connected to the 50 Ohm microstrip line for tuning and impedance matching.

Design Evolution

Figure 2a shows the design evolution. Antenna 1 is a simple CPW-fed square patch. Antenna 2 introduces circular slots in the square patch and adds matching elements to the feedline. Antenna 3 adds rectangular slots to the CPW ground plane and slots to the matching elements. In the final design of Antenna 4, a circular parasitic element is added on the backside. The dimensions of all design parameters are optimized through parametric analysis of $|S_{11}|$. ***Figure 2b*** shows the progressive performance improvement. ***Figure 3*** shows the effect of the stepped ground, improving the return loss and impedance bandwidth. The frequency band shifts higher due to increased capacitance introduced by the ground slots.

Varying the Parasitic Element Radius and Position

The effect on $|S_{11}|$ of varying the parasitic element radius (R_p) from 4.5 to 5.5 mm is shown in ***Figure 4a***. The $|S_{11}|$ performance of the antenna is best at R_p = 5.5 mm. As R_p decreases, the resonant frequency shifts upwards as the antenna's impedance bandwidth decreases. The position of the parasitic element, d, is varied from 6.57 to 10.57 mm with the results shown in ***Figure 4b***. It is clear that d = 6.57 mm mini-

TABLE 1
ANTENNA DIMENSIONS

Parameter	*Value (mm)*
Substrate length (L)	28
Substrate width (W)	20
Length of patch (L_p)	13
Width of patch (W_p)	13
Width of ground (W_1)	8
Length of ground (L_1)	6
Width of feedline (W_f)	2
Length of feedline (L_f)	14.5
Parasitic element radius (R_p)	5.5
Diameter of circular slot in patch (d_c)	2.5
Diameter of leaf (d_f)	4.51
Length of branch (t)	3.62
Length of leaf (l)	3.31
L_2	2.5
L_3	2.5
W_2	4.4
W_3	3

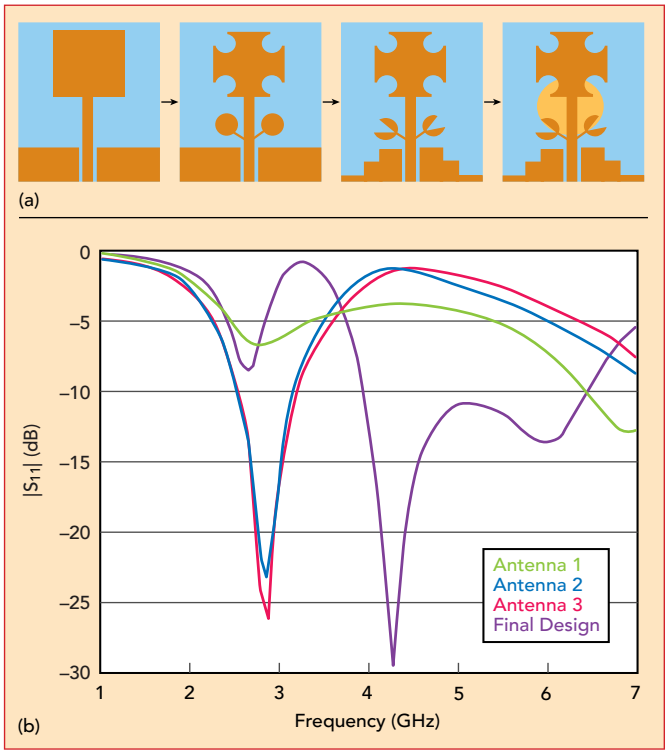

Fig. 2 **Antenna design evolution (a) and corresponding $|S_{11}|$ simulations (b).**

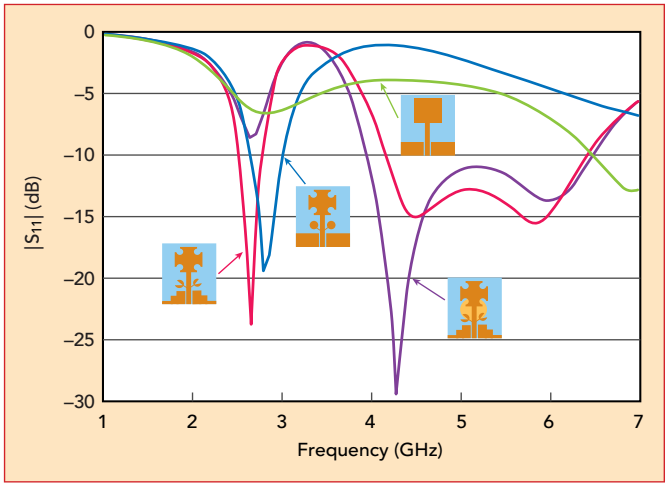

Fig. 3 **Effect of ground slots on $|S_{11}|$.**

mizes $|S_{11}|$ over the frequency band from 3.96 to 6.45 GHz. The center frequency shifts upwards and the impedance bandwidth decreases with an increasing value of d. ***Figure 5a*** shows one side of the optimized prototype antenna and ***Figure 5b*** shows the other side of the circuit board.

SIMULATED AND MEASURED RESULTS

Without the parasitic element, the simulation shows the antenna resonates at 2.9 GHz with a 588 MHz bandwidth (2.6 to 3.19 GHz). The simulated and measured bandwidths for the antenna containing the parasitic element are 2490 MHz (3.96 to 6.45 GHz) and 2470 MHz (3.95 to 6.42 GHz), respectively, as shown in ***Figure 6***. The parasitic element enhances the impedance bandwidth by creating an additional resonance at 4.2 GHz.

Figure 7 and ***Figure 8*** show radiation patterns across the operating band. The E-plane patterns in Figure 7 are bidirectional, while the H-plane patterns in Figure 8 are omnidirectional. The antenna gain is approximately 2.5 dBi.

The surface current distribution at 4.2 GHz is shown in ***Figure 9***. The current density is high on the microstrip line, parasitic element, a tiny section of the ground plane, radiating patch and branch strips. This leads to several conclusions:

- The high current density in areas like the radiating patch and branch strips suggests that these parts are vital for the effective radiation of electromagnetic waves.
- High current density on the microstrip line indicates efficient power transfer from the feed line to the antenna, suggesting good impedance matching.
- High current density on the parasitic element significantly influences the antenna's performance, likely altering its radiation pattern or other characteristics.
- High current density in a section of the ground plane indicates its role in shaping the electromagnetic field distribution and potentially affecting the antenna's radiation pattern.

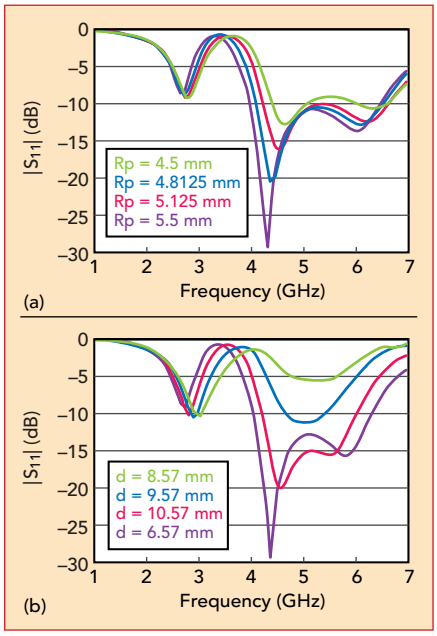

Fig. 4 **Effect of the variation of parasitic element dimensions on $|S_{11}|$: Rp (a) and d (b).**

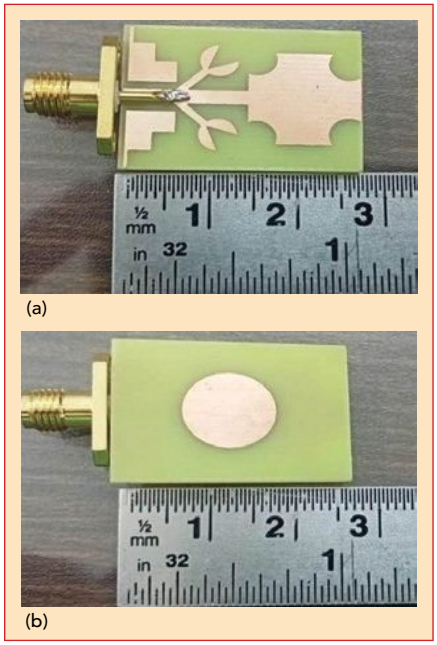

Fig. 5 **Antenna prototype: front view (a) and back view (b).**

Table 2 compares this antenna with previously reported antenna designs. Considering bandwidth, gain, size and design flexibility, this

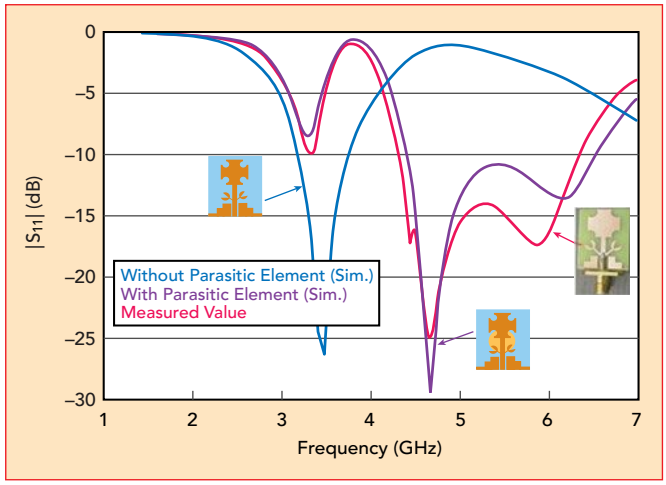

Fig. 6 **Simulated and measured antenna $|S_{11}|$.**

approach offers an alternative that may be better suited for high data rate applications.

ML APPROACH

Advancements in wireless technology and IoT are driving the use of smart ML techniques like ANN, KNN, decision tree and random forest for efficient antenna design, improved prediction accuracy and process streamlining.[9,10] These methods replace traditional, time-consuming approaches by analyzing data and revealing statistical relationships.

ANN

ANNs mirror biological neural networks. They contain input, hidden and output layers with interlinked nodes and have been used in radar, antenna design and remote sensing applications since 1990.[7,8,16] Each associated node from every single layer is linked to every other one in the successive layer. The ANN architecture, comprising neurons and synapses, uses weighted stimulation for information interpretation and output generation.[9,10] This three-tier structure, as shown in ***Figure 10***, replicates the equation y = M(x) by integrating input, output and latent layers. This is shown in ***Equation 1***:

$$M(x) = a\left(\sum_{i=1}^{l} \psi i(x) wi + \theta\right) \quad (1)$$

Where:

$\Phi_l(x)$, i = 1 to l, is implemented in neurons in the hidden layer

w_i i = 1 to l represents the hidden neuron and network output weights

θ is the bias value

M(*x*) = a () is the activation function.

For the patch antenna, an ANN is constructed with four layers: one input layer, two hidden layers and one output layer. The activation function for the input layer, which has a six-unit output, is the rectified linear unit (ReLU). The first dense layer has an output of eight units using ReLU as its activation function. One of the three units in the second hidden layer has the ReLU as a function. The output layer has only one unit because only $|S_{11}|$ is predicted for the antennas. The output layer's activation function is linear.

As seen from the patch antenna's predicted versus actual values plot in ***Figure 11***, the model prediction fits well for smaller values of $|S_{11}|$, but there is some variation for larger values.

KNN

The KNN algorithm, an unsupervised ML method, classifies new data by selecting the nearest K points. The optimal value of K = 5.0 is determined via a ten-fold cross-validation for minimal error, using the five closest neighbors for predictions. KNN predicts the correct class by calculating the distance between the test data and the training point. KNN uses Euclidean distance as defined in ***Equation 2***:

$$d(m,n) = \sqrt{\sum_{i=1}^{n} (n_i - m_i)^2} \quad (2)$$

The model works very well for smaller values of $|S_{11}|$, as seen by the plots of expected and actual values shown in ***Figure 12***.

Decision Tree

Regression, crucial for predicting continuous values, is known for its accuracy and efficiency. Decision tree regression reduces the standard deviation and error in subsets by dividing datasets and optimizing split criteria. This focus contrasts with ML's usual emphasis on classification, showcasing regression's significance in research and practical applications.

Suppose y is the target variable and x is a particular attribute of the dataset. In that case, the reduction in the standard deviation of the i^{th} data point can be calculated using ***Equation 3***:

$$SDR = sd(y) - \sum_i \frac{x_i}{y} sd(x_i) \quad (3)$$

The result is shown in ***Figure 13***.

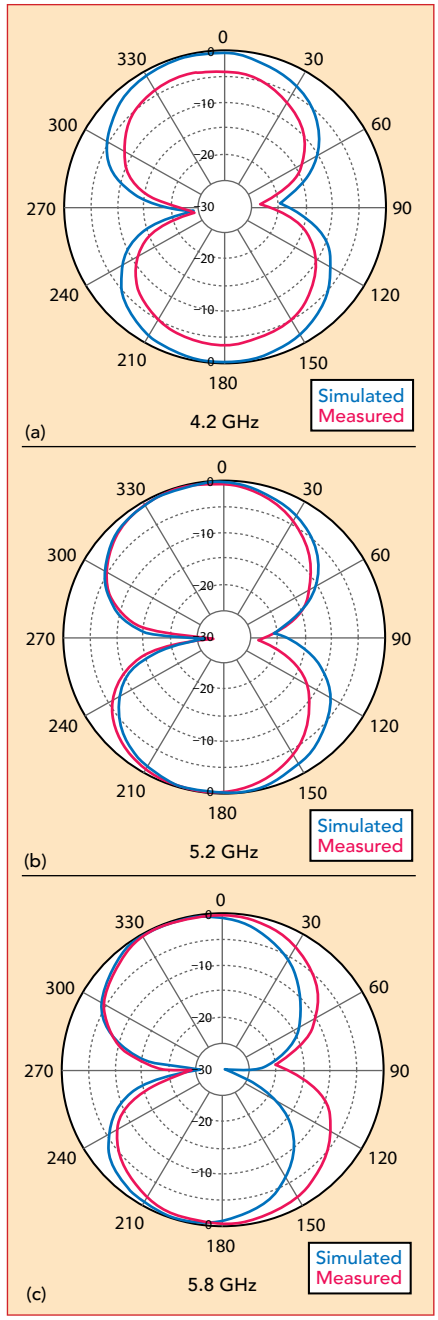

Fig. 7 **E-plane radiation patterns at 4.2 (a), 5.2 (b) and 5.8 (c) GHz.**

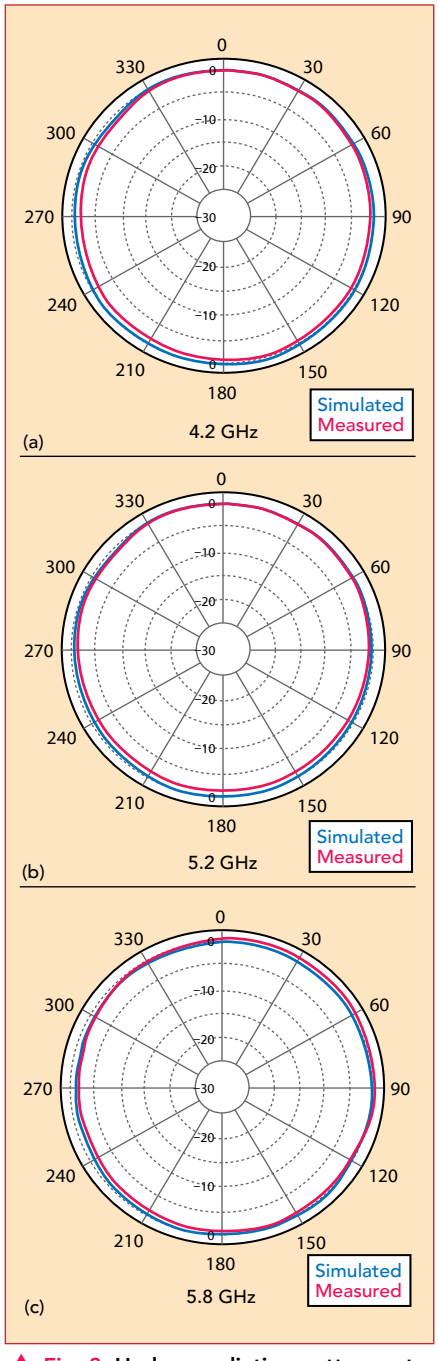

Fig. 8 H-plane radiation patterns at 4.2 (a), 5.2 (b) and 5.8 (c) GHz.

TABLE 2

COMPARISON WITH PREVIOUS WORK

Reference	Size (mm)	Frequency Band (GHz)	Gain (dBi)	Application	Parasitic Concept	Design Flexibility
12	37 × 37	2.25 to 5.44	-	Wideband	Yes	No
13	38.2 × 8.8	5.06 to 6.18	1.8	Wideband	No	No
14	29 × 38	2.15 to 6.1	-	Wideband	No	No
15	80 × 60	2.21 to 4.0	6.2	Wideband	No	Yes
This Work	28 × 20	3.96 to 6.45	2.5	Wideband	Yes	Yes

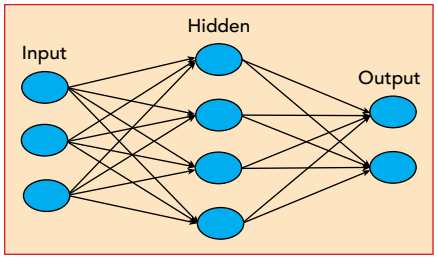

Fig. 10 ANN interconnections.

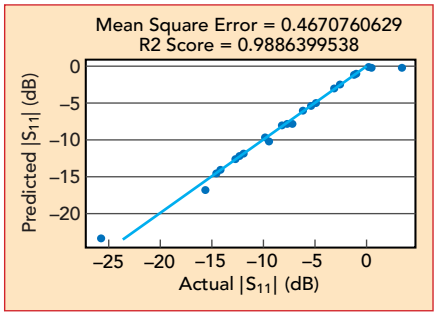

Fig. 11 ANN predicted versus actual values for $|S_{11}|$.

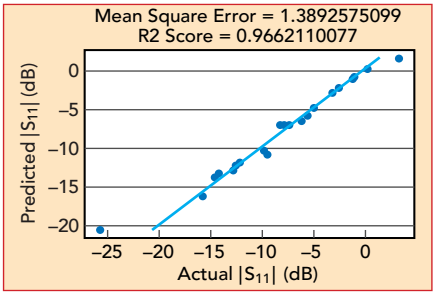

Fig. 12 KNN predicted versus actual values for $|S_{11}|$.

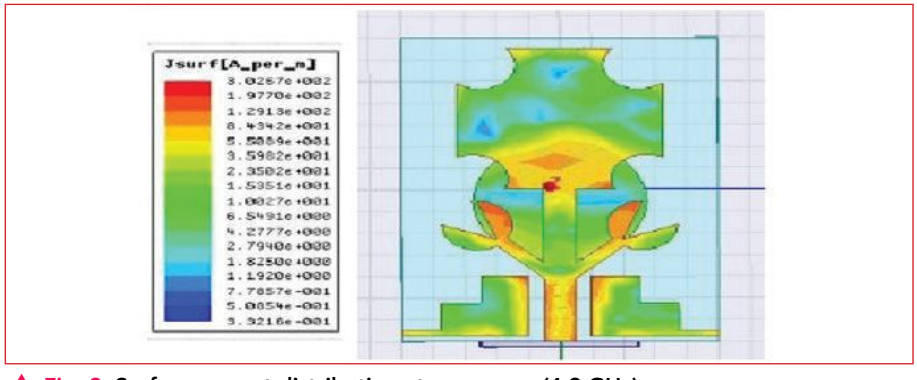

Fig. 9 Surface current distribution at resonance (4.2 GHz).

Random Forest

Random forest regression uses multiple decision trees on random subspaces, avoiding overfitting/underfitting in large datasets with mean-squared error (MSE) for node splitting; its output, x_i, aligns with actual values for N data points. If N is the number of data points, the value returned by the model, x_i, is the actual value of the i^{th} data point. The MSE calculation method can be described in ***Equation 4***.

$$MSE = \frac{1}{N}\sum_{i=1}^{N}(y_i - x_i)^2 \quad (4)$$

The comparison for the patch antenna generated using the random forest model is shown in ***Figure 14***. The MSE is extremely low and the correlation value (R2 score) is excellent.

CONCLUSION

A CPW-fed microstrip patch antenna optimized using ML techniques, including ANN, KNN, random forest and decision tree, demonstrates significant improvements for high data rate wireless applications. The antenna's compact size, enhanced by triangular and semicircular slots, along with an 1882 MHz bandwidth increase due to the parasitic element, improves efficiency and cost-effectiveness. The integration of ML, using Ansys HFSS software for data creation, expedites the design process and reduces simulation errors. This innovative approach is verified through measurement and simulation. ■

References

1. Y. Cao, Y. Cai, W. Cao, B. Xi, Z. Qian, T. Wu and L. Zhu, "Broadband and High-Gain Microstrip Patch Antenna Loaded with Parasitic Mushroom-Type Structure," *IEEE Antennas and Wireless*

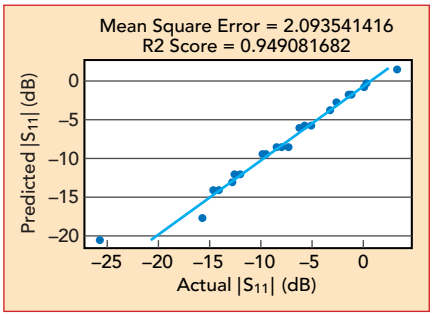

Fig. 13 Decision tree predicted versus actual values for $|S_{11}|$.

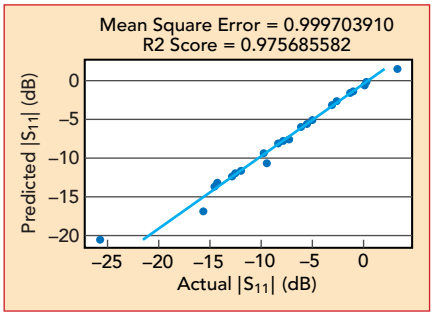

Fig. 14 Random forest predicted versus actual values for $|S_{11}|$.

Propagation Letters, Vol. 18, No. 7, July 2019, pp. 1405–1409.

2. L. Ge, C. Y. D. Sim, H. L. Su, J. Y. Lu and C. Ku, "Single Layer Dual Broadband Circularly Polarized Annular-Slot Antenna for WLAN Applications," *IET Microwaves, Antennas & Propagation*, Vol. 12, No. 1, January 2018, pp. 99–107.
3. W. J. Yang, Y. M. Pan and S. Y. Zheng, "A Low-Profile Wideband Circularly Polarized Crossed-Dipole Antenna with Wide Axial-Ratio and Gain Beamwidths," *IEEE Transactions on Antennas and Propagation*, Vol. 66, No. 7, July 2018, pp. 3346–3353.
4. K. Ding, Y. -X. Guo and C. Gao, "CPW-Fed Wideband Circularly Polarized Printed Monopole Antenna with Open Loop and Asymmetric Ground Plane," *IEEE Antennas and Wireless Propagation Letters*, Vol. 16, September 2016, pp. 833–836.
5. Y. -J. Chen, T. -W. Liu and W. -H. Tu, "CPW-Fed Penta-Band Slot Dipole Antenna Based on Comb-Like Metal Sheets," *IEEE Antennas and Wireless Propagation Letters*, Vol. 16, May 2016, pp. 202–205.
6. M. R. Abkenar and P. Rezaei, "EBG Structures Properties and Their Application to Improve Radiation of a Low Profile Antenna," *Journal of Information Systems and Telecommunications*, Vol. 1, No. 4, January 2013, pp. 251–259.
7. Q. Zhang, C. Liu, X. Wan X, L. Zhang, S. Liu, Y. Yang and T. J. Cui, "Machine-Learning Designs of Anisotropic Digital Coding Metasurfaces," *Advanced Theory and Simulations*, Vol. 2, No. 2, February 2019.
8. H. J. Delgado and M. H. Thursby, "A Novel Neural Network Combined with FDTD for the Synthesis of a Printed Dipole Antenna," *IEEE Transactions on Antennas and Propagation*, Vol. 53, No. 7, July 2005, pp. 2231–2236.
9. P. Ranjan, A. Maurya, H. Gupta, S. Yadav and A. Sharma, "Ultra-Wideband CPW Fed Band-Notched Monopole Antenna Optimization Using Machine Learning," *Progress In Electromagnetics Research M*, Vol. 108, 2022, pp. 27–38.
10. P. Ranjan, A. Krishnan, A. K. Dwivedi, S. K. Singh and A. Sharma, "Design and Optimization of MIMO Dielectric Resonator Antenna Using Machine Learning for Sub-6 GHz Based on 5G IoT Applications," *Arabian Journal for Science and Engineering*, Vol. 48, March 2023, pp. 4671–14679.
11. P. Ranjan, S. Yadav, H. Gupta and A. Bage, "Design and Development of Machine Learning Assisted Cylindrical Dielectric Resonator Antenna," *EVERGREEN Joint Journal of Novel Carbon Resource Sciences & Green Asia Strategy*, Vol. 10, No. 1, March 2023, pp. 308–316.
12. Y. Sung, "Bandwidth Enhancement of a Microstrip Line-Fed Printed Wide-Slot Antenna with a Parasitic Center Patch," *IEEE Transactions on Antennas and Propagation*, Vol. 60, No. 4, April 2012, pp. 1712–1716.
13. X. Yang, Y. Liu and S. -X. Gong, "Design of a Wideband Omnidirectional Antenna with Characteristic Mode Analysis," *IEEE Antennas and Wireless Propagation Letters*, Vol. 17, No. 6, June 2018, pp. 993–997.
14. D. D. Krishna, M. Gopikrishna, C. K. Aanandan, P. Mohanan and K. Vasudevan, "Compact Wideband Koch Fractal Printed Slot Antenna," *IET Microwaves, Antennas & Propagation*, Vol. 3, No. 5, August 2009, pp. 782–789.
15. M. O. Sallam, S. M. Kandil, V. Volski, G. A. E. Vandenbosch and E. A. Soliman, "Wideband CPW-Fed Flexible Bow-Tie Slot Antenna for WLAN/WiMax Systems," *IEEE Transactions on Antennas and Propagation*, Vol. 65, No. 8, August 2017, pp. 4274–4277.
16. L. -Y Xiao, W. Shao, F. -L. Jin, B. -Z. Wang and Q. H. Liu, "Inverse Artificial Neural Network for Multiobjective Antenna Design," *IEEE Transactions on Antennas and Propagation*, Vol. 69, No. 10, October 2021, pp. 6651–6659.